Regulation of the NAD⁺-dependent deacetylase SIRT2 by CDK5

Von der Fakultät für Mathematik, Informatik und Naturwissenschaften der Rheinisch-Westfälischen Technischen Hochschule Aachen zur Erlangung des akademischen Grades einer Doktorin der Naturwissenschaften genehmigte Dissertation

vorgelegt von

Diplom-Biologin
Franziska Flick

aus Ludwigslust

Berichter: Universitätsprofessor Dr. rer. nat. Bernhard Lüscher
               Universitätsprofessor Dr. rer. nat. Werner Baumgartner

Tag der mündlichen Prüfung: 25. Januar, 2012

Die Dissertation ist auf den Internetseiten der Hochschulbibliothek online verfügbar.

Abstract

SIRT2 belongs to the protein family of sirtuins, which are homologs of the yeast silencing information regulator 2 (Sir2), an NAD^+-dependent histone deacetylase. Seven different sirtuins, SIRT1-7, have been identified in mammals, which share a common catalytic core domain but possess distinct N- and C-terminal extensions. In the case of SIRT2 this core domain elicits an NAD^+-dependent deacetylase activity. SIRT2 is the only sirtuin, which is predominantly localized in the cytoplasm. It is highly abundant in the brain, especially in myelin-forming oligodendrocytes. Cellular processes, in which SIRT2 is implicated, include differentiation, neurite outgrowth, autophagy, and spindle checkpoint activation. In addition, SIRT2 is associated with neurodegenerative diseases, such as Huntington's and Alzheimer's disease. These findings strongly suggest that SIRT2 is tightly controlled and potentially responsive to different signal transduction pathways. However, very little is known about how SIRT2 is regulated both in normal and deregulated cell physiology. Because deregulation of cellular processes account for many diseases, it is important to understand the mechanisms that determine SIRT2 function.

Here I demonstrate that a p35/CDK5-mediated signaling pathway mediates the phosphorylation of SIRT2 at serine 368/331 (S368/331) and S372/335 (numbering according to SIRT2 isoform 1 or isoform 2, respectively) in cells. Thereby p35/CDK5 phosphorylates S368/331 directly, whereas the phosphorylation of S372/335 is effected indirectly. A candidate kinase acting downstream of CDK5 is CDK16, which also induces phosphorylation of SIRT2 at S335 in cells. Furthermore my results support the hypothesis that the C-terminal region of SIRT2 administrates an inhibitory effect on the catalytic activity of SIRT2, which might be enhanced by phosphorylation. In addition I discovered a potential feedback-loop between SIRT2 and CDK5, which includes a cytoplasmic acetyltransferase, GCN5.

My results provide further knowledge about a regulatory signaling pathway that targets SIRT2 and CDK5, two proteins involved in postmitotic cell physiology and whose deregulation support and are associated with neurodegeneration.

Zusammenfassung

SIRT2 ist eine NAD^+-abhängige Deacetylase, die zur Proteinfamilie der Sirtuine gehört. Diese wird aus Homologen des Hefe-Proteins Sir2 gebildet. Bislang wurden sieben humane Sirtuine identifiziert, SIRT1-7, welche sich durch eine konservierte katalytische Domäne auszeichnen. Abgesehen von dieser Sirtuin-typischen Domäne unterscheiden sich die einzelnen Sirtuine in ihren N- und C-terminalen Regionen, für die regulatorische Eigenschaften nachgewiesen werden konnten. SIRT2 ist im Gegensatz zu den anderen Sirtuinen hauptsächlich im Zytoplasma lokalisiert. Außerdem wurden hohe *SIRT2*-Expressionslevel im Gehirn, insbesondere in den Myelin-bildenden Oligodendrozyten gemessen. SIRT2 ist in verschiedene zelluläre Prozesse involviert, wie zum Beispiel Zelldifferenzierung, Neuritenwachstum, Makroautophagie und Spindel-Kontrollpunkt-Aktivierung im Zellzyklus. Außerdem ist SIRT2 mit neurodegenerativen Erkrankungen, wie zum Beispiel Huntington und Alzheimer, assoziiert. Diese Erkenntnisse deuten darauf hin, dass SIRT2 Regulationsmechanismen unterliegt, welche durch verschiedene Signalwege gesteuert werden können. Bisher ist nur wenig über solche Regulationsmechanismen für SIRT2 bekannt. Um zu verstehen, wie es zu bestimmten Krankheitsbildern kommt, ist es wichtig diese Regulationsmechanismen zu kennen.

In dieser Arbeit zeige ich, dass ein p35/CDK5-abhängiger Signalweg die Phosphorylierung von SIRT2 in der C-terminalen Region an Serin 368/331 (S368/331) und S372/335 (Nummerierung gibt Position der Aminosäure in Isoform 1 oder 2 an) in Zellen vermittelt. P35/CDK5 phosphoryliert SIRT2 dabei an S368/331 direkt, während die Phosphorylierung von S372/335 jedoch indirekt erfolgt. Eine mögliche Kinase, welche durch CDK5 aktiviert wird, ist CDK16. Mit Hilfe von Mutationsanalysen konnte ich eine inhibierende Funktion der C-terminalen Region nachweisen, welche vermutlich durch Phosphorylierung verstärkt wird. Außerdem zeige ich einen Feedback-Signalweg zwischen SIRT2 und CDK5, welcher möglicherweise eine neue zytoplasmatische Funktion der Acetyltransferase GCN5 beschreibt. Meine Ergebnisse geben Aufschluss über einen Signalweg, der sowohl SIRT2 als auch CDK5 reguliert: Zwei Proteine, die die postmitotische Zellphysiologie kontrollieren und deren Fehlregulation mit der Ausbildung von neurodegenerativen Erkrankungen assoziiert ist.

Table of content

1. Introduction

Sirtuins are homologs of the yeast silencing information regulator 2 (Sir2) protein, an NAD^+-dependent (histone) deacetylase. In mammals 7 different sirtuins, SIRT1-7, have been identified, which share a common catalytic core domain but possess distinct amino- (N-) and carboxy- (C-) terminal extensions. This core domain elicits NAD^+-dependent deacetylase and in some cases also ADP-ribosyltransferase activity. Sirtuins have been implicated in key cellular processes, including cell survival, autophagy, apoptosis, gene transcription, DNA repair, stress response and genome stability. In addition some sirtuins are associated with disease, including cancer and neurodegeneration. These findings suggest strongly that sirtuins are tightly controlled and potentially responsive to different signal transduction pathways. However, very little is known about how these proteins are regulated both in normal and deregulated cell physiology and as deregulation of cellular processes are the basis for many diseases, it is important to understand the mechanisms that determine sirtuin function.

1.1 Posttranslational modifications (PTMs)

The term "posttranslational modification" (PTM) is generally used to summarize covalent modifications, which are inflicted upon a protein after its translation. These can involve structural changes of a protein or the addition of functional groups or proteins to individual amino acids of a protein. Posttranslational structural changes can be achieved, e.g. by disulfide bridges between cysteines or by proteolytic cleavage of peptide bonds. Prominent functional groups, which can be added posttranslationally are acetyl- (acetylation) or phosphate-groups (phosphorylation). SUMOylation and ubiquitination are processes, which involve the addition of small proteins. More than 200 different PTMs have been described to date. While these are usually catalyzed by enzymes, non-enzymatic modifications occur as well, e.g. glycation (Wold, 1981). Within the enzyme-mediated PTM group one can distinguish between those that are catalyzed in an uni-directional manner and those that are reversible and thus can function as on-off switches for biological activities (Yan et al., 1989).

PTMs expand the functional properties of proteins as they can influence their activity, subcellular distribution, interactions and/or turnover (Wold, 1981).

Many proteins are posttranslationally modified in multiple ways and in some of these cases single PTMs can influence each other. This so-called PTM crosstalk can be of positive or negative nature. While in positive crosstalk one PTM mediates the removal or addition of a

second PTM or structural change, negative crosstalk is defined by competition between PTMs, e.g. SUMOylation and acetylation target the same lysine residue and thus excludes the other (Hunter, 2007). In another example of negative crosstalk one modification prevents binding of an enzyme because it masks the consensus site. Furthermore direct crosstalk between PTMs occurs if a modification affects the activity of a PTM-catalyzing enzyme or the accessibility of this enzyme to its substrate (Hunter, 2007). This complex program of protein regulation is essential for normal development. Thus deregulation of PTM mechanisms are often implicated in diseases including cancer and neurodegeneration (Rodier et al., 2007).

1.1.1 Phosphorylation

Reversible phosphorylation of proteins, catalyzed by protein kinases and protein phosphatases, can regulate protein functions in multiple ways, e.g. modifying the biological activity, stability, subcellular distribution or intra- and intermolecular interactions. About 30 % of cellular proteins are shown to be phosphorylated, which reflects the importance of this PTM in regulation of cellular function (Cohen, 2000). Protein phosphorylation involves the transfer of a phosphate moiety from a donor molecule, in general ATP, to an amino acid residue of the target protein. There are nine amino acids in proteins, which can be phosphorylated (tyrosine, serine, threonine, cysteine, arginine, lysine, aspartate, glutamate and histidine) with serine, threonine and tyrosine being predominantly phosphorylated in eukaryotic cells (Moorhead et al., 2009).

Cyclin-dependent kinases (CDKs) are a protein family of kinases, which are involved in multiple cellular processes, such as cell cycle regulation and gene transcription. As the name indicates the activity of these kinases is dependent on their association with specific cyclin subunits. The human genome encodes 21 CDK genes (CDK1-CDK20, including CDK11A and CDK11B) and five additional genes for CDK-like kinases (CDKL1-5) (Malumbres et al., 2009).

Enzymes that remove phosphate groups from eukaryotic proteins can be grouped into four main classes. These are termed PPPs (phospho-protein phosphatases), PPMs (metallo-dependent protein phosphatases), PTPs (protein tyrosine phosphatases) and aspartate-based phosphatases. In contrast to its name the PTP class is defined by the catalytic signature CX_5R rather than a common substrate preference. The majority of PTPs dephosphorylates phosphotyrosine. In some cases, however, phosphoserine and -threonine are targeted. The

PTP class can be further subdivided into subclass I and class II PTPs with class I containing the classic and dual-specific enzymes (DUSPs) (Moorhead et al., 2009).

There are several cases, in which a crosstalk between phosphorylation and other PTMs is reported, e.g. with ubiquitination. This crosstalk takes place at several levels as phosphorylation can modify the activity of E3 ligases, influence the recognition of a protein by an E3 ligase or influence the accessibility of a protein for an E3 ligase in a temporal-spatial manner by regulating their subcellular distribution (Hunter, 2007).

1.1.2 Acetylation

In vivo lysine acetylation as a PTM was initially described 47 years ago (Allfrey and Mirsky, 1964). To date at least 1750 acetylated proteins have been identified in mammals. Comparative analysis revealed that acetylation sites are significantly higher conserved than phosphorylation sites (Choudhary et al., 2009; Choudhary et al., 2011). Because the first acetylated proteins described were histones, enzymes catalyzing the addition or removal of acetyl groups are often referred to as histone acetyltransferases (HATs) or histone deacetylases (HDACs). As many of these enzymes are subsequently shown to target non-histone targets as well, Allis and colleagues introduced in 2007 a new nomenclature, in which HATs became lysine acetyltransferases (KATs) (Allis et al., 2007). Accordingly HDACs are sometimes referred to as KDACs (lysine deacetylases).

Based on structural and functional similarities, mammalian KDACs can be divided into four major classes. Class I KDACs are similar to yeast Rpd3 and contain HDAC1, -2, -3 and -8 whereas class II KDACs are homologs of yeast Hda1 and include HDAC4, -5, -6, -7, -9 and -10. Sirtuins, which are related to yeast Sir2 are also termed class III KDACs and HDAC11 forms the class IV on its own (Voelter-Mahlknecht et al., 2006).

Beside acetylation, lysine side chains are also targeted by other PTMs, e.g. ubiquitination, SUMOylation or methylation. As these PTMs cannot occur simultaneously on the same lysine, acetylation has the potential for negative cross-regulation (Yang and Seto, 2008).

Furthermore acetylation can crosstalk with phosphorylation. For example it was recently reported that acetylation regulates the subcellular localization of the kinases AKT and PDK1 and thus their substrate-accessibility (Sundaresan et al., 2011).

1.1.3 ADP-ribosylation

ADP-ribosylation, which was first observed by P. Chambon and colleagues in 1963 (Chambon et al., 1963) can be grouped into four major reaction types: mono-ADP-ribosylation, poly-ADP-ribosylation, ADP-ribose cyclization and formation of O-acetyl-ADP-ribose. However, only the first two reactions are involved in posttranslational modification of proteins, while the products of the latter two reaction types are thought to function as second messengers. ADP-ribosylation is carried out by ADP-ribosyltransferases (ARTs) and involves the transfer of an ADP-ribose moiety from NAD^+ to a specific amino acid residue of a substrate, typically a protein. Simultaneously nicotinamide is released. The type of amino acid residue that is mono-ADP-ribosylated depends on the specificity of the distinct mono-ART. Bacterial mono-ARTs are reported to target amino acids including arginine, asparagine, glutamate, aspartate, cysteine, and modified histidine. Non-enzymatic mono-ADP-ribosylation can occur at lysine or cysteine residues. Poly-ADP-ribosylation (PAR) describes the formation of an homopolymer of ADP-ribose molecules, which are linked by glycosidic bonds as the result of an iterative transfer of multiple ADP-ribose units to substrates by ARTs. These polymers can have varying lengths of up to 400 ADP-ribose units. ADP-ribosylation is a reversible process and ADP-ribose is removed from substrates by glycohydrolases that are still ill defined (Hottiger et al., 2010).

There is an interesting link between PARylating enzymes and sirtuins. The majority of sirtuins catalyzes an NAD^+-dependent deacetylase reaction (Smith et al., 2000). Therefore one NAD^+ is cleaved between nicotinamide and ADP-ribose for each acetyl group that is removed from a substrate (Landry et al., 2000). The ADP-ribose moiety is necessary for the deacetylase reaction as it serves as an acceptor for the removed acetyl group and forms a novel *O*-acetyl-ADP-ribose (*O*-AADPr) product (Tanner et al., 2000). In addition selected sirtuins are also reported to catalyze an NAD^+-dependent ADP-ribosyltransfer reaction (Liszt et al., 2005; Ahuja et al., 2007). This tight connection between sirtuin reactions and ADP-ribosylating enzymes provides potential for crosstalk. Thus Zhang et al. suggested in 2003 that the competition for NAD^+ links both reaction types (Zhang, 2003).

1.1.4 Methylation

The transfer of a methyl group to an amino acid residue is termed methylation and the most common substrates are lysines or arginines of histones and non-histone proteins. Methylation

catalyzing enzymes (methyltransferases) use S-adenosyl-L-methionine (SAM) as a methyl donor generating the methylated substrate and S-adenosyl-L-homocysteine as a by-product. Lysine methyltransferases (KMTs) catalyze the transfer of up to three methyl groups to the ε-nitrogen of lysine residues thereby generating mono-, di- or trimethylated residues. They are specified according to a conserved SET domain that facilitates the interaction with the targeted lysine and the binding of SAM, e.g. SET7/9. The SET domain is named after the three *Drosophila* proteins, in which this conserved region was originally identified: SU(VAR)39, Enhancer of zeste,   and Trithorax (Pradhan et al., 2009). KMTs target predominantly lysine residues in N-terminal histone tails thereby contributing to the so-called "histone code". These modifications together with other posttranslational histone modifications are involved in the control of chromatin structure and DNA accessibility for replication, repair, and transcription (Strahl and Allis, 2000). Few non-histone proteins such as the tumor suppressor p53 are also reported to be subject to lysine methylation. On the other hand, many protein arginine methyltransferases (PRMTs) can catalyze methylation of non-histone proteins. In particular, shuttling proteins are a target of arginine methylation. Arginine methylation involves the transfer of one or two methyl groups to the ω-nitrogen of the guanidinium side chain of arginine. The resulting dimethylarginines are either symmetric or asymmetric (Di Lorenzo and Bedford, 2011).

At least lysine methylation is a reversible modification. Thus in 2004 Shi et al. discovered a lysine specific demethylase (KDM) that is able to demethylate mono- and dimethylated lysines. It uses FAD as a co-factor and generates formaldehyde and hydrogen peroxide as by-products (Pradhan et al., 2009).

1.1.5 Ubiquitination

Ubiquitination is an ATP-requiring PTM, in which a small protein (ubiquitin) is covalently bound to a primary amino group on the acceptor protein. In general, ubiquitin is linked either to the ε-amino group of a lysine residue or to the N-terminus of a polypeptide (Ciechanover and Ben-Saadon, 2004). However, it has been reported that ubiquitin can additionally be attached to cysteine, serine and threonine residues in proteins (Hochstrasser, 2009).

Ubiquitin consists of 76 amino acids and has a predicted molecular size of 8.4 kDa. It is sequentially activated and attached to acceptor proteins by a series of enzymes, which are termed according to their functions ubiquitin-activating enzyme (E1), ubiquitin-conjugating enzyme (E2) and ubiquitin-ligating enzyme (E3). Out of these three types of enzymes E3-

ligases determine the substrate specificity of the reaction. There are seven lysine residues in ubiquitin itself (K6, K11, K27, K29, K33, K48 and K63) allowing further conjugation of another ubiquitin to form a polyubiquitin chain. The linkage between ubiquitin-subunits within a chain can be homo- or heterotypic with homo-K48- or homo-K63-linked chains being the most common types (Pickart, 2001).

The attachment of ubiquitin can have different effects on the acceptor protein. Whereas monoubiquitination is reported to alter protein activity or subcellular distribution, polyubiquitin chains can serve as signals for degradation, immune signaling or DNA repair. These modifications are recognized by different types of ubiquitin-binding domains (UBDs) (Dikic et al., 2009).

Ubiquitination is reversible as ubiquitin can be removed from a protein by enzymes known as deubiquitinating enzymes (DUBs) (Amerik and Hochstrasser, 2004). To date two ubiquitin E1 enzymes, and about 50 E2s, 600 E3s, 90 DUBs and 20 types of UBDs have been identified in the human proteome (Bhoj and Chen, 2009).

1.1.6 SUMOylation

SUMOylation shares substantial similarities with ubiquitination as it includes the reversible attachment of small ubiquitin-related modifiers (SUMOs) to internal lysine residues of substrate proteins in a posttranslational manner. SUMOs resemble ubiquitin in their three-dimensional structure but they share only ~18 % amino acid sequence homology. Four human SUMO proteins have been identified so far (SUMO1-4). Similar to ubiquitin they are synthesized as immature preforms, which need to be cleaved at the C-terminus before conjugation to a substrate. The actual mechanism for SUMOylation proceeds in a similar three-step way as ubiquitination with the alteration that E1-E3 enzymes are SUMO-specific (Geiss-Friedlander and Melchior, 2007). SUMOylation occurs at a short consensus sequence ΨKXE, in which Ψ is a large hydrophobic (isoleucine, leucine, or valine) and X any amino acid (Song et al., 2004). In general, SUMOylation results in attachment of a single moiety. However, an unstructured N-terminal extension of SUMO proteins can mediate the formation of polySUMO chains as is regularly observed for ubiquitin. The removal of SUMO modifications is carried out by specific proteases, which are also responsible for the generation of mature SUMO forms by cleaving the preforms. Six proteases have been identified in humans that are responsible for SUMO processing, and which are termed sentrin-specific proteases (SeNP1-3, SeNP5-7). They are homologues of yeast Ulp1 and Ulp2 (Geiss-

Friedlander and Melchior, 2007).

SUMOylation usually positively regulates protein-protein interactions thereby promoting the assembly of multi-protein complexes. Thus it is involved in transcriptional regulation, nuclear transport, maintenance of genome integrity, and signal transduction. The modification can be recognized by so-called SUMO-interaction motifs (SIMs), which consist of a hydrophobic core that is enclosed by up to five acidic amino acids (Johnson, 2004).

Crosstalk of SUMOylation with other PTMs has been observed for phosphorylation, ubiquitination, and acetylation. For example a phosphorylated serine and proline residue following the SUMO-motif can enhance SUMOylation (Hietakangas et al., 2006). Furthermore phosphorylation-dependent SIMs have been reported, which recognize SUMO only after phosphorylation. Negative crosstalk occurs if SUMO and ubiquitin and also acetylation target the same lysine (Desterro et al., 1998). Additionally, crosstalk between ubiquitination and SUMOylation takes place when enzymes of one system are modified by the other system (Prudden et al., 2007). This interplay is also observed for acetylation as for example SIRT1 is SUMOylated and thereby its activity enhanced (Yang et al., 2007).

1.1.7 Posttranslational mitochondrial translocation and proteolytic cleavage

Usually, inner-mitochondrial proteins are synthesized as precursor proteins with N-terminal extensions, which are cleaved off during passage into the mitochondria (Chacinska et al., 2009). These so-called presequences are recognized in the cytoplasm by chaperones, which maintain an "import-competent" conformation of the precursor and prevent its aggregation and degradation. Furthermore the presequences contain a positively charged mitochondrial matrix-targeting signal of up to 60 amino acid residues, which is often followed by an intra-mitochondrial sorting signal. These signals determine whether the mature protein is localized in the mitochondrial matrix, inner-membrane or inter-membrane space (Chacinska et al., 2009). Mitochondrial import of precursor proteins is driven by the TIM/TOM-complex system. Therefore the precursor is translocated across the mitochondrial outer membrane by electrostatic interactions between the positively charged presequence and proteins of the "translocase of the outer membrane" (TOM) complex. Then the precursor is pulled across the inner membrane via the "translocase of the inner membrane" (TIM) complex in an ATP-dependent manner. In the mitochondrial matrix the matrix targeting signal of the presequence is cleaved off by the mitochondrial processing peptidase (MPP) thereby unmasking potential

intra-mitochondrial sorting signals. In most cases MPP-cleavage generates a biologically active protein. However, there are mitochondrial proteins that require an additional cleavage by the mitochondrial intermediate peptidase (MIP) to become fully active. Inter-membrane space proteins often undergo an additional cleavage by the inner membrane peptidase (IMP) during their passage back across the inner membrane (Gakh et al., 2002).

1.2 Sirtuins and their regulation by PTMs

The sirtuin protein family was founded by the yeast silent information regulator 2 (Sir2) (Brachmann et al., 1995). Sir2 is a nicotinamide adenine dinucleotide (NAD$^+$)-dependent histone deacetylase (Imai et al., 2000) and initial findings from genetic studies suggested that Sir2 controls chromatin and gene expression. In particular Sir2 was identified to participate in silencing of homothallic mating (HM) loci and telomeric chromosomal regions and to interfere with rDNA recombination (Braunstein et al., 1993; Gottlieb and Esposito, 1989). These functions have obtained wide interest because they have been linked to lifespan regulation. Indeed overexpression of Sir2 was shown to increase lifespan in yeast (Kaeberlein et al., 1999). Although similar effects were reported for *Drosophila melanogaster* and *Caenorhabditis elegans*, more recent findings suggest that Sir2 does not affect longevity in these organisms (Burnett et al., 2011).

Sir2-like proteins are conserved from prokaryotes to mammals and they all share a common core domain comprising approximately 200-275 amino acid residues. A phylogenetic analysis of the catalytic domain allows subdividing the sirtuin into five classes, i.e. I-IV and U, with the latter only found in gram-positive bacteria (Frye, 2000). Besides the founding member Sir2, the yeast *Saccharomyces cerevisiae* expresses four additional sirtuin genes, whose gene products are termed "homologs of sir two" (Hst1-4). Seven human sirtuins have been identified so far, which can be grouped into four of the phylogenetic classes: SIRT1, SIRT2 and SIRT3 (class I), SIRT4 (class II), SIRT5 (class III) and SIRT6 and SIRT7 (class IV) (Frye, 2000). Of these, SIRT1 share the highest sequence similarities with yeast Sir2 and Hst1, and SIRT2 and SIRT3 with Hst2. SIRT4 to SIRT7 are more closely related to prokaryotic sirtuins or sirtuins of *Drosophila melanogaster* and *Caenorhabditis elegans* (Figure 1).

The mammalian sirtuins are localized in different subcellular compartments. While SIRT1, SIRT6 and SIRT7 are predominantly localized in the nucleus, albeit with different subnuclear distributions, SIRT3, SIRT4 and SIRT5 are mitochondrial. SIRT2 is the only human sirtuin, which is primarily localized in the cytoplasm (Michishita et al., 2005).

The majority of sirtuins catalyzes an NAD$^+$-dependent deacetylase reaction (Smith et al., 2000). Therefore one NAD$^+$ is hydrolyzed for each acetyl group removed from a substrate with the nicotinamide moiety being released (Landry et al., 2000). The acetyl group is transferred to ADP-ribose to form a novel *O*-acetyl-ADP-ribose product (Tanner et al., 2000), which has been suggested to function as a second messenger (Tong and Denu, 2010).

Additionally, distinct sirtuins (SIRT4 and SIRT6) were reported to catalyze the transfer of ADP-ribose from NAD$^+$ to substrate proteins (Ahuja et al., 2007; Liszt et al., 2005), thus providing evidence that some sirtuins may be able to perform two different biochemical reactions.
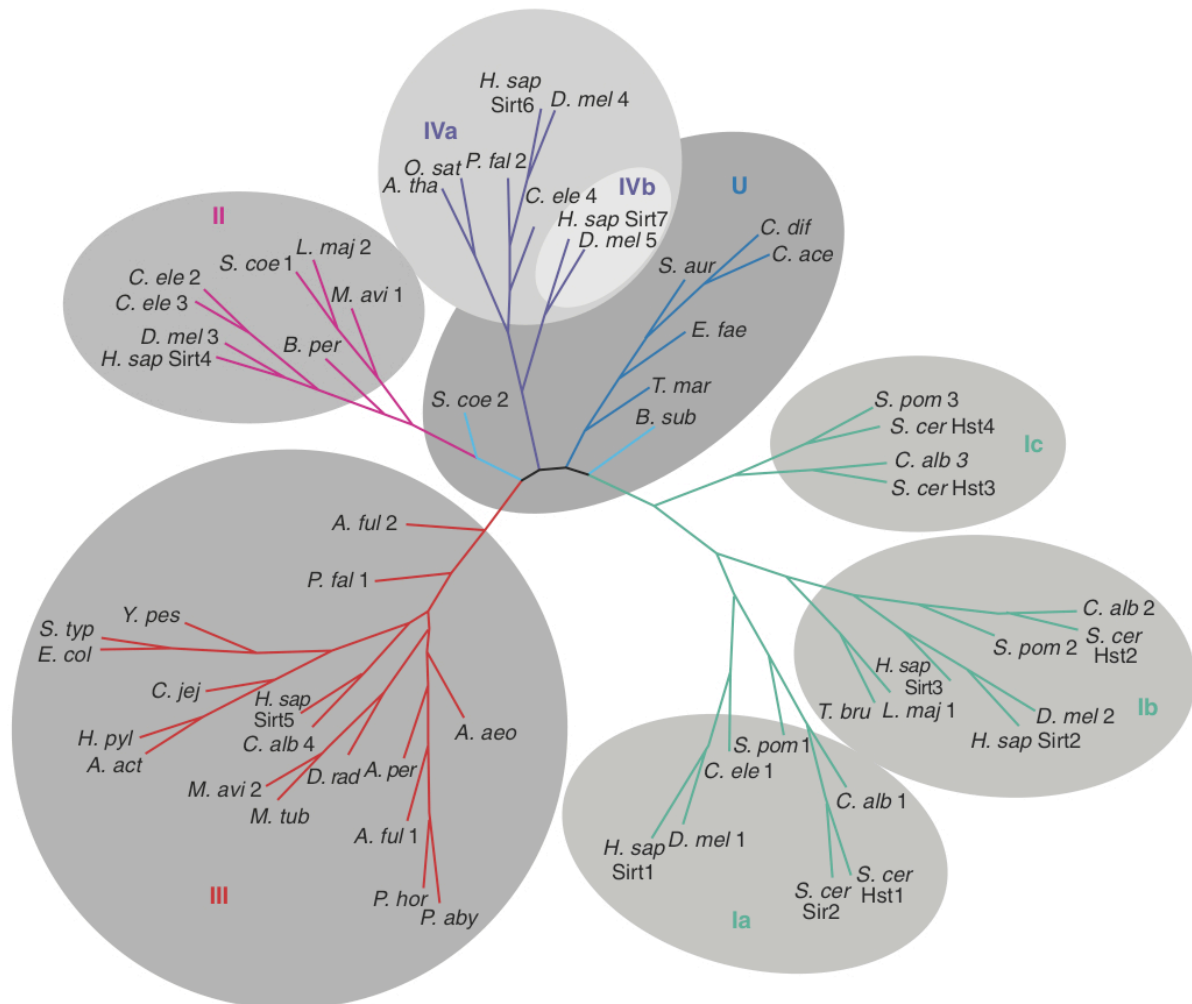
Figure 1: Phylogenetic classification of Sirtuins derived from phylogenetic analysis of the conserved domains of 60 sirtuin sequences. Classes I, II, III, IV, and U and subdivisions of classes I and IV are indicated. Organism abbreviations: *A. act, Actinobacillus actinomycetemcomitans; A. aeo, Aquifex aeolicus; A. ful, Archaeoglobus fulgidus; A. per, Aeropyrum pernix; A. tha, Arabidopsis thaliana; B. per, Bordetella pertussis; B. sub, Bacillus subtilis; C. ace, Clostridium acetabutylicum; C. alb, Candida albicans; C. dif, Clostridium difficile; C. ele, Caenorhabditis elegans; C. jej, Campylobacter jejuni; D. mel, Drosophila melanogaster; D. rad, Deinococcus radiodurans; E. col, Escherichia coli; E. fae, Enterococcus faecalis; H. sap, Homo sapiens; H. pyl, Helicobacter pylori; L. maj, Leishmania major; M. avi, Mycobacterium avium; M. tub, Mycobacterium tuberculosis; O. sat, Oryza sativa; P. aby, Pyrococcus abyssi; P. fal, Plasmodium falciparum; P. hor, Pyrococcus horikoshii; S. aur, Staphylococcus aureus; S. coe, Streptomyces coelicolor; S. pom, Schizosaccharomyces pombe, S. typ, Salmonella typhimurium; S. cer, Saccharomyces cerevisiae; T. bru, Trypanosoma brucei; T. mar, Thermotoga maritima; Y. pes, Yersinia pestis* (North and Verdin, 2004).

The findings summarized above, including the observations on longevity in yeast, the role of NAD$^+$ as cofactor, and the localization of the different sirtuins to distinct subcellular compartments, notably the mitochondria, suggested early on that sirtuins might have

fundamental roles in metabolism. Indeed Sir2 is mediating at least in part the effects elicited by caloric restriction (Lu and Lin, 2010). Of note is also that sirtuins in higher organisms have been suggested to contribute to longevity (Guarente, 2011). Moreover the findings that sirtuins carry out NAD^+-dependent reactions suggest an involvement of these enzymes in mammalian metabolic control and offer the possibility for modulation of their activity by small molecules. The involvement of sirtuins in many physiological processes (see also below) suggests that these enzymes themselves are most likely controlled by different signaling pathways in response to both extracellular and intracellular cues. The use of NAD^+ must be controlled because of its central function in metabolic pathways, suggesting that enzymes that consume NAD^+ will most likely be part of feedback control mechanisms of such pathways. In addition the enzymatic processes of deacetylation and of ADP-ribosylation need to be regulated to adjust for optimal, functionally relevant levels of substrate acetylation and ADP-ribosylation. Despite the many reasons for posttranslational control of sirtuin function, we know relatively little about such mechanisms. The available evidence suggests that the N- and C-terminal extensions relative to the catalytic core domains of the seven mammalian sirtuins are targets of PTMs, while hardly any information is available on how the catalytic domain itself is controlled (Figure 2).
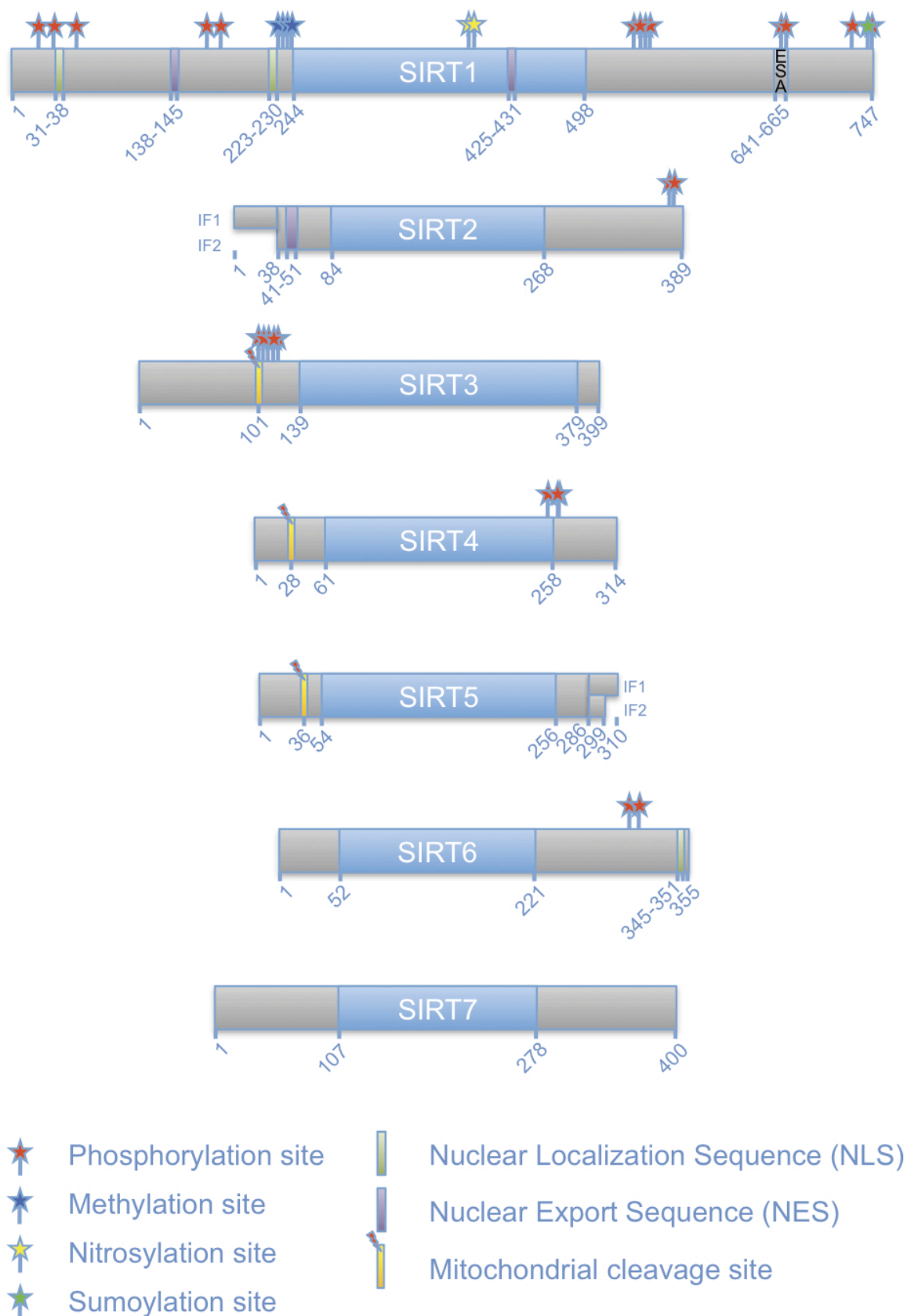
Figure 2: Schematic overview of human sirtuins and their PTMs. The seven mammalian sirtuins are schematically indicated with the blue boxes depicting the sirtuin-typic catalytic core domain. The catalytic domains are flanked by distinct N- and C-terminal extensions (grey boxes). The numbers below indicate amino acid numbers for orientation. Two isoforms (IF) are shown for SIRT2 and SIRT5, respectively. The ESA ("essential for SIRT1 activity") sequence of SIRT1 (see below) is indicated. PTMs, nuclear localization sequences, nuclear export sequences, and proteolytic cleavage sites are indicated.

1.2.1 SIRT1

Among the seven human sirtuins SIRT1 shares the highest sequence homology with yeast Sir2 (Voelter-Mahlknecht and Mahlknecht, 2006). In addition SIRT1, similar to its ancestor Sir2, is localized in the nucleus and involved in chromatin remodeling as it deacetylates several lysine residues of histone tails, including acetylated lysines 9 of histones H3 (H3K9ac), H3K14ac, H4K16ac, and H1K26ac (Vaquero et al., 2004). Moreover SIRT1 targets also non-histone proteins and its activity can be regulated by its ability to shuttle between nuclear and cytoplasmic compartments (Tanno et al., 2007; Hisahara et al., 2008). The increasing number of known SIRT1 substrates includes the transcription factor and tumor suppressor p53 as well as several other transcriptional regulators and cofactors, among them NF-κB, members of the forkhead family (FOXOs), PPAR (peroxisome proliferator-activated receptors) and p300 (Rahman and Islam, 2011). Molecular studies revealed that SIRT1 is involved in the regulation of diverse cellular processes ranging from lipid and glucose metabolism, cancer, aging to stress response. Of particular relevance for many of these processes is the AMP-activated protein kinase (AMPK)-SIRT1 signaling axis. AMPK is activated in response to increasing amounts of AMP and thus functions as an energy sensor that responds to cellular metabolic stress, including calorie restriction. Thereupon it increases the intracellular NAD^+/NADH ratio in a nicotinamide (NAM) phosphoribosyltransferase (NAMPT)-dependent way, promoting the activity of SIRT1 (Fulco et al., 2008). Maybe not surprising then is the finding that *Sirt1* knockout mice display a severe phenotype. These mice are viable but sterile and have a high prenatal or early postnatal death rate. Surviving animals are smaller than their wildtype littermates and exhibit developmental defects, e.g. delayed eyelid opening. Furthermore they are reported to suffer from several dysfunctions of the heart, lung and pancreas (Cheng et al., 2003; McBurney et al., 2003).

With the identification of the tumor suppressor p53 as a SIRT1 substrate, a role of this enzyme in tumor formation was postulated (Vaziri et al., 2001; Luo et al., 2001). Upon deacetylation by SIRT1, the activity of p53 is reduced and thus SIRT1 appears to function as an oncoprotein (Chen et al., 2005; Kim et al., 2007; Yuan et al., 2011). However, there are also reports that describe SIRT1 as a tumor suppressor (Yi and Luo, 2010). These alternative activities are possibly the result of cell-type specific effects and/or a consequence of distinct regulation of SIRT1 that might differentially affect the activities of substrates.

SIRT1 is ubiquitously expressed with highest mRNA levels measured in the brain, skeletal muscle, kidney and thymus (Michishita et al., 2005).

Despite being the best studied human sirtuin relatively little is known about mechanisms that regulate SIRT1 itself. The 747 amino acids long protein is by far the largest human sirtuin, due to its extensive N- and C-terminal sequences (Figure 2). SIRT1 has a predicted molecular size of 81.7 kDa and the conserved catalytic domain is found between amino acid residues 244 and 498 (Voelter-Mahlknecht and Mahlknecht, 2006). The N-terminal extension of SIRT1 contains two functional nuclear localization signals (NLS) between amino acid residues 31-38 and 223-230. These are counteracted by two nuclear export signals (NES) between amino acid residues 138-145 and 425-431. Both types of signal sequences are responsible for the nucleo-cytoplasmic shuttling of SIRT1 (Tanno et al., 2007), which determines at least in part the enzyme's ability to interact with distinct substrates (Hisahara et al., 2008). Furthermore the nuclear-cytoplasmic distribution of SIRT1 is regulated by signals, for example during differentiation (Tanno et al., 2007). While SIRT1 is nuclear in proliferating C2C12 myoblasts, it is cytoplasmic in differentiated cells. Moreover inhibition of PI3K prevents the nuclear localization of SIRT1 in proliferating cells, suggesting that PI3K-dependent signaling controls the shuttling. Whether the PI3K signaling cascade targets directly SIRT1 or some accessory factor or factors is not known. One kinase that might be involved in this process is JNK, although this kinase is not typically activated downstream of PI3K. JNK interacts with SIRT1 upon oxidative stress, phosphorylates SIRT1 at S27, S47, and T530, thereby enhancing its nuclear localization (Nasrin et al., 2009). Furthermore these phosphorylations increase the enzymatic activity of SIRT1 in a substrate-specific manner with histone H3, but not p53, becoming a better substrate. In contrast to the findings with JNK, mTOR-dependent phosphorylation of S47 alone results in inhibition of SIRT1 deacetylase activity (Back et al., 2011). Thus combinatorial effects of different phosphorylations appear to control SIRT1 function.

Using a mass spectrometry approach, 13 phosphorylation sites were identified in SIRT1 (Sasaki et al., 2008a). Seven of these sites are located in the N-terminal region, including S27 and S47, and six in the C-terminal region, including T530 (Figure 2). Two of the identified sites, T530 and S540, are potential substrates of cyclin B/cyclin-dependent kinase 1 (CDK) complexes. The functional analysis suggests that these two phosphorylation sites are required for normal cell cycle progression. For example, while wildtype SIRT1 rescues the growth defect of cells lacking endogenous SIRT1, a mutant, in which T530 and S540 are substituted by alanines, is unable to rescue the knockout cells (Sasaki et al., 2008a).

In addition to the sites mentioned above, two protein kinase CK2 phosphorylation sites have

been identified at S659 and S661 in the C-terminal extension (Zschoernig and Mahlknecht, 2009). Although it is not fully clear if these sites are also used in cells because they were not identified in the mass spectrometry approach described above and no site-specific antibodies have been reported, these phosphorylation sites are potentially of considerable functional relevance. They lie within a domain of SIRT1 that is referred to as the ESA (for essential for SIRT1 activity) (Figure 3), which spans a small region from amino acids 641 to 665 in human SIRT1 (Kang et al., 2011). The ESA interacts with the catalytic domain, activates the catalytic activity, and increases the affinity for substrates. Moreover the binding site for ESA in the catalytic domain is also the interaction site of DBC1, an endogenous SIRT1 inhibitor (Kim et al., 2008). The two postulated CK2 phosphorylation sites flank one of the two identified key residues within ESA that are important to control catalytic activity (Figure 3). Thus it is well possible that these phosphorylation sites modulate the interaction of the C-terminal region with the catalytic domain, thereby regulating SIRT1 activity and substrate recognition and possibly the interaction with DBC1. Thus the control of SIRT1 function by its own C-terminal domain and the regulation of this interaction by CK2, although molecularly not fully explored yet, may represent an important regulatory mechanism (Figure 3).

Besides phosphorylation, SIRT1 is modified by additional PTMs, including sumoylation. SUMO, a small ubiquitin-related modifier, can be attached *in vitro* close to the C-terminal end of SIRT1 at lysine 734 (K734), which lies within a sumoylation consensus sequence (ΨKXE). This modification increases catalytic activity as measured by p53 deacetylation (Yang et al., 2007). Upon stress SIRT1 associates with the nuclear desumoylase SENP1, which reduces the catalytic activity of SIRT1 and consequently allows efficient activation of p53. How modification by SUMO stimulates the catalytic activity of SIRT1 is not known. However, the recent findings that the C-terminal region is key to enhance SIRT1 activity suggests that sumoylation may participate in this regulation. A possibility is that sumoylation enhances the interaction of the ESA motif with the catalytic domain or modifies CK2 phosphorylation (Figure 3). Thus it appears that sumoylation of SIRT1 is relevant for stress control in cells.
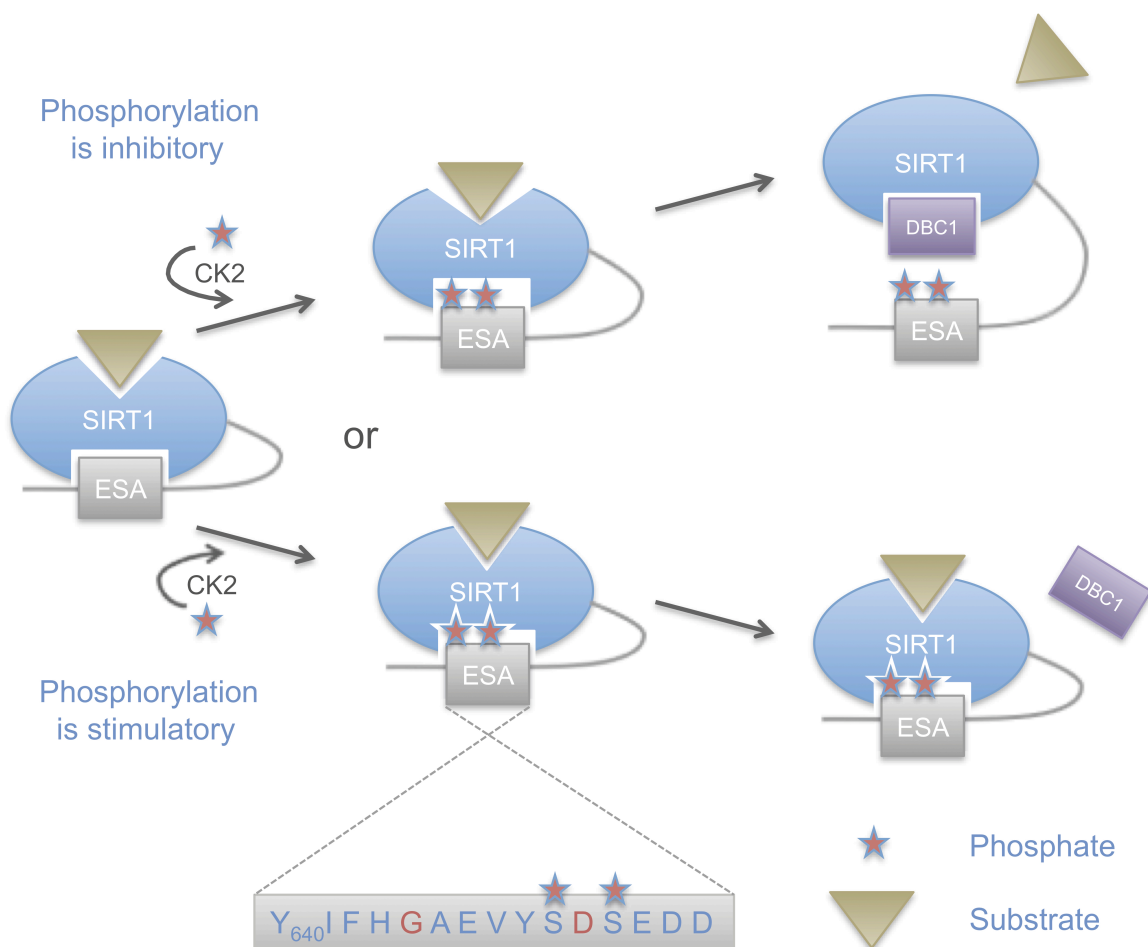
Figure 3: Control of SIRT2 catalytic activity by the ESA motif and hypothetical regulation by phosphorylation. The CK2 phosphorylation sites lie within the ESA ("Essential for SIRT1 activity") sequence motif found in the C-terminal extension of SIRT1. The two phosphorylation sites flank one of the two key residues of the ESA motif. CK2-mediated phosphorylation might either enhance the interaction of ESA with the catalytic core thereby increasing SIRT1 affinity for substrates or weaken the interaction. The latter scenario would allow DBC1 to bind SIRT1 more efficiently and thus interfere with SIRT1 activity.

Furthermore, SIRT1 is also targeted by methylation. The methyltransferase Set7/9 interacts with and methylates SIRT1 at K233, K235, K236, and K238 of the N-terminal extension. Although it is unclear whether methylation affects directly SIRT1 deacetylase activity, the interaction of Set7/9 with SIRT1 disrupts the binding of SIRT1 with p53. Consequently p53 acetylation and transactivating activity is enhanced (Liu et al., 2011). Despite the lack of information about direct consequences of lysine methylation, it is worth remembering that lysines can be modified by multiple PTMs and thus methylation may compete with acetylation and ubiquitination (Yang and Seto, 2008).

Recently it was reported that nuclear SIRT1 is transnitrosylated by nitrosylated GAPDH (Kornberg et al., 2010). As a consequence acetylation of PGC1α, a SIRT1 substrate, increases

in cells, suggesting that SIRT1 deacetylation activity is inhibited by nitrosylation. Mutational analysis implies that two cysteines, C387 and C390, within the catalytic core of SIRT1 are targeted by nitrosylation. These cysteines are of special interest because they participate in the coordination of a structurally relevant Zn^{2+} ion and nitrosylation might result in protein misfolding (Kornberg et al., 2010). It will be of interest to define whether nitrosylation is a general regulatory mechanism of sirtuins.

Similar to yeast Hst2, purified endogenous SIRT1 can exist as a homotrimer (Zhao et al., 2003; Vaquero et al., 2004). Because SIRT2 was also purified as a homotrimer (Vaquero et al., 2006), this structural organization may be characteristic for sirtuins. Structural analysis of the Hst2 trimer suggests that the N-terminal region is involved in trimer formation. Whether this is also true for SIRT1 and SIRT2 remains to be determined. Because of the many PTMs that have been mapped in the N-terminal extension of SIRT1, it is well possible that trimer formation is regulated by signaling, an aspect that needs further exploration.

1.2.2 SIRT2

SIRT2 is the only sirtuin that is predominantly localized in the cytoplasm (Afshar and Murnane, 1999). There, it colocalizes at least in part with the microtubule network. Consistent with this finding is that K40 of α-tubulin is a SIRT2 substrate (North et al., 2003). Moreover, SIRT2 can also translocate into the nucleus and a predominant nuclear or chromatin-associated SIRT2 localization is detected during G2/M transition and in mitosis of the cell cycle in chemically synchronized cells (Vaquero et al., 2006; North and Verdin, 2007a). Nuclear substrates of SIRT2 include H4K16ac and H3K56ac, modifications that are implicated in DNA damage response and cancer (Vaquero et al., 2006; Vempati et al., 2010).

Human *SIRT2* is ubiquitously expressed in at least two isoforms. The longer SIRT2 isoform 1 consists of 389 amino acids and has a predicted molecular size of 43.2 kDa, whereas SIRT2 isoform 2 lacks the first 37 N-terminal amino acids of isoform 1 and spans a total length of 352 amino acids with a predicted molecular size of 39.5 kDa (Figure 2). The catalytic domain of SIRT2 isoform 1 and 2 is found between amino acids 84-268 and 47-231, respectively (Voelter-Mahlknecht et al., 2005). Highest SIRT2 mRNA levels were measured in human brain, heart and skeletal muscle tissues (Afshar and Murnane, 1999; Michishita et al., 2005; Voelter-Mahlknecht et al., 2005). Particularly high SIRT2 protein level in the brain are found in myelin-forming oligodendrocytes (OLs) (Li et al., 2007; Southwood et al., 2007). There, SIRT2 level increase after birth and peak at adulthood, thereby correlating with expression

profiles of the OL differentiation markers CNPase (2′,3′-cyclic nucleotide 3′-phosphodiesterase) and MBP (myelin basic protein) (Li et al., 2007; Werner et al., 2007; Ji et al., 2011). In mature OLs SIRT2 abundantly resides in the myelin sheath surrounding the axon (Southwood et al., 2007). However, its physiological function in these postmitotic cellular structures remains to be elucidated. Interestingly only the shorter isoform 2 is present in the myelin-enriched fraction of adult mouse brain or in the cytoplasm of murine cerebellar granule cells (Suzuki and Koike, 2007; Werner et al., 2007), suggesting that the N-terminal region is involved in controlling the subcytoplasmic localization.

Luthi-Carter et al. demonstrated recently that SIRT2 positively regulates the transcription factor SREBP-2 (sterol response element binding protein 2) thereby promoting cholesterol biosynthesis in neurons (Luthi-Carter et al., 2010). Cholesterol influences membrane thickness and fluidity and is essential for myelin membrane growth (Saher et al., 2005). In contrast, cholesterol is also reported to have a detrimental effect in neurons and presents a risk factor in neurodegenerative diseases like Alzheimer's (AD) and Parkinson's diseases (PD) (Stefani and Liguri, 2009; Huang et al., 2011). Consistently, Luthi-Carter et al. reported in 2010 that SIRT2 inhibition reduces toxicity of mutant huntingtin by decreasing sterol biosynthesis (Luthi-Carter et al., 2010). Furthermore, *SIRT2* knockdown or SIRT2 inhibition decreases α-synuclein toxicity, which is a hallmark of the neurodegenerative PD (Outeiro et al., 2007).

Besides SREBP-2, SIRT2 is also involved in the regulation of other transcription factors like NF-κB (Rothgiesser et al., 2010), FOXO1 (Jing et al., 2007; Zhao et al., 2010b), and FOXO3 (Wang et al., 2007; Wang and Tong, 2009), thereby providing potential for regulation of multiple cellular processes, e.g. inflammation, autophagy and stress response.

The predominant cytoplasmic localization of SIRT2 is dictated by an NES in its N-terminal extension (amino acids 41-51 and 4-14 of the long and short protein variants, respectively) (Wilson et al., 2006; North and Verdin, 2007a). However, it is unclear how SIRT2 translocates into the nucleus, because the protein lacks any obvious NLS and it also remains to be defined how the cell cycle-dependent nuclear localization is regulated. One possibility is that signals in late G2 control the activity of the NES. Indeed in chemically synchronized cells SIRT2 is hyperphosphorylated during the G2/M transition and in M phase, which is paralleled by a mobility shift in SDS-PAGE (Dryden et al., 2003; North and Verdin, 2007b). This correlates with the nuclear translocation of SIRT2 and suggests a regulatory role for Cyclin B/CDK1 and other mitose-specific kinases (Morgan, 2008). But alternative mechanisms may also be in

place, such as stimulation of nuclear uptake and/or tight interaction with nuclear structures in late G2 or mitosis.

To date two putative phosphorylation sites have been identified in SIRT2 (Figure 2). They are located in the C-terminal extension in close proximity to each other at S368/331 and S372/335 (numbering according to the two SIRT2 isoforms). The phosphorylation of each site results in a mobility shift of the protein in SDS-PAGE, which results in a characteristic triple band pattern (Nahhas et al., 2007; Pandithage et al., 2008). S368/331 is part of a cyclin-dependent kinase (CDK) consensus motif and has been demonstrated to be a substrate of Cyclin B/CDK1, Cyclin E/CDK2, Cyclin A/CDK2, Cyclin D3/CDK4 and p35/CDK5 (North and Verdin, 2007b; Pandithage et al., 2008). Consistent with these *in vitro* studies is the finding that S368/331 is phosphorylated when cells enter S phase, suggesting that this phosphorylation is not the signal for nuclear accumulation of SIRT2, which begins in late G2 (Pandithage et al., 2008). Phosphorylation of SIRT2 at S368/331 reduces its enzymatic activity as measured by deacetylation of core histones and α-tubulin (Pandithage et al., 2008). Moreover SIRT2 interferes with neurite outgrowth in primary neurons, correlating with α-tubulin deacetylation, a process that is antagonized by phosphorylating S368/331 providing evidence that the C-terminal extension of SIRT2 controls activity in cells (Pandithage et al., 2008). So far, nothing is known about a kinase responsible for phosphorylation of S372/335 or about its influence on SIRT2 functions.

Additionally SIRT2 is acetylated by the KAT p300. This acetylation, although the site of modification has not been mapped, interferes with the catalytic activity of SIRT2 (Han et al., 2008). Predictions of acetylation sites indicate that the C-terminal extension provides multiple target lysine residues (Li et al., 2006), further supporting the concept that the N- and C-terminal regions are particularly relevant to control catalytic activities of sirtuins.

Finally, SIRT2 was purified as a homotrimer out of cell extracts similar to SIRT1 and Hst1 (see above) (Vaquero et al., 2006). It is not known how trimer formation is regulated and what the consequences are for SIRT2 function.

1.2.3 SIRT3

Three sirtuins are located in mitochondria. Of these *SIRT3* is the best studied. It is broadly expressed including brown but not white adipose tissue (Shi et al., 2005). Indeed, SIRT3 is required for PGC-1α-mediated differentiation of brown adipose tissue in an estrogen-related receptor α (ERRα)-dependent manner (Giralt et al., 2011; Kong et al., 2010). The

transcriptional coactivator PGC-1α (peroxisome proliferator-activated receptor gamma coactivator 1 alpha) regulates genes involved in energy metabolism, suggesting that SIRT3 participates in this process (Shi et al., 2005). Moreover, SIRT3 regulates the cellular response to oxidative stress and calorie restriction. Thus, upon cellular stress, e.g. increase in reactive oxygen species or nutrient deprivation, human *SIRT3* transcription is stimulated (Shi et al., 2005; Chen et al., 2011), and the protein translocates to the mitochondrial inner membrane (IMS) (Scher et al., 2007; Michishita et al., 2005), where it becomes activated by proteolytic cleavage (Schwer et al., 2002). SIRT3 deacetylates and thereby activates the enzymes isocitrate dehydrogenase 2 (Idh2) and superoxide dismutase 2 (SOD2), which are involved in reducing cellular oxidants, including oxidized glutathione (GSSG) and reactive oxygen species (ROS) (Schlicker et al., 2008; Someya et al., 2010; Qiu et al., 2010; Chen et al., 2011). In addition, SIRT3 promotes alternative energy providing pathways by deacetylating and thereby activating central enzymes, which are involved in fatty acid oxidation (*3-Hydroxy-3-methylglutaryl-CoA synthase*/HMGCS2, *Long-chain acyl-CoA dehydrogenase*/LCAD, *Acetyl-CoA synthetase 2*/AceCS2) or the urea cycle *(Ornithine transcarbamoylase*/OTC) (Hallows et al., 2006; Hirschey et al., 2010; Shimazu et al., 2010; Hallows et al., 2011).

Recently, it has been discovered that SIRT3 acts as a tumor suppressor, as SIRT3-deficiency is sufficient to transform mouse embryonic fibroblasts (MEFs) with Myc or RAS alone to form tumors in xenograft models (Kim et al., 2010). This transformation is closely linked to an elevation in ROS level, which in turn increases the stability and activity of the transcription factor hypoxia inducible factor 1α (HIF-1α). HIF-1α target genes are involved in glucose metabolism, angiogenesis, and metastasis (Finley et al., 2011; Bell et al., 2011).

Human SIRT3 is synthesized as a latent inactive preform of 399 amino acids and a predicted molecular size of 43.7 kDa. The conserved domain, which is characteristic for all sirtuins, stretches from amino acids 139-379. The N-terminal extension contains a mitochondrial targeting signal peptide within the first 25 amino acids, which is responsible for the characteristic subcellular distribution of the protein. During import of SIRT3 into the mitochondrial matrix, the preform is proteolytically cleaved at position 101 and thus enzymatically activated (Schwer et al., 2002) (Figure 2). It has been postulated that the proteolytically shortened N-terminal region and the C-terminal extension form a module that might regulate the access of substrate proteins to the active site (Schlicker et al., 2008).

Presently we know very little about the regulation of SIRT3 function. The biological

significance, as summarized briefly above, would suggest strongly that SIRT3 is regulated by signaling. Indeed, six phosphorylated serine residues (out of a total of eight possible sites) between positions 101 and 118 have been identified in a high-resolution mass spectrometry-based phosphoproteome analysis (Olsen et al., 2010). But their biological relevance or influence on SIRT3 function has not been analyzed yet. These phosphorylation sites are close to the mitochondrial cleavage site in the N-terminal extension (Figure 2). Therefore it is possible that phosphorylation modulates the enzymatic activity of SIRT3 in mitochondria either by regulating the proteolytic cleavage, by influencing the interaction between the N- and C-terminal extension, or by regulating the interaction of the N-terminal region with the catalytic domain.

1.2.4 SIRT4

SIRT4 is an additional mitochondrial sirtuin (Michishita et al., 2005; Haigis et al., 2006). It resides as a soluble protein in the mitochondrial matrix (Ahuja et al., 2007; Nakamura et al., 2008). Similar to the other sirtuins, *SIRT4* is ubiquitously expressed (Michishita et al., 2005; Haigis et al., 2006; Ahuja et al., 2007).

Sirt4 knockout mice are viable, fertile and did not display apparent phenotypic abnormalities. However, these mice exhibit increased insulin levels when compared with wildtype littermates (Haigis et al., 2006). This anomaly points to a function of SIRT4 in the insulin producing β-cells of the pancreatic islets. Indeed, SIRT4 negatively regulates glutamate dehydrogenase (GDH) via ADP-ribosylation. GDH is a mitochondrial enzyme, which catalyzes the conversion of glutamate into α-ketoglutarate in the tricarboxylic acid (TCA) cycle and induces insulin secretion (Haigis et al., 2006). A second possible explanation for the increased insulin levels measured in Sirt4-deficient mice is that IDE (insulin-degrading enzyme) interacts with SIRT4 (Ahuja et al., 2007). IDE regulates insulin levels and SIRT4 appears to be a negative regulator of this enzyme. Whether this occurs through direct interaction or by ADP-ribosylation has not been determined. It is worth pointing out that so far no deacetylase activity of SIRT4 has been identified. It remains to be determined whether this enzyme is indeed deficient of deacetylase activity or whether this is a reflection of the lack of appropriate substrates.

In addition to a function in pancreatic β-cells, SIRT4 is implicated in fatty acid oxidation (FAO) in liver cells. A *Sirt4* knockdown in primary murine hepatocytes elevates FAO in a transcriptional manner. The negative regulation of FAO gene transcription by SIRT4 is

mediated by SIRT1, as an additional knockdown of this sirtuin prevents the effect (Nasrin et al., 2010). This implies that sirtuins crosstalk with each other.

SIRT4 is expressed as a 314 amino acid long preform with a predicted molecular size of 35.2 kDa. Analogous to the murine SIRT4 protein sequence the highly conserved sirtuin-typic core domain spreads from amino acids 61 to 258 in the human ortholog (Mahlknecht and Voelter-Mahlknecht, 2009). The N-terminal extension protruding the conserved domain contains a mitochondrial targeting signal peptide within the first ten amino acids. Similar to SIRT3, SIRT4 is proteolytically cleaved within the N-terminal extension upon entry into the mitochondrial matrix resulting in a 28 amino acids shortened protein (Ahuja et al., 2007) (Figure 2). It is not known whether the proteolytic cleavage of SIRT4 influences its enzymatic activity, as was reported for SIRT3 (Schwer et al., 2002).

Three phosphorylation sites have been identified in SIRT4 at S255, S261 and S262 in an proteomic approach using a phosphopeptide enrichment procedure in combination with data-dependent neutral loss nano-RPLC-MS2-MS3 analysis (Yu et al., 2007). These findings were not further developed to address the biological relevance or influence of these PTMs on SIRT4 function.

1.2.5 SIRT5

SIRT5, the third mitochondrial sirtuin, is ubiquitously expressed (Michishita et al., 2005; Nakagawa et al., 2009). Very little is known about SIRT5 function. *Sirt5* knockout mice develop inconspicuously until at least 18 months of age (Lombard et al., 2007). However, they exhibit significantly elevated blood ammonia levels compared to wildtype animals after calorie restriction or fasting, which are presumably caused by a deregulated urea cycle. In this support SIRT5 can deacetylate and activate the carbamoyl phosphate synthetase 1 (CPS1), an mitochondrial enzyme of the urea cycle (Nakagawa et al., 2009). It was suggested that elevated mitochondrial NAD$^+$ levels during starvation activate SIRT5 and in turn CPS1 is activates and initiates the detoxification of excess ammonia under physiological conditions (Nakagawa et al., 2009). In addition to its deacetylase activity SIRT5 was very recently reported to elicit also NAD$^+$-dependent demalonylase and desuccinylase activities (Jintang Du, 2011). In line with thess observations CPS1 succinylation at K1291 is strongly increased in *Sirt5* knockout mice compared to wildtype littermates. Furthermore Schlicker et al. demonstrated in 2008 that SIRT5 can *in vitro* deacetylate the mitochondrial intermembrane space (IMS) protein cytochrome c, which is involved in oxidative metabolism and apoptosis

(Schlicker et al., 2008). Up to now, the functional relevance of this observation has not been clarified.

SIRT5 is expressed in two distinct transcriptional variants due to alternative splicing, encoding proteins with distinct C-terminal regions (Figure 2). The longer transcriptional variant one is translated into a 310 amino acid protein with a predicted molecular size of 33.9 kDa. The alternative transcriptional variant two is translated into a shorter protein of 299 amino acids with a predicted molecular size of 32.7 kDa. The highly conserved core domain spreads from amino acids 54 to 256 in both isoforms (Mahlknecht et al., 2006a). Both isoforms can be cleaved after the first 36 amino acids at a consensus sequence for the mitochondrial processing peptidase (MPP) upon entry into the mitochondrial matrix (Michishita et al., 2005). Similar to SIRT4 no data are available about a relationship between the N-terminal truncation of SIRT5 and its enzymatic activity (Schwer et al., 2002).

Both cleaved SIRT5 isoforms display a mitochondrial localization. There SIRT5 can enter the IMS and the mitochondrial matrix (Schlicker et al., 2008). In contrast to the cleaved isoform 2 (IF2, derived from the shorter splice variant), which seems to reside exclusively in the mitochondria, cleaved IF1 is found additionally in the cytoplasm. It appears that the different C-termini of the two SIRT5 isoforms are responsible for their distinct subcellular distribution. The C-terminal extension of IF2 is rich in hydrophobic amino acids and functions as a mitochondrial membrane insertion signal (Matsushita et al., 2011). Presently no post-translational modifications of SIRT5 are described besides the proteolytic cleavage and thus nothing is known about the role of this protein in signaling processes.

1.2.6 SIRT6

SIRT6 is expressed in most tissues (Liszt et al., 2005; Mostoslavsky et al., 2006). It is, similar to SIRT1 and SIRT7, predominantly localized in the nucleus (Michishita et al., 2005; Liszt et al., 2005), where it associates with the chromatin (Mostoslavsky et al., 2006). A nuclear localization signal was discovered between amino acids 345 and 351 in the distal region of the C-terminal extension of SIRT6 (Figure 2). This signal is necessary and sufficient for proper nuclear localization of the protein (Tennen et al., 2010). In comparison to other sirtuin knockout mice, *Sirt6*-deficient mice display a severe phenotype. Despite normal development for several weeks after birth, these mice die at about one month of age due to degenerative processes of multiple organs. These processes include loss of subcutaneous fat and metabolic defects displayed by dramatic drops of serum glucose and insulin-like growth factor 1 (IGF1)

levels. Additional symptoms are lordokyphosis, colitis, and severe lymphopenia (Mostoslavsky et al., 2006). One suggestion is that this phenotype is the consequence of a loss of Sirt6-mediated inhibition of NF-κB target gene expression (Kawahara et al., 2009; Kawahara et al., 2011). The absence of SIRT6-dependent repression of HIF1α might also account for the phenotype (Zhong et al., 2010). Under physiologic conditions SIRT6 interacts with these transcription factors and is transported to their target gene promoters where it deacetylates H3K9ac or H3K56ac. (Michishita et al., 2008; Kawahara et al., 2009; Yang et al., 2009). In both cases, the binding of the respective transcription factor to its target gene promoters is enhanced in *Sirt6*-deficient cells due to locally elevated acetylation levels of H3K9. Further investigations revealed that upon TNF-α signaling, SIRT6 binds up to 5050 gene promoters, which are highly enriched for NF-κB, SP1, STAT1/3, ELK1, E2F1, and FOXO1/4 binding motifs (Kawahara et al., 2011). Thus SIRT6 appears to have widespread activities as a regulator of transcription, in particular of genes whose products are involved in glucose and lipid metabolisms.

Moreover SIRT6 seems to be involved in DNA repair and thus in the maintenance of genomic integrity. Indeed MEFs derived from *Sirt6*-deficient mice are more sensitive to irradiation and display multiple chromosomal aberrations, i.e. fragmentations, detached centromeres and translocations (Mostoslavsky et al., 2006). In addition SIRT6 associates with chromatin in response to DNA damage and stabilizes the DNA-dependent protein kinase (DNA-PK) at DNA double-strand breaks (DSBs) (McCord et al., 2009). SIRT6 also deacetylates CtIP [C-terminal binding protein (CtBP) interacting protein] in response to DNA damage, which promotes the ability of CtIP to mediate DSB repair by homologous recombination (Kaidi et al., 2010). Finally SIRT6 is required for telomere maintenance (Tennen and Chua, 2011). Together these findings provide strong evidence for a role of SIRT6 in controlling genomic stability.

SIRT6 is expressed as a 355 amino acids long protein with a predicted molecular size of 39.1 kDa. The sirtuin-typic core domain, which spreads from amino acids 52 to 221 (Mahlknecht et al., 2006b), is not sufficient to deacetylate H3K9ac or H3K56ac (Tennen et al., 2010). For SIRT6 the available evidence suggests that the N-terminal region is essential for deacetylase activity as a SIRT6 mutant that lacks the N-terminal regions fails to deacetylate H3K9ac or H3K56ac. This is reminiscent of the findings with other sirtuins, which require either N- or C-terminal regions to activate catalytic function as described above.

In addition to its deacetylase activity, SIRT6 has been reported to mono-ADP-ribosylate substrates. One substrate identified is PARP1/ARTD1, which is activated by SIRT6 (Mao et al., 2011). This provides an additional link to genomic stability because ARTD1 is a DNA damage sensor and upon activation synthesizes ADP-ribose polymers that are docking sites for repair enzymes (Kleine and Luscher, 2009). SIRT6 can also auto-ADP-ribosylate but the site of modification and the functional relevance are unclear (Liszt et al., 2005). It remains to be elucidated whether the N-terminal extension is essential for the ADP-ribosylation activity of SIRT6 as it is for the deacetylase activity. Of note is that besides ADP-ribosylation, two C-terminal phosphorylation sites at Y294 and SS303 have been discovered in a proteomic approach (Dephoure et al., 2008) (Figure 2). It remains to be seen whether these phosphorylations influence SIRT6 function.

1.2.7 SIRT7

Of the seven human sirtuins, SIRT7 is the least studied. It is a nuclear protein that is concentrated in the nucleoli (Michishita et al., 2005) where it interacts with components of the rDNA transcription machinery, like the RNA polymerase I (Pol I) and the rDNA transcription factor UBF. SIRT7 positively regulates rDNA transcription (Ford et al., 2006; Grob et al., 2009). Knockdown of SIRT7 in human cancer cell lines blocks cell proliferation and causes apoptosis. This drastic effect implies that SIRT7 is required for cancer cell viability (Ford et al., 2006). Further evidence supporting this hypothesis is provided by enhanced *SIRT7* expression levels in breast carcinoma biopsies compared to normal, 'nonmalignant' tissue (Ashraf et al., 2006). The tumor suppressor factor p53 is a substrate of SIRT7 and thus this sirtuin appears to interfere with p53 function, similar to SIRT1 (Vakhrusheva et al., 2008b). *Sirt7*-knockout mice are viable but suffer from progressive heart hypertrophy, accompanied by inflammation and decreased stress resistance, possibly a consequence of altered p53 activity (Vakhrusheva et al., 2008b; Vakhrusheva et al., 2008a).

SIRT7 is expressed as a 400 amino acids long protein with a predicted molecular size of 44.9 kDa. The highly conserved core domain spreads from amino acids 107 to 278 (Voelter-Mahlknecht et al., 2006). Little is known about regulatory mechanisms of the catalytic activity of SIRT7. Thus despite the fact that SIRT7 resides in the nucleus, no corresponding localization signals have been described so far. However, indirect evidence suggests that SIRT7 is phosphorylated during mitosis by a CDK complex, but no sites have been mapped nor functional consequences defined (Grob et al., 2009).

1.3 Cyclin-dependent Kinase 5 (CDK5)

CDK5 is a proline-directed serine/threonine kinase and belongs to the protein family of cyclin-dependent kinases (CDKs). It was discovered in 1992 by Lew and colleagues who purified the kinase from bovine brain extracts (Lew et al., 1992). In contrast to the initially identified CDKs that are regulators of the cell cycle, CDK5 is not regulated by cell cycle-dependent cyclins and seems not to play a role in the control of cell cycle. CDK5 associates with its regulatory subunits p35 or p39, which determine its activity, substrate specificity and subcellular localization. Both activators carry an N-terminal myristoylation motif, which anchors them at the plasma membrane and the cytoskeleton of the cell periphery. The association with peripheral membranes is disrupted by calpain-mediated cleavage of p35/p39 at the N-terminus. The resulting truncated forms p25/p29 are also able to activate CDK5 but they alter its target phosphorylation and subcellular distribution, because they are no longer myristylated (Patrick et al., 1999). An alternative mechanism to activate CDK5 is phosphorylation. C-Abelson (c-Abl) and Fyn are two kinases, which are reported to phosphorylate CDK5 at tyrosine 15 (Y15) and thereby activate kinase activity (Zukerberg et al., 2000; Sasaki et al., 2002).

Cdk5 knockout mice die around birth due to severe abnormal brain organization, which is explained by neuronal migration defects (Ohshima et al., 1999). In addition, mice lacking p35 display similar but attenuated defects of the central nervous system (Chae et al., 1997). These observations promoted the assumption that CDK5 as well as its activators p35/p39 are neuron specific. Indeed, CDK5 is involved in several neuronal processes including neuronal migration, axon guidance and synaptic transmission. In this context the best studied CDK5 substrates are the microtubule-associated protein Tau and the focal adhesion kinase (FAK). Consistently, deregulation of CDK5 is part of several pathologic disorders, e.g. AD, PD, and amyotrophic lateral sclerosis. In this regard, CDK5 deregulation is often caused by neurotoxin-induced cleavage of p35 to p25 (Liebl et al., 2011).

An increasing number of publications provide evidence that CDK5 also plays a role in non-neuronal tissues, including skeletal muscle, pancreas, leukocytes, glia cells and germ cells. CDK5 is involved in differentiation of oligodendrocytes, myocytes and monocytes. Furthermore CDK5 promotes secretion, not only in neuronal synapsis, but also of insulin in pancreatic β-cells. Consistent with the involvement of CDK5 in neuronal migration and cell adhesion, CDK5 also promotes adhesion in keratinocytes. In addition, CDK5 influences

transcription by interacting and modulating several transcription factors such as p53, myocyte enhancing factor-2 (MEF2) and STAT3 (Lalioti et al., 2010). The latter seems to play a role in DNA damage response mediated by CDK5 (Courapied et al., 2010). Initial evidence for a role of CDK5 in DNA damage response was provided by Turner et al. in 2008. The group revealed that treatment of cells with a PARP1 inhibitor, which provokes DNA damage, is synthetically lethal in combination with the knockdown of CDK5. These findings suggest that CDK5 is required for DNA damage checkpoint activation during cell cycle progression (Turner et al., 2008).

Together with the above-summarized studies implicating SIRT2 in stress response in cells of the nervous system the findings suggest that the interaction with SIRT2 and SIRT2 regulation by CDK5 may be part of a stress-signaling network.

1.4 State of research and objectives

SIRT2 is highly expressed in the brain especially in myelin-forming oligodendrocytes (OLs) (Li et al., 2007; Southwood et al., 2007) and its expression profile correlates with that of OL differentiation markers (Li et al., 2007; Werner et al., 2007; Ji et al., 2011). In mature OLs SIRT2 abundantly resides in the myelin sheath surrounding the axon (Southwood et al., 2007) but its physiological function in these postmitotic cellular structures remains to be elucidated. Luthi-Carter et al. demonstrated recently that SIRT2 positively regulates the transcription factor SREBP-2 (sterol response element binding protein 2) thereby promoting cholesterol biosynthesis in neurons (Luthi-Carter et al., 2010). Cholesterol influences membrane thickness and fluidity and is essential for myelin membrane growth and integrity (Saher et al., 2005). In contrast, cholesterol is also reported to have a detrimental effect in neurons and presents a risk factor in neurodegenerative diseases like AD and PD (Stefani and Liguri, 2009; Huang et al., 2011). Consistently, Luthi-Carter et al. reported in 2010 that SIRT2 inhibition reduces toxicity of mutant huntingtin by decreasing sterol biosynthesis (Luthi-Carter et al., 2010). In addition, SIRT2 knockdown or SIRT2 inhibition decreases α-synuclein toxicity, which is a hallmark of PD (Outeiro et al., 2007). An alternative explanation for the positive effect of SIRT2 downregulation on toxicity of aggregation-prone proteins is its postulated implication in macroautophagy (autophagy). Autophagy together with the ubiquitin-proteasomal system is responsible for elimination of protein-aggregates, which are a feature of many neurodegenerative diseases (Madeo et al., 2009). In this regard Zhao and colleagues provided evidence that cytoplasmic FOXO1 is required for stress-induced autophagy. FOXO1 is a transcription factor but its function in autophagy is independent of its gene regulatory properties. The authors demonstrated that stress induction disrupts an interaction between SIRT2 and FOXO1, which results in increased acetylation of FOXO1. Acetylated FOXO1 in turn activates the autophagy-regulating protein Atg7 and thus promotes autophagy (Zhao et al., 2010a).

Very little is known about how SIRT2 is regulated both in normal and deregulated cell physiology. In this regard phosphorylation of SIRT2 at serine 368/335 (S368/335) and S372/335 in its C-terminal extension by p35/CDK5 is especially interesting because similar to SIRT2, CDK5 is highly expressed in the brain and its protein levels are upregulated in differentiating cells, i.e. OLs (He et al., 2011). Furthermore CDK5 is an important cell cycle suppressor in postmitotic neurons (Cicero and Herrup, 2005). Its cell cycle suppressor

activities require a nuclear localization of CDK5, which is mediated by an interaction with p27 (Zhang et al., 2008). Upon stress, e.g. induced by β-amyloid expression in an AD model, association between p27 and CDK5 is disrupted resulting in reduced nuclear CDK5 levels (Zhang et al., 2010). Further evidence for CDK5 dysregulation as a component of neurodegenerative diseases is provided by accumulation of CDK5 and p25, a p35 cleavage product, in Levy bodies of AD patients (Lau and Ahlijanian, 2003).

The aim of this work was to analyze mechanisms that regulate SIRT2 with emphasis on its postmitotic function. In regard of regulatory mechanisms that target sirtuin function, PTMs play an important role. In sirtuins these occur, as far as analyzed, almost exclusively in the regions neighboring the conserved catalytic domain. These modifications influence enzymatic activity, intracellular distribution and/or inter- and intramolecular interaction of individual sirtuins. I focused my studies on SIRT2 phosphorylation, especially phosphorylation of S372/335. On that account I studied CDK5-SIRT2 signaling as both proteins are implicated in postmitotic cell physiology. Finally, generation of specific antibodies recognizing S368/335 will help to monitor SIRT2 regulation in cells.

2. Results and discussion

2.1 CDK5 induced mobility shift of SIRT2 is caused by phosphorylation

SIRT2 is expressed in two isoforms due to an alternative start codon (Voelter-Mahlknecht et al., 2005) and in some cases these differ in their subcellular distribution. Thus Suzuki et al. reported in 2007 that only the shorter isoform 2 is present in the myelin-enriched fractions of adult mouse brains and Werner et al. observed that only isoform 2 is found in the cytoplasm of murine cerebellar granule cells (Suzuki and Koike, 2007; Werner et al., 2007). Both heterologously expressed or endogenous SIRT2 isoforms display a characteristic triple band pattern in SDS-PAGE, which can be reversed to a single band after phosphatase treatment (Dryden et al., 2003; Nahhas et al., 2007). This indicates that phosphorylation reduces the mobility of SIRT2 in SDS-PAGE, which is displayed by a shift of the SIRT2-specific band on the corresponding Western blots. Mutational analysis revealed that two sites in the C-terminal extension of SIRT2 are targets of phosphorylation, namely S368 (S331 in isoform 2) and S372 (S335 in isoform 2). Their substitution to an alanine abolishes the mobility shift of SIRT2 and results in a single band pattern comparable to the phosphatase treatment suggesting that the mobility shift is caused by phosphorylation of these sites (Nahhas et al., 2007). Interestingly, hyperphosphorylation of SIRT2 at S368/331 and S372/335 is observed in cells treated with microtubule inhibitors such as Nocodazole (Nahhas et al., 2007; North and Verdin, 2007b). Nocodazole is a synthetic anti-tubulin agent, which reversibly interferes with the polymerization of microtubules (Samson et al., 1979). It is often used to arrest cells in G2/M phase of the cell cycle as treated cells are unable to form mitotic spindles. Therefore hyperphosphorylation of SIRT2 in cells treated with nocodazole implies that SIRT2 is phosphorylated in a cell cycle-dependent manner. Indeed, we and others discovered that S368/331 is part of a CDK-motif and can be phosphorylated by diverse CDK complexes, such as Cyclin B1/CDK1, Cyclin A/CDK2, Cyclin E/CDK2, Cyclin D3/CDK4, and p35/CDK5 (North and Verdin, 2007b; Pandithage et al., 2008). But synchronization studies with SIRT2 mutants, in which either S368/331 or S372/335 was substituted by an alanine (single phospho-mutants) (Nahhas et al., 2007), indicate that a phosphorylation of the second site, S372/335, is actually responsible for the hyperphosphorylation status of SIRT2 observed in Nocodazole treated cells. To date, no kinase has been identified, which targets S372/335. An alternative effect of Nocodazole treatment is the activation of the spindle assembly

checkpoint. Once activated it halts cell cycle progression when mitotic spindle positioning or assembly are impaired (Cuschieri et al., 2007). In fact further studies of Inoue and colleagues provided evidence that SIRT2 is required for mitotic stress induced cell death mediated by spindle checkpoint activation (Inoue et al., 2007; Inoue et al., 2009). However, the expression profile of SIRT2 implies a postmitotic function, which is supported by the positive effect of SIRT2 inhibition or knockdown on toxicity of neurodegenerative proteins. In this regard I focused my studies on SIRT2 phosphorylation by p35/CDK5.

To analyze phosphorylation of SIRT2 by p35/CDK5 I transiently co-expressed p35/CDK5 with SIRT2 isoform 2 wildtype (wt) and mutants in HEK293 cells. In the SIRT2 mutants each or both described phosphorylation sites were substituted by an alanine. Cell lysates were subjected to SDS-PAGE and SIRT2 was detected by Western blotting (Figure 4).
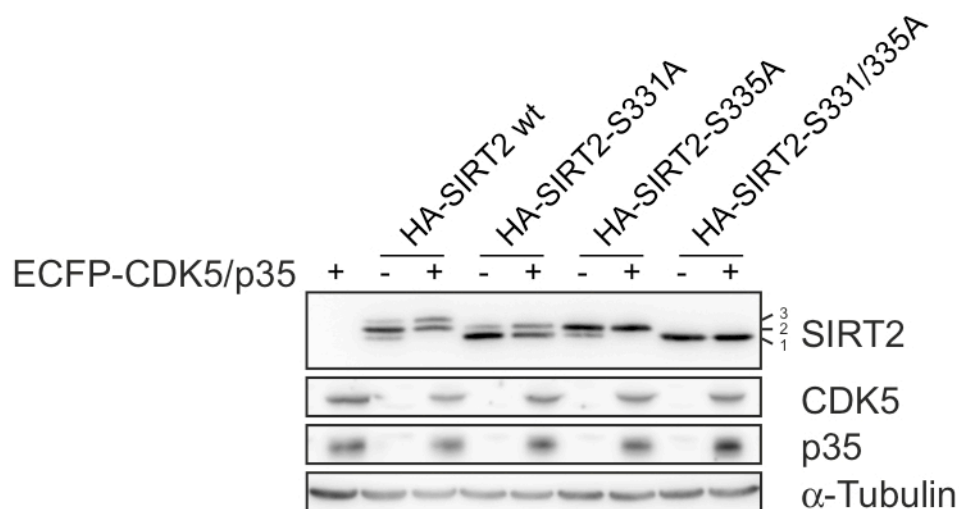
Figure 4: Mobility shift of SIRT2 wt and phosphorylation mutants induced by co-expression of p35/CDK5. HEK293 cell were transiently transfected with the indicated expression plasmids. After 48 hours cells were harvested and lysed in CoIP buffer. SIRT2 was immuno-precipitated with a tag-specific antibody. Immuno-precipitated SIRT2 and the co-expressed p35/CDK5 complex were detected by Western blotting with tag-specific (α-HA, α-GFP) or protein-specific (α-p35) antibodies. Detection of α-tubulin was used as a loading control. Small numbers highlight phosphorylation-dependent mobility shift of SIRT2 (1: unphosphorylated, 2: single-phosphorylated, 3: double-phosphorylated).

Consistent with the literature SIRT2 wt displayed a characteristic triple band pattern (lane 2). According to Nahhas et al. the first band represents unphosphorylated SIRT2 whereas phosphorylation of either S331 or S335 results in a mobility shift (band 2). Hyperphosphorylation of both sites causes an additional shift of the SIRT2 band (band 3) (Nahhas et al., 2007). Congruously the single phospho-mutants S331A and S335A form a double band pattern (lanes 4, 6) and the double phospho-mutant S331/335A a single band (lane 8). Co-expression of p35/CDK5 correlated with a change of the mobility shift pattern of SIRT2 wt, as it enhanced the third band and abolished the first band (lane 3). Interestingly,

p35/CDK5 co-expression also enhanced the mobility shift of the single phosho-mutant S331A (lane 5), in which the CDK5 target site was substituted. The double-phospho-mutant S331/335A (lane 9) showed no mobility shift upon p35/CDK5 co-expression.

To confirm that these mobility shifts are caused by phosphorylation, I performed a phosphatase assay. Therefor I transiently co-expressed HA-tagged SIRT2 wt or phospho-mutants with the p35/CDK5 complex in HEK293 cells. After 48 hours I harvested the cells and lysed them in CoIP buffer. I immunoprecipitated SIRT2 with a tag-specific antibody and subjected the immunoprecipitate to a phosphatase assay. Addition of phosphatase inhibitors or mock-treatment served as controls. Afterwards, samples were subjected to SDS-PAGE and SIRT2 was detected by Western blotting and a tag-specific antibody (α-HA) (Figure 5). Again p35/CDK5 co-expression altered the mobility shift pattern of SIRT2 wt and of the single phospho-mutants but had no effect on the double phospho-mutant. Phosphatase treatment but not control treatments reversed the band patterns of SIRT2 wt and of the single phospho-mutants to a single band pattern. The single band pattern of the double phospho-mutant stayed unchanged.
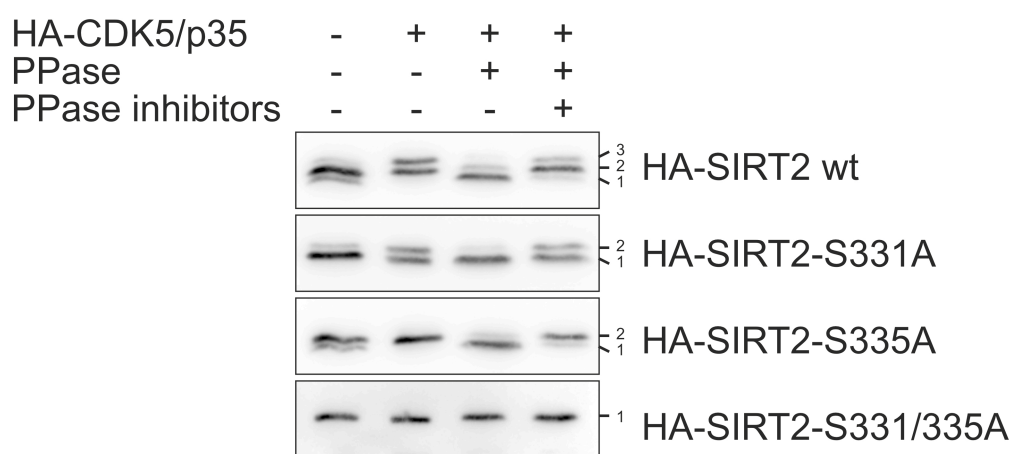
Figure 5: Phosphatase assay of SIRT2 wt and phosphorylation site mutants. HEK293 cells were transiently transfected with SIRT2- and p35/CDK5-expressing plasmids. Cells were harvested after 48 hours and lysed in CoIP buffer containing phosphatase inhibitors. SIRT2 was immunoprecipitated with a tag-specific antibody and subjected to a phosphatase (PPase) assay. Afterwards SIRT2 was detected by Western blotting and a tag-specific antibody (α-HA). Small numbers highlight phosphorylation-dependent mobility shift of SIRT2 (1: unphosphorylated, 2: single phosphorylated, 3: double phosphorylated).

Next, I wanted to test whether I can also induce hyperphosphorylation of endogenous SIRT2. Therefor I immunoprecipitated SIRT2 out of CoIP buffer lysates of HEK293 cells, which transiently expressed p35/CDK5 (Figure 6). Both immunoprecipitated SIRT2 isoforms displayed an altered band pattern upon co-expression of p35/CDK5, which was similar to SIRT2 wt in the preceding experiments.

HA-CDK5/p35   -   +

⊒ Isoform 1
⊒ Isoform 2
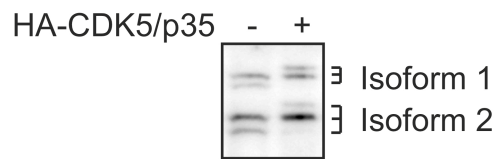
Figure 6: Mobility shift of endogenous SIRT2. HEK293 cells were transiently transfected as indicated. Cells were harvested after 48 hours and transfected cells were selected due to co-expression of CD4. Selected cells were lysed in CoIP buffer and endogenous SIRT2 immunoprecipitated with a polyclonal antibody serum (T749). Immunoprecipitated SIRT2 was detected by Western blotting with a monoclonal α-SIRT2 antibody (7G5). Both SIRT2 isoforms (Isoform 1, 2) were detected. The three phosphorylation-specific isoforms are indicated for the two protein isoforms.

These results confirmed that co-expression of CDK5 induces phosphorylation of S368/331. In addition CDK5 mediates phosphorylation of SIRT2 at S372/335 and causes hyperphosphorylation of SIRT2 as it was observed in Nocodazole-treated cells (Nahhas et al., 2007). Furthermore SIRT2 is targeted by phosphorylation even without co-expression of p35/CDK5 indicated by a prominent second band of endogenous SIRT2 or SIRT2 wt. This can be explained by the activity of endogenous CDK-complexes, which are reported to phosphorylate SIRT2 at S368/331 (Pandithage et al., 2008), and whose activities are indispensable for proliferating cells, such as HEK293 cells.

2.2 Phosphorylation of SIRT2 at S372/335

To further elucidate CDK5 mediated phosphorylation of SIRT2 I tested whether p35/CDK5 directly phosphorylates SIRT2 at S372/335 as this was already demonstrated for S368/331 (Pandithage et al., 2008). For that purpose I generated fusion proteins consisting of a GST-tag and the C-terminal extension of SIRT2 (sequence in Figure 7a), which contained both phosphorylation sites either in a wt conformation (CT wt) or substituted by an alanine (CT-S331A, -S335A, -S331/335A). Note that this region is common in both SIRT2 isoforms but for simplicity the numbering refers to isoform 2 only. I incubated these proteins in the presence of radioactively labeled ATP (^{32}P-γ-ATP) with the p35/CDK5 complex, which I immunoprecipitated out of transiently transfected HEK293 cells. I used a catalytically inactive CDK5 (CDK5-Δcat) mutant as a negative control to exclude unspecific phosphorylation of the SIRT2 C-terminal extension by a co-precipitated kinase. A sample containing GST instead of a GST-fusion protein was included in the assay to exclude unspecific phosphorylations at the GST-tag. After an incubation at 30 °C for 30 minutes the samples were subjected to SDS-PAGE and phosphorylation signals were detected via autoradiography. Incubation of CT wt with p35/CDK5 but not with p35/CDK5-Δcat produced

a radioactive signal corresponding to the GST-fusion protein stained by Coomassie blue. This signal was specific for the CT wt as no signal appeared in the GST control sample, which was treated in parallel. Furthermore no corresponding phosphorylation signal was detected in the samples containing the double phospho-mutant CT-S331/335A or the single phospho-mutant CT-S331A. On the other hand incubation of p35/CDK5 with the single phospho-mutant CT-S335A resulted in a distinct signal corresponding to the GST-tagged C-terminal extension.

A

G_{320}AGVPNPSTSAS_{331}PKKS_{335}PPPAKDEARTTEREKPQ -C

B

	GST	CT wt			CT-S331A	CT-S335A	CT-S331/335A
HA-CDK5	+	+	-	-	+	+	+
HA-CDK5-Δcat	-	-	+	-	-	-	-
myc-p35	+	+	+	-	+	+	+

^{32}P

← GST-SIRT2-CT
← GST

CB

← GST-SIRT2-CT
← GST
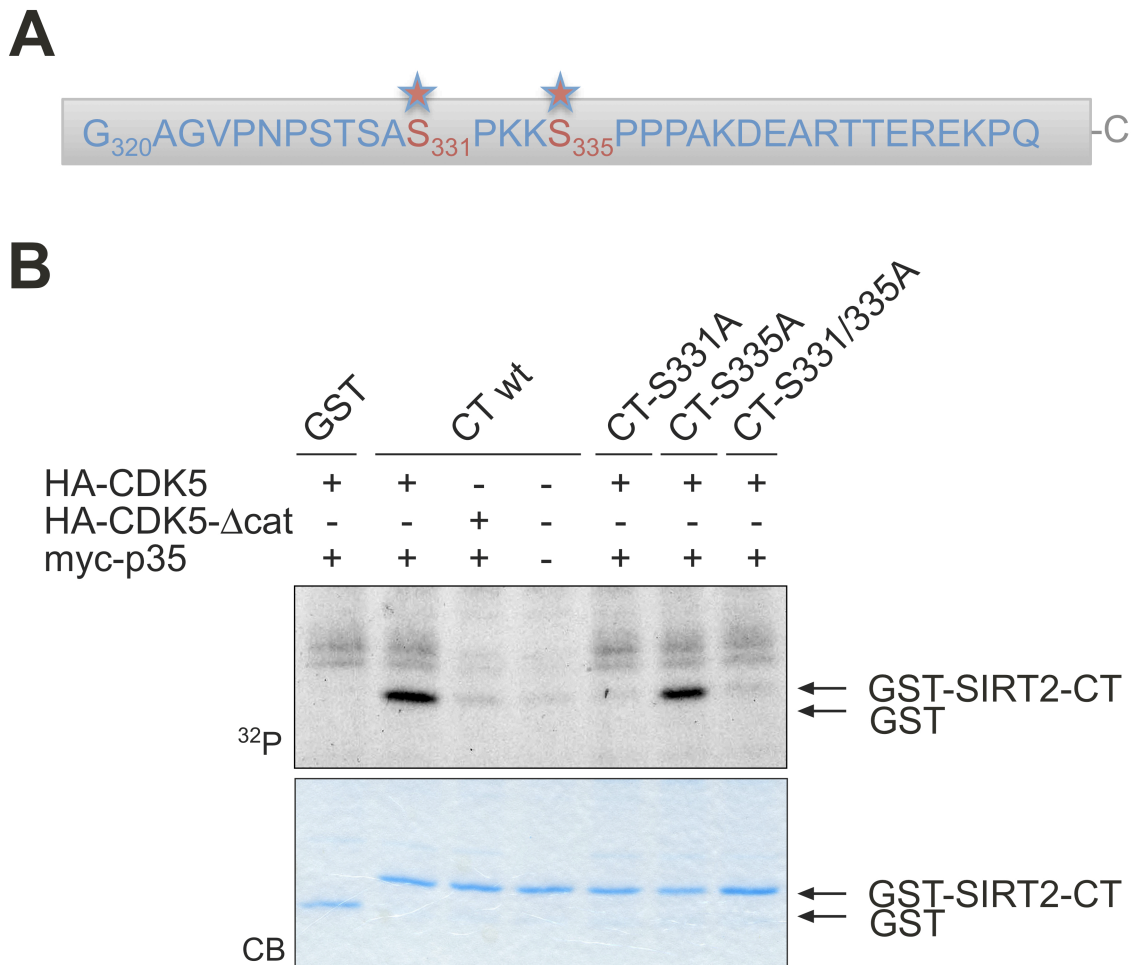
Figure 7: Kinase assay with p35/CDK5 and SIRT2 C-terminus (CT). A) Amino acid sequence of the SIRT2-CT that was fused to the GST-tag. Numbering according to SIRT2 isoform 2. Phosphorylation sites are indicated. B) HEK293 cells were transiently transfected with plasmids expressing HA-tagged CDK5 or a catalytically inactive CDK5 mutant (Δcat) and p35. Cells were lysed after 48 hours and p35/CDK5 complexes immunoprecipitated with a tag-specific antibody (α-HA) A) Bacterially expressed and purified GST-SIRT2 C-terminus or the respective phosphorylation site mutant were incubated with the immunoprecipitated p35/CDK5 complexes and radioactively-labeled ATP (^{32}P). Samples were subjected to SDS-PAGE and gels stained with coomassie blue (CB). Phosphorylation was detected by autoradiography.

These results confirmed that p35/CDK5 directly targets S331 in SIRT2 but does not phosphorylate S335. It is unlikely that phosphorylation of S335 depends on phosphorylation of S331 because both single phospho-mutants are phosphorylated upon p35/CDK5 co-expression in cells. Hence phosphorylation of SIRT2 at S335 upon CDK5 co-expression in

cells is most likely mediated by a kinase downstream of p35/CDK5 (Figure 7b).

A putative candidate kinase, which is activated downstream of p35/CDK5, is CDK16. Similar to SIRT2, CDK16 is predominantly localized in the cytoplasm and highly expressed in terminally differentiated cells of brain and testis (Besset et al., 1999). Furthermore CDK16 can interact with p35. CDK16 is phosphorylated by p35/CDK5 at S95 and thereby activated (Cheng et al., 2002). To test whether CDK16 phosphorylates SIRT2 at S335 I co-expressed CDK16 and its activator Cyclin Y with SIRT2 wt and phospho-mutants and monitored the SIRT2 mobility shift in a SDS-PAGE gel by Western blotting with tag-specific antibodies as described before (Figure 8).
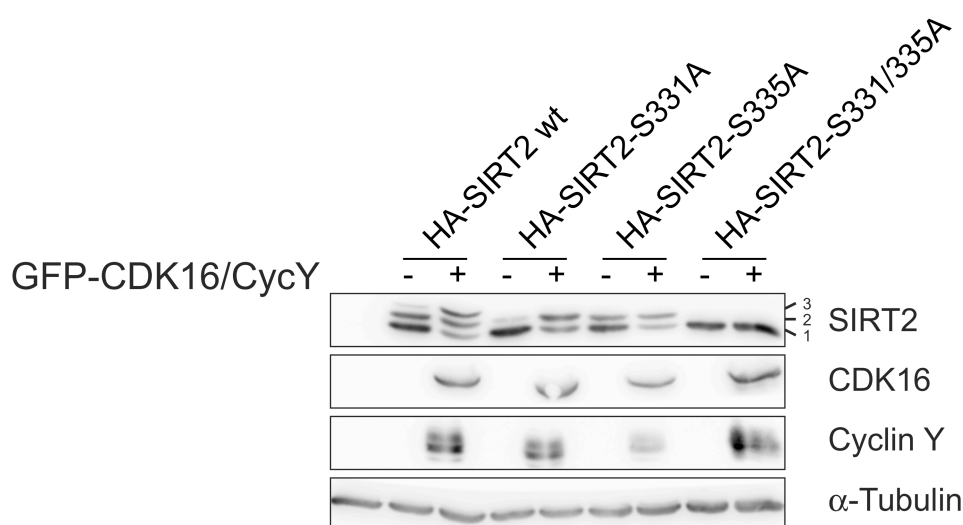
Figure 8: Mobility shift of SIRT2 wildtype (wt) and phosphorylation site mutants induced by co-expression of Cyclin Y/CDK16. Experimental procedures as in Figure 4. HCT116 cells served as model cell line and detection of transiently expressed proteins was carried out with tag-specific antibodies (α-HA, α-GFP, α-Flag). Tubulin was detected as a loading control. Small numbers highlight phospho-specific isoforms (1: unphosphorylated, 2 single phosphorylated, 3: double phosphorylated).

Similar to p35/CDK5, co-expression of Cyclin Y/CDK16 induced a change of the specific band pattern of SIRT2 wt and the single phospho-mutant S331A. The effect was not as strong as for p35/CDK5 because despite the occurrence of the third band (wt, lane 3), which represents double phosphorylated SIRT2, a subset of SIRT2 remained unphosphorylated, indicated by the lowest band. Furthermore co-expression of Cyclin Y/CDK16 had no effect on the single phospho-mutant S335A and the double phospho-mutant S331/335A. According to these results Cyclin Y/CDK16 co-expression mediates the phosphorylation of SIRT2 at S335 but it seems to have no effect on S331 as no enhanced mobility shift of the single phospho-mutant S335A occurred. It remains to be elucidated whether Cyclin Y/CDK16 phosphorylates SIRT2 directly and whether CDK5-mediated phosphorylation of SIRT2 at S335 requires CDK16 or vice versa. These questions will be addressed by siRNA experiments

and in vitro kinase assays in the future. Furthermore it is possible that phosphorylation of SIRT2 at S335 by CDK5 requires association of CDK5 with a different activator, such as p39 or the cleavage products p25 or p29. In vitro kinase assays using these alternative CDK5 complexes shall help to study this possibility.

2.3 α-SIRT2 antibody characterization

To decipher the biological function of SIRT2 phosphorylation at S335 I generated SIRT2-specific antibodies in a cooperation with E. Kremmer. Therefore I designed a peptide comprising 14 amino acids of the SIRT2 C-terminal extension including the phosphorylation sites S331 and S335, in which either S335 or both phosphorylation sites were conjugated with a phosphate group (Peptide production by PSL GmbH). These peptides were then used to immunize rats and mice. Antibody producing B cells of these animals were then fused with myeloma cells and the resulting hybridoma cell lines grown in tissue culture. Monoclonal antibodies from cell culture supernatants were screened initially in an enzyme-linked immunosorbent assay (ELISA) (Antibody production by E.Kremmer). I tested 107 positively screened antibody clones for SIRT2 specificity and their ability to detect phosphorylation of S331 and S335. These tests included a set of previously described α-SIRT2 antibodies generated with a peptide, in which S331 was phosphorylated (Pandithage et al., 2008). I wanted to expand their characterization concerning S335 phosphorylation, as both phosphorylation sites are situated in close proximity and might interfere with antigen recognition.

My tests consisted of two types of assays. First I generated cell lysates of HEK293 cells, which transiently expressed either HA-tagged SIRT2 wt or one of the two single phospho-mutants (S331A or S335A) and p35/CDK5 to induce phosphorylation of S335. Mock-transfected cells served as negative control. These cell lysates were subjected to SDS-PAGE and SIRT2 was detected via Western blot using either a tag-specific antibody (α-HA) or one of the antibodies to be analyzed (Figure 9a, c). Comparisons of immuno-reactivities between tag-specific and putative protein-specific antibodies allowed identification of SIRT2-specific antibody clones (summarized in Table 1). Furthermore antibody clones that detected SIRT2 wt specifically but not the phospho-mutant were delineated as phospho-specific. In a second screen I controlled phospho-specificity in a phosphatase assay as described before (Figure 9b,d).
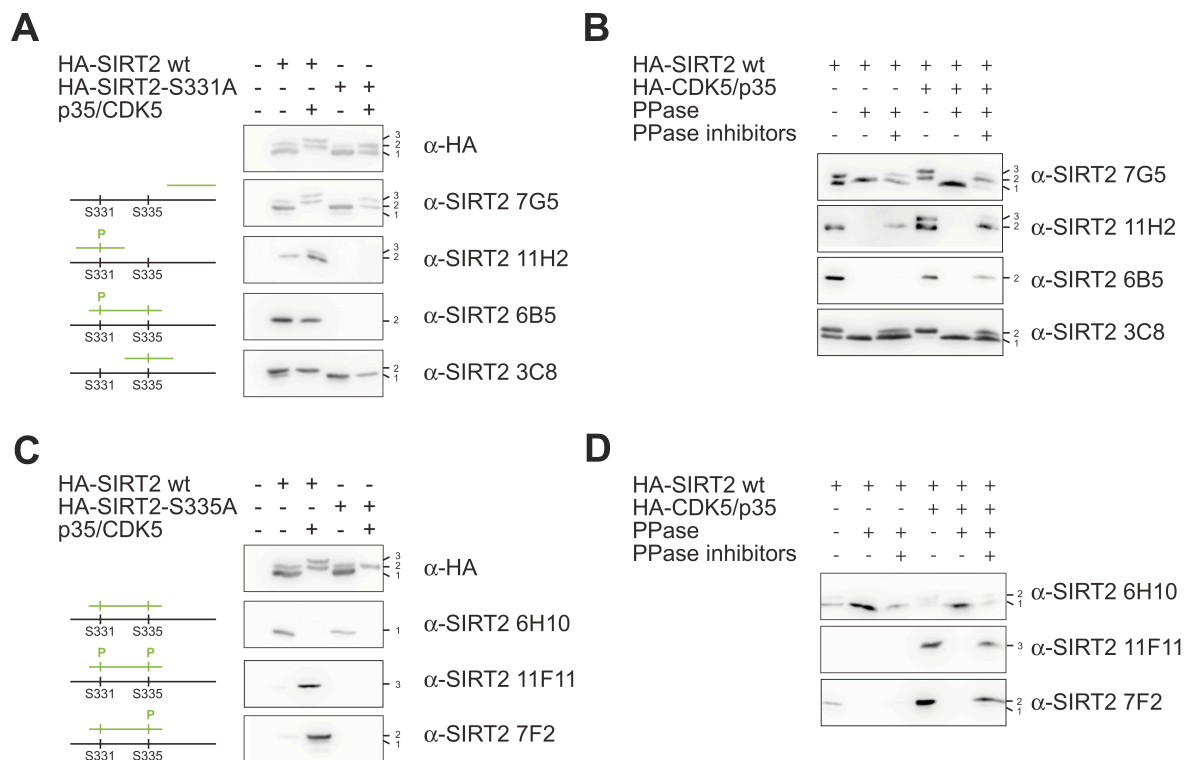
Figure 9: Results of selected α-SIRT2 antibody clones tested. To examine the specificity of the monoclonal α-SIRT2 antibodies HEK293 cells were transiently transfected with HA-tagged SIRT2 wildtype (wt) or single phospho-mutant (S331A or S335A) expressing plasmids. Co-expression of the p35/CDK5 complex induced phosphorylation of S335 and the corresponding mobility shift in SDS-PAGE. As a negative control cells were mock transfected. Cells were harvested after 48 hours and lysed in CoIP-buffer containing phosphatase inhibitors. Small numbers highlight phosphorylation-specific isoforms (1: unphosphorylated, 2 single phosphorylated, 3: double phosphorylated). A, C) Lysates were subjected to SDS-PAGE and SIRT2 detected by Western blotting and a tag-specific or a monoclonal α-SIRT2 antibody. Pictograms on the right illustrate the epitopes, which are recognized by the antibodies (green). B, D) SIRT2 was immunoprecipitated with a tag-specific antibody and subjected to a phosphatase (PPase) assay. PPase inhibitors were included in control samples. Afterwards samples were subjected to SDS-PAGE and SIRT2 was detected by Western blotting and a monoclonal α-SIRT2 antibody. A, B) Previously described antibody clones (Pandithage et al., 2008). C, D) Newly generated antibody clones.

α-SIRT2 Clone	Species	S331		S335	
		-	P	-	P
7G5	Rat	+	+	+	+
11H2	Rat	-	+	+	+
6B5	Rat	-	+	+	-
3C8	Rat	+	+	+	-
6H10	Mouse	+	-(*)	+	-
4C4	Mouse	-	+	-	+
7F2	Mouse	+	-	-	+
1C5	Rat	-	+	-	+
11F11	Rat	-	+	-	+

Table 1: List of all positively tested monoclonal SIRT2-specific antibodies. The list displays properties of all positively tested α-SIRT2-antibody sera incl. the type species it was generated in and phosphorylation status (unphosphorylated "-" or phosphorylated "P") it is specific for (recognition "+", no recognition "-"). The asterisk marked background detection when using a very low antibody dilution.

Of nine positively tested antibody clones only the previously described clone 7G5 detected SIRT2 independently of phosphorylation at S331 or S335 as it can recognize all three bands comparable to the tag-specific antibody. The previously described clone 11H2 recognized SIRT2 only when S331 was phosphorylated, even when S335 was also phosphorylated, as it recognizes the second band and the third band of SIRT2 wt but displayed no signal for the single phospho-mutant S331A. In addition, the 11H2 signal vanished after phosphatase treatment and was restored by addition of phosphatase inhibitors verifying its phospho-specificity. The antibody clones 6B5 and 7F2 were phospho-specific for S331 and S335, respectively. But their epitope was masked if the other site was phosphorylated as well. Thus they stained only the second band of SIRT2 wt but displayed no signal for the respective single phospho-mutant. Phosphatase treatment abolished the signals, whereas phosphatase inhibitors restored them at least in part. The newly generated clones 4C4, 1C5 and 11F11 detected SIRT2 only when both sites were phosphorylated as they only stained the third band of SIRT2 wt but not the phospho-mutant (Figure 9 and data not shown). Their signals vanished after phosphatase treatment and were restored by addition of phosphatase inhibitors. The antibody clone 6H10 recognized SIRT2 only when S331 and S335 were unphosphorylated because it only stained the first band of either SIRT2 wt or the single phospho-mutant. Furthermore the signal was enhanced by phosphatase treatment and restored when phosphatase inhibitors were included in the experiment. Properties of all antibodies positively tested are summarized in table 1.

2.4 Function of the SIRT2 C-terminal extension

Next I wanted to elucidate the effect of the C-terminal extension and its modifications on SIRT2 function. According to phylogenetic analysis of the sirtuin typic core domain, SIRT2 is most closely related to the yeast sirtuin Hst2 and the human sirtuin SIRT3 and more distantly to SIRT1 (Figure 1) (Frye, 2000). Similar to SIRT2, Hst2 and SIRT1 contain at least one functional nuclear export signal and their subcellular localizations are reported to determine their deacetylase activities (Wilson et al., 2006; Tanno et al., 2007). Furthermore Hst2 and SIRT1 are shown to form homotrimers. Hst2 trimerization is influenced by its C-terminal extension and influences the enzyme's activity (Zhao et al., 2003; Vaquero et al., 2004). Schlicker et al. demonstrated in 2008 that a deletion of the C-terminal extension in SIRT3 increased the deacetylase activity of the enzyme. Based on crystallographic structures the authors postulated that the N- and C-terminal extensions of SIRT3 form a module that might

regulate access of substrate proteins to the catalytic domain (Schlicker et al., 2008). Finally, phosphorylation of SIRT1 can have different effects on its substrate specificity or activity dependent on the sites that are targeted (Sasaki et al., 2008b; Zschoernig and Mahlknecht, 2009).

From these data at least three hypotheses concerning a function of the SIRT2 C-terminal extension (CT) are conceivable. First, the CT might regulate the interaction of SIRT2 with other proteins including substrates. Second, the CT might modulate activity of the catalytic core domain. And third, the CT might be involved in the subcellular distribution of SIRT2.

To test the first hypothesis I studied the interaction of SIRT2 and HDAC6. HDAC6 is a class II lysine deacetylase, which is dependent on Zn^{2+} rather than NAD^+. Similar to SIRT2, HDAC6 is predominantly localized in the cytoplasm and can deacetylate alpha-tubulin at lysine 40 (de Ruijter et al., 2003). Both deacetylases are reported to interact. Nahhas et al. demonstrated in 2007 that mutants of SIRT2, in which S331 or S335 are substituted by alanines, have no effect on the interaction between SIRT2 and HDAC6 in co-immunoprecipitations (Nahhas et al., 2007). However, it is not clear whether phosphorylation of these sites or the CT in general influences such an interaction. Therefore I cloned a SIRT2 mutant, in which I deleted the complete CT (SIRT2-ΔCT) and used it for co-immunoprecipitation studies with HDAC6. I transiently transfected HEK293 cells with plasmids encoding ECFP-tagged SIRT2 or SIRT2-ΔCT and co-expressed HA-tagged HDAC6. 48 hours after transfection, cells were harvested and lysed in CoIP-buffer. SIRT2 or HDAC6 were immunoprecipitated with tag-specific antibodies (α-HA or α-GFP). Immunoprecipitates and whole cell lysates were subjected to SDS-PAGE and proteins were detected by Western blotting with tag-specific antibodies (α-HA or α-CFP). Tubulin detection served as a loading control (Figure 10). Both SIRT2 and the truncated mutant were co-immunoprecipitated by HDAC6 and conversely, HDAC6 was co-immunoprecipitated by SIRT2 wt as well as by SIRT2-ΔCT. These results are consistent with previous experiments of Nahhas et al., in which the interaction between SIRT2 and HDAC6 was unaffected by substitutions of either phosphorylation site by alanines. These observations suggest that the unphosphorylated CT does not influence the interaction between SIRT2 and HDAC6 in cells. However, it remains to be elucidated whether phosphorylation of the CT promotes a conformational change of SIRT2 that blocks the HDAC6 interaction domain of SIRT2. The newly generated SIRT2 antibodies will help to address this question as they can be used to clarify, which phospho-specific SIRT2 isoform is co-immunoprecipitated by HDAC6.

Furthermore it needs to be investigated whether the binding of an alternative interacting protein is influenced by the CT in a similar way.
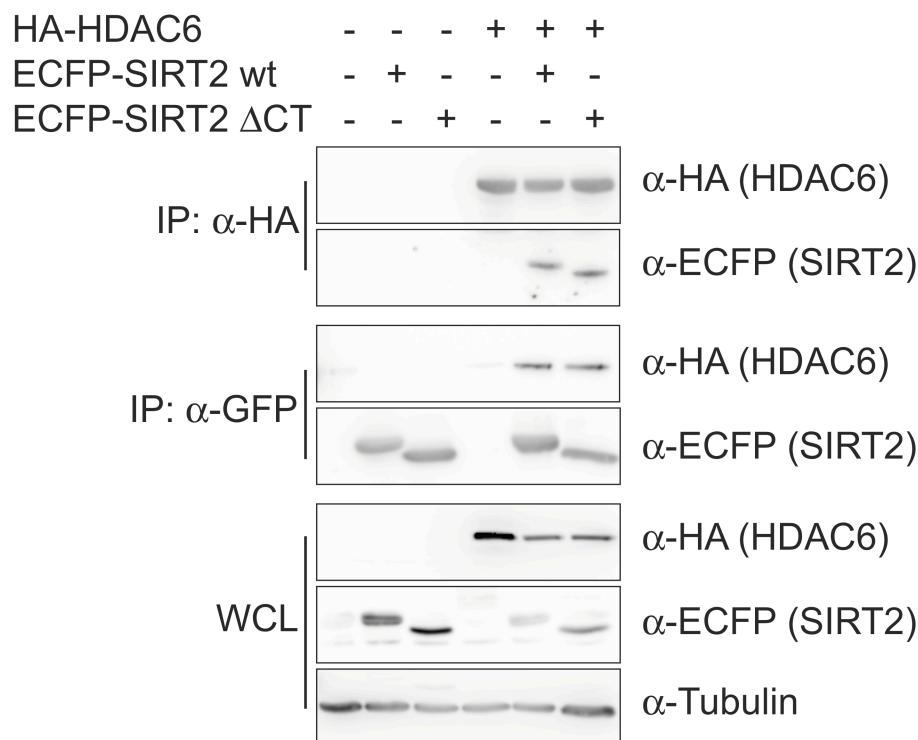
Figure 10: Interaction between SIRT2 and HDAC6 is independent of the SIRT2 CT in cells. HEK293 cells were transfected with HA-tagged HDAC6 or ECFP-tagged SIRT2 wildtype (wt) or a C-terminally truncated mutant (ΔCT) expressing plasmids. Cells were harvested after 48 hours and lysed in CoIP-buffer. SIRT2 or HDAC6 were immunoprecipitated with tag-specific antibodies (α-HA or α-GFP) and precipitates subjected to SDS-PAGE. Proteins were detected by Western blotting and tag-specific antibodies (α-HA or α-CFP). Whole cell lysates (WCL) were subjected to SDS-PAGE and Western blot as expression controls. Tubulin detection served as a loading control.

Next I tested the effect of the CT on the catalytic activity of SIRT2. Therefor I incubated GST-SIRT2 wt or the C-terminally truncated GST-SIRT2-ΔCT fusion protein with commercially available purified tubulin in the presence of NAD$^+$. As a control of unspecific deacetylation of tubulin, I included a sample with GST in the experiment. After an incubation step for up to 90 minutes, samples were subjected to SDS-PAGE and either stained by Coomassie blue or the tubulin acetylation status was detected via Western blot with a specific antibody for acetylated tubulin (Figure 11). The tubulin acetylation status was already markedly reduced after 30 minutes of incubation in the samples containing SIRT2 wt as well as SIRT2-ΔCT in comparison to the GST control sample. Furthermore tubulin incubated with the truncated SIRT2 mutant was deacetylated significantly faster compared to the wt protein. This indicates that the unphosphorylated CT has an inhibitory function.

A
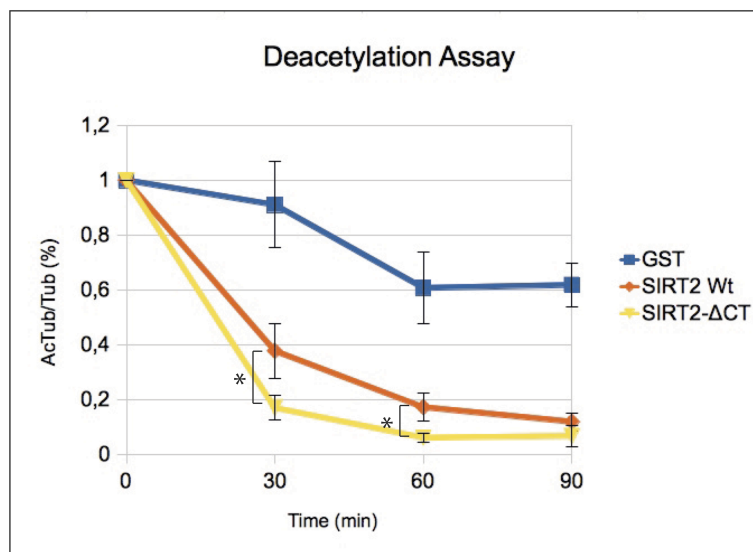
B
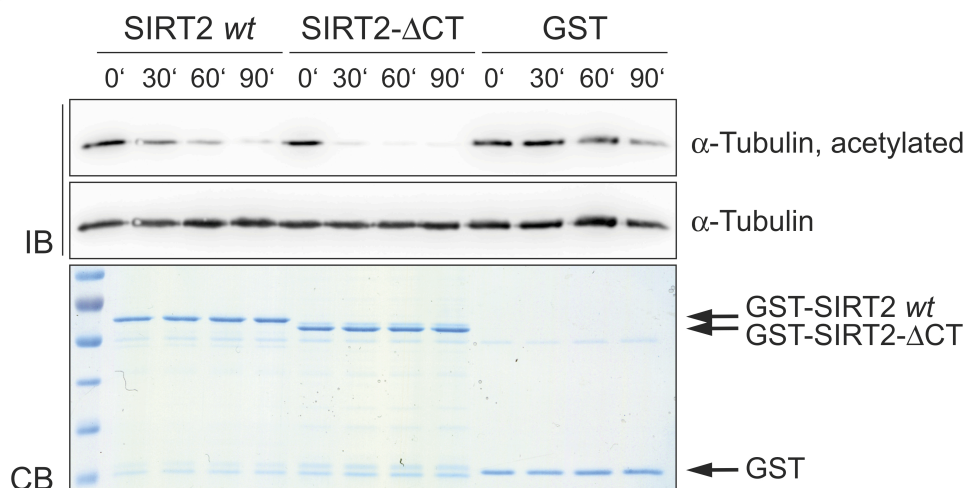
Figure 11: Tubulin-deacetylation assay with SIRT2. GST-SIRT2 wildtype (wt) or a C-terminally truncated GST-SIRT2-ΔCT fusion protein were incubated with commercially available purified tubulin in the presence of NAD^+ for the indicated periods of time (0 to 90 minutes). GST protein was included as a negative control for unspecific deacetylation of tubulin. Afterwards samples were subjected to SDS-PAGE and either stained by Coomassie blue (CB) or the tubulin acetylation status was detected via Western blot with a specific antibody for acetylated tubulin (IB). A) Quantification of three independent experiments. Standard deviations are indicated. Significant differences were indicated by an asterisk (two-sided students T-test). B) Western blot (IB) and Coomassie blue staining of one experiment.

Unfortunately this assay is not sensitive enough to determine exact Michaelis-Menten kinetics of the reactions. However, the results allow the conclusion that the CT interferes with the enzymatic activity of SIRT2. Hence posttranslational modifications targeting this part of SIRT2 provide the potential to regulate the negative effect of the CT on SIRT2 catalytic activity. The results are consistent with previously published data, which demonstrate that

phosphorylation of S331 reduces enzymatic activity of SIRT2 (Pandithage et al., 2008). In addition the assay provides further evidence that the CT is not involved in ligand binding as it is necessary for SIRT2 to be in physical contact with its substrate to remove the acetyl-group. Taken together the results of the HDAC6-SIRT2 co-immunoprecipitation and of the deacetylation assay point to a putative intramolecular effect of S335 phosphorylation. Further studies involving the newly characterized SIRT2 phospho-specific antibodies and more sensitive enzymatic assays with SIRT2 phospho-mutants shall help to shed light on the signaling pathways that target S335 and its effect on SIRT2 function.

2.5   SIRT2 interferes with CDK5 acetylation

In 2009 Choudhary and colleagues identified 3600 acetylation sites in 1750 proteins using a high-resolution mass spectrometry approach. One of these sites was lysine 56 (K56) in CDK5 (Choudhary et al., 2009). The only other member of the CDK family, which is reported yet to be a target of acetylation is CDK9 (Sabò et al., 2008). CDK9 is acetylated by GCN5 and P/CAF in the catalytic core domain at lysine 48 (K48), which coordinates ATP binding and the phosphotransfer reaction. Hence acetylation of K48 inhibits catalytic activity of CDK9. Interestingly K48 is conserved in the CDK family and is located in CDK5 at position 33 (K33) (Sabò et al., 2008). The previously reported substitution of K33 to a threonine (K33T) in CDK5 renders the protein catalytically inactive. This mutant was already used in the kinase assays shown before. A third interesting link between GCN5 and the CDK5-SIRT2 signaling pathway was recently provided by Conacci-Sorrel et al. in 2010, who demonstrated that GCN5 can acetylate α-tubulin, which correlates with muscle differentiation (Conacci-Sorrell et al., 2010). These data allow the hypothesis that GCN5 can also acetylate CDK5 providing the potential for a feedback loop between SIRT2 and CDK5 as SIRT2 would be a candidate deacetylase for CDK5.

To test the hypothesis whether CDK5 was acetylated in our model system as well, I transiently transfected HEK293 cells with HA-tagged CDK5- and GCN5-encoding plasmids. Besides CDK5 wt I also included two mutants, in which either K33 or K56 were substituted by a threonine (K33T) or arginine (K56R). To exclude unspecific acetylation signals, control cells were mock-transfected. Cells were harvested and lysed in CoIP-buffer containing deacetylase inhibitors after 48 hours. CDK5 was immunoprecipitated with a tag-specific antibody. Immunoprecipitates and whole cell lysates were subjected to SDS-PAGE and Western blot. Acetylated CDK5 was detected with an antibody specific for acetylated lysines.

Tubulin detection served as a loading control (Figure 12a).
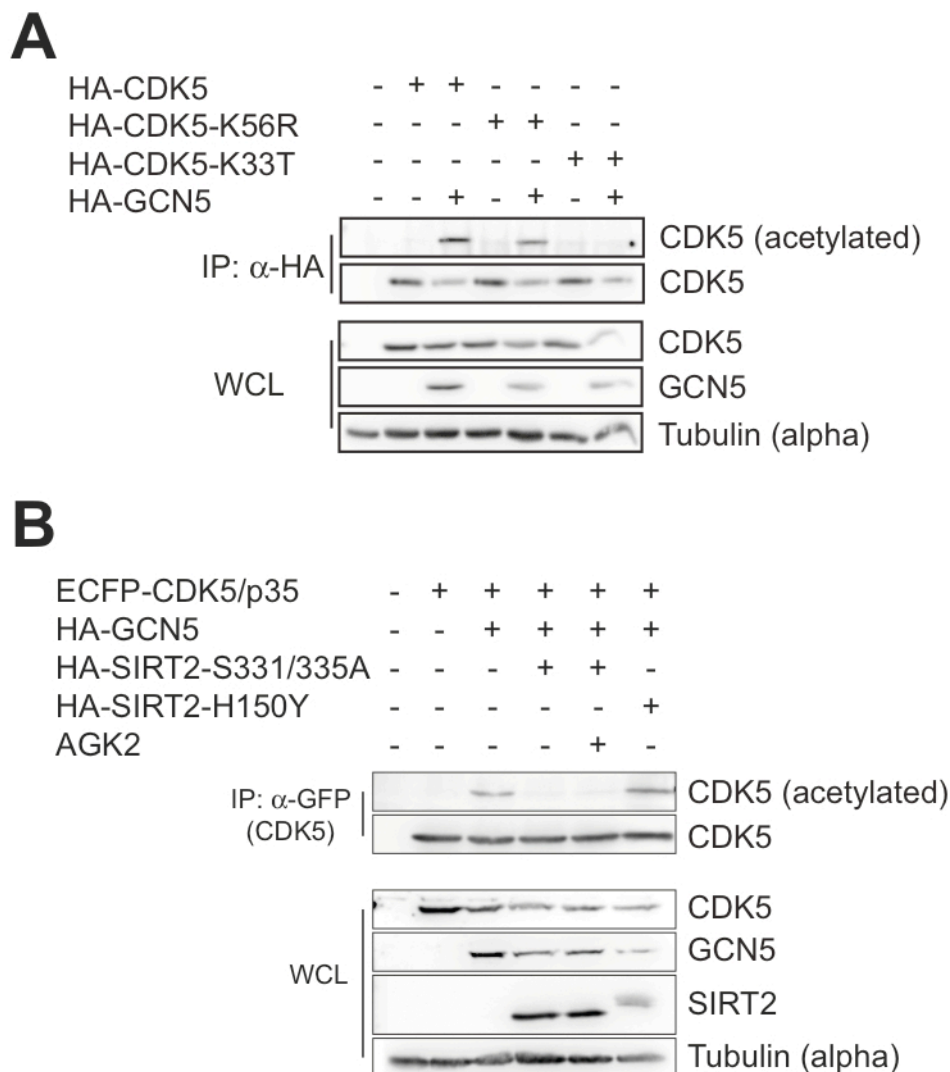
Figure 12: SIRT2 reverses GCN5-mediated acetylation of CDK5 at K33 in cells. HEK293 cells were transiently transfected with expression plasmids as indicated. After 48 hours cells were harvested and lysed in CoIP-buffer containing deacetylase inhibitors. CDK5 was immunoprecipitated with a tag-specific antibody. Immunoprecipitates (IP) and whole cell lysates (WCL) were subjected to SDS-PAGE and Western blot. Acetylated CDK5 was detected with an antibody specific for acetylated lysines. Tubulin detection served as a loading control. A) Acetylation of CDK5 and CDK5 mutants after co-expression of GCN5. B) Effect of SIRT2 co-expression on GCN5-mediated acetylation of CDK5. The SIRT2-specific inhibitor AGK2 was added to cells 16 hours prior to lysis.

A CDK5-specific acetylation signal was detected in the samples containing GCN5 and either CDK5 wt or CDK5-K56R but no signal occurred in samples containing GCN5 and CDK5-K33T. Furthermore no acetylation signal was detectable with the Kac-specific antibody for CDK5 wt and mutants that were expressed alone. These results indicate that co-expression of GCN5 mediates acetylation of CDK5 at K33 in cells. Next, I addressed the question whether SIRT2 can deacetylate CDK5. Therefore I repeated the last experiment and additionally co-

expressed the SIRT2 double phospho-mutant (S331/335A) and a catalytically inactive SIRT2 mutant (SIRT2-H150Y) to CDK5 wt and GCN5. The double mutant was included in the assay to exclude phosphorylation-dependent inhibition of SIRT2 by CDK5. Furthermore I treated cells with a specific SIRT2 inhibitor (AGK2) 16 hours prior to cell lysis (Figure 12b). Consistent with the last experiment GCN5 co-expression induced a CDK5-specific acetylation signal, which was abolished after co-expression of SIRT2-S331/335A and enhanced in the sample containing SIRT2-H150Y. Unfortunately, treatment of cells with AGK2 did not restore the acetylation signal of CDK5 in the sample containing SIRT2-S331/335A. But as nicotinamide treatment in a similar experimental outline restored CDK5 acetylation to a certain extent (data not shown), I conclude that SIRT2 deacetylase activity interferes with CDK5 acetylation at least in cells.

To test whether GCN5 acetylates CDK5 directly I performed an in vitro-acetylation assay. Therefore I incubated purified GCN5 (kindly provided by M. Hottiger) with the commercially available purified p35/CDK5 complex in presence of acetyl-CoA. To test for unspecific acetylation a BSA control was included in the assay. Acetyl-transferase activity was tested in two different buffer conditions. Buffer A1 contained DTT and EDTA whereas buffer A2 contained salts such as $MgCl_2$, $NaCl_2$ and $ZnCl_2$. After incubation samples were subjected to SDS-PAGE and acetylated CDK5 was detected via Western blot with a specific antibody for acetylated lysines. Proteins were detected by Ponceau staining before antibody incubation (Figure 13a). An acetylation signal was detected only in the sample containing GCN5 and p35/CDK5 just under 35 kDa, which correlates with the predicted molecular size of 33 kDa for CDK5. P35 was fused to a GST-tag and should run between 50 and 55 kDa. Furthermore the acetylation signal occurs only when the proteins were incubated in buffer A2. The results indicate that GCN5 directly acetylates CDK5 in vitro. In a similar approach I tested whether other acetyltransferases, such as P/CAF, p300, CBP or TIP60, are also able to acetylate CDK5 (Figure 13b). P/CAF, which belongs to the same class of lysine acetyltransferases as GCN5 displayed a similar activity in the assay as GCN5, with preference for buffer A2. CBP and p300 induced a slightly different acetylation signal pattern. In both samples a CDK5-specific signal was detected with preference for buffer A1. Additionally both enzymes acetylated p35, which was indicated by an acetylation signal at about 55 kDa. An additional acetylation signal slightly above the 35 kDa mark might be explained by p35 without its GST-tag. To my knowledge there are no reports about an acetylation of p35 published yet.
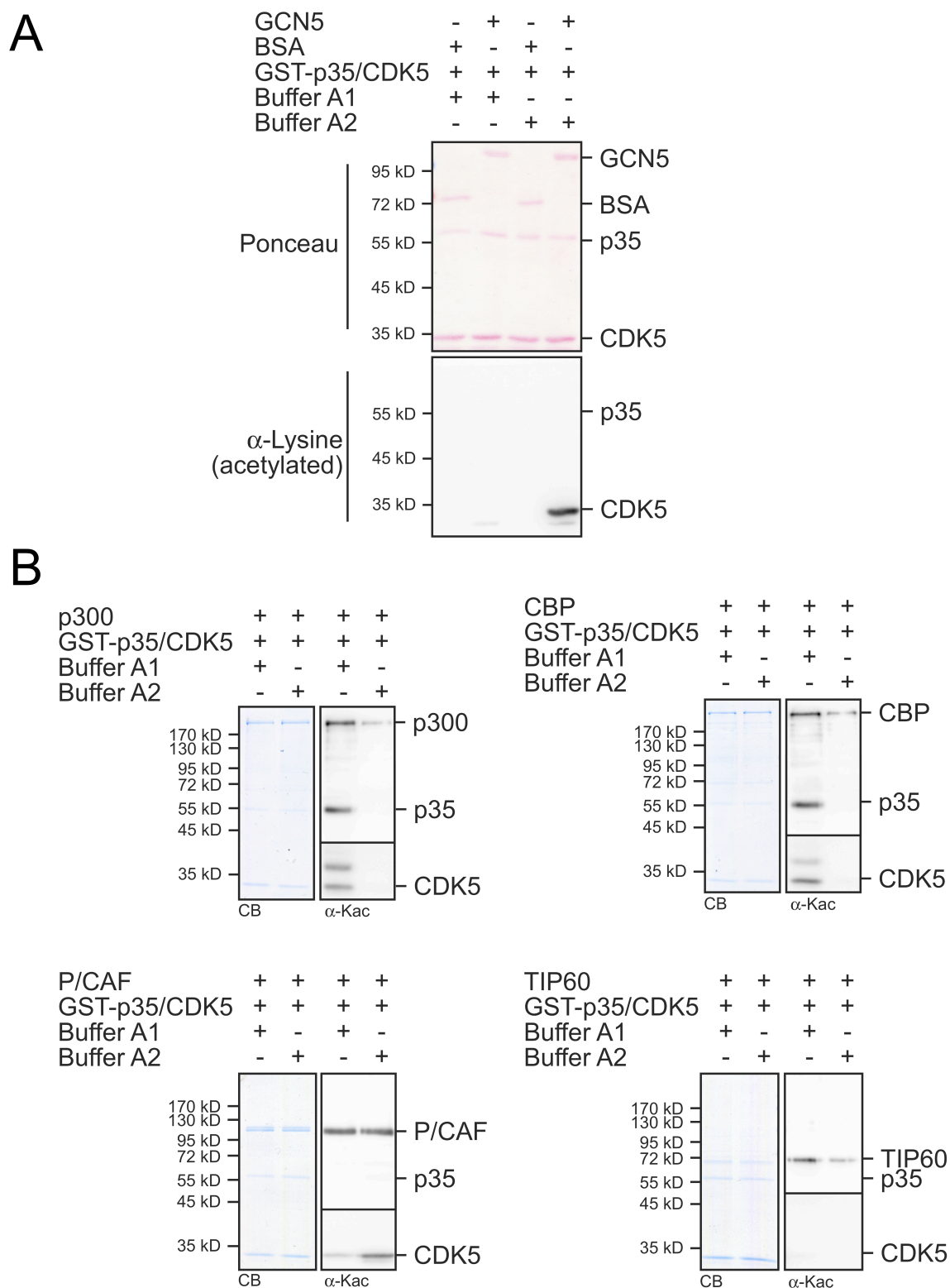
Figure 13: Figure 13: In vitro-acetylation assay of p35/CDK5 with different lysine acetyltransferases. Commercially available p35/CDK5 proteins were incubated with baculovirally expressed and purified KATs (M. Hottiger) in presence of acetyl-CoA. KAT activity was tested in two different buffers. To exclude unspecific acetylation a BSA control was included in the assay. Afterwards samples were subjected to SDS-PAGE and acetylated CDK5 was detected via Western blot with a specific antibody for acetylated lysines (α-AcK). A) GCN5. Proteins were detected by Ponceau staining before antibody incubation. B) p300, CBP, P/CAF and TIP60. Proteins were detected by Coomassie blue (CB) staining.

3. Conclusions

SIRT2 is expressed in two isoforms due to an alternative start codon (Voelter-Mahlknecht et al., 2005) and in some cases these differ in their subcellular distribution. Thus Suzuki et al. reported in 2007 that only the shorter isoform 2 is present in the myelin-enriched fractions of adult mouse brains and Werner et al. observed that only isoform 2 is found in the cytoplasm of murine cerebellar granule cells (Suzuki and Koike, 2007; Werner et al., 2007). Inhibition of SIRT2 is reported to reduce neurotoxicity of mutant huntingtin and α-synuclein toxicity, which are hallmarks of neurodegenerative Huntington's and Parkinson's disease (Luthi-Carter et al., 2010; Outeiro et al., 2007).

Two phosphorylation sites have been identified in SIRT2, which are located in the CT in close proximity to each other at S368/331 and S372/335 (Nahhas et al., 2007). S368/331 is part of a cyclin-dependent kinase (CDK) recognition motif and has been shown to be a substrate of Cyclin B/CDK1, Cyclin E/CDK2, Cyclin A/CDK2, Cyclin D3/CDK4 and p35/CDK5 (North and Verdin, 2007b; Pandithage et al., 2008). Phosphorylation of SIRT2 at S368/331 reduces its enzymatic activity (Pandithage et al., 2008). Upon mitotic stress induction by nocodazole SIRT2 gets hyper-phosphorylated (Nahhas et al., 2007; North and Verdin, 2007b) caused by the additional phosphorylation of S372/335 by an unknown kinase. Due to its expression profile and implication in neurodegenerative diseases I studied the regulation of SIRT2 by CDK5.

Of the CDK complexes that target SIRT2 at S368/331, CDK5 is particularly interesting, as it is highly abundant in the brain and its protein levels are upregulated in differentiating cells, i.e. oligodendrocytes (He et al., 2011). Furthermore CDK5 is an important cell cycle suppressor in postmitotic neurons (Cicero and Herrup, 2005). Its cell cycle suppressor activities require a nuclear localization of CDK5, which is mediated by an interaction with p27 (Zhang et al., 2008). Upon stress, e.g. induced by β-amyloid accumulation in an Alzheimer's disease (AD) model, association between p27 and CDK5 is disrupted resulting in reduced nuclear CDK5 levels (Zhang et al., 2010). Further evidence for CDK5 dysregulation as a component of neurodegenerative diseases is provided by accumulation of CDK5 and p25 in Levy bodies of AD patients (Lau and Ahlijanian, 2003).

Here I confirmed that p35/CDK5 phosphorylates SIRT2 at S331 in cells and in vitro. Additionally I demonstrated that p35/CDK5 co-expression mediates phosphorylation of SIRT2 at S335. A candidate kinase acting downstream of CDK5 is CDK16, which also

induced phosphorylation of SIRT2 at S335 in cells. It is conceivable that CDK5 translocates to the cytoplasm in postmitotic cells upon stress induction, e.g. by aggregating proteins, where it activates CDK16 and phosphorylates SIRT2 at S331. CDK16 in turn phosphorylates SIRT2 at S335. It remains to be elucidated how hyper-phosphorylation of SIRT2 affects cells. One possible cellular process, which might be activated in this way is autophagy, which is a critical process for degradation of protein aggregates. Recently, Zhao and colleagues provided evidence that cytoplasmic FOXO1 is required for stress-induced autophagy independent of its transcription factor properties in cancer cell lines. They demonstrated that stress induction disrupted an interaction between SIRT2 and FOXO1, which resulted in increased levels of acetylated FOXO1. Acetylated FOXO1 in turn activated the autophagy-regulating protein Atg7 and thus promoted autophagy and cell death (Zhao et al., 2010a). My results support the hypothesis that the CT of SIRT2 administrates an inhibitory effect on the catalytic activity of SIRT2 rather than ligand binding. Perhaps stress-induced hyper-phosphorylation of SIRT2 enhances the inhibitory effect of the CT. This would consequently allow an increase in acetylated FOXO1 levels and in turn-over rates of protein-aggregates by autophagy. The feedback-loop between SIRT2 and CDK5 allows a fine-tuning of this model system. Assuming acetylation of CDK5 by GCN5 inhibits its kinase activity as it did with CDK9 (Sabò et al., 2008), the repressive phosphorylation of SIRT2 would be interrupted. GCN5 is already described to respond to stress such as aggregation of misfolded proteins by inducing gene transcription (Welihinda et al., 1999). However, it has been reported that GCN5 is also found in the cytoplasm of differentiating cell, where it acetylates α-tubulin (Conacci-Sorrell et al., 2010). Therefore it is conceivable that cytoplasmic GCN5 is also activated upon stress signaling to prevent excessive autophagy induction.

My results provide further knowledge about regulatory mechanisms that target SIRT2 and CDK5, two proteins that are involved in postmitotic cell physiology and whose deregulation support neurodegeneration. Therefore my results will help to understand the development of neurodegeneration, which is important to design new drugs to treat affected patients.

4. Experimental Procedures

Materials and Methods are described according to standard protocols used in the Institute of Biochemistry and Molecular Biology, RWTH Aachen University, and modified regarding individual differences in experimental procedures.

4.1 Consumables and reagents

4.1.1 Consumables

Used consumables were purchased from the following companies:

Amersham Biosciences, Ansell, Becton Dickinson, Biometra, Bio-Rad, Biosan, Biotron, Biozym, Brand, Braun, Cellstar, Costar, Eppendorf, eBioscience, Falcon, Fisher Scientific, Fuji, Gibco BRL, Heidolph, Hirschmann, Integra Biosciences, Komberley-Clark, Kojair, Millipore, Nalgene, Nerbe Plus, Omnilab, Rainin, Roth, Sanyo, Sarstedt, Sartorius, Schott Duran, Semper med, Siemens, TPP, VWR

4.1.2 Reagents

Used reagents met at least the criteria for the purity standard *p.a.* and were purchased from the following companies:

Amersham Pharmacia Biotech, AppliChem, Bayer, BD Biosciences, Bode, Biometra, Bio-Rad, Calbiochem, Chroma, Clontech, Eurogentec, Fermentas, Finnzymes, Fluka BioChemika, Gibco, Invitrogen, Invivogen, Merck, New England Biolabs, PAA, Pierce, Qiagen, Roche, Santa Cruz Biotechnology, Seromed, Serva, Sigma, Zymo Research

Reaction kits

- GeneJET™ Plasmid Miniprep Kit (Fermentas)
- NucleoBond® Xtra Maxi Plus (Macherey-Nagel)
- Zymoclean™ Gel DNA Recovery Kit (Zymo Research)
- Zyppy™ Plasmid Miniprep Kit (Zymo Research)

4.2 Oligonucleotides

The following oligonucleotides were purchased from MWG/Operon or Sigma:

Oligonucleotide Name	Sequence: 5' → 3'
CDK5-277-F	AGT TGC AAT GGT GAC CTC GAT CCT
CDK5-279-F	TTG CAA TGG TGA CCT CGA TCC TGA
CDK5-attB1-F	GGG GAC AAG TTT GTA CAA AAA AGC AGG CTC GAT GCA GAA ATA CGA GAA A
CDK5-attB2-R	ACC CAG CTT TCT TGT ACA AAG TGG TCC CCC CTA GGG CGG ACA GAA GTC G

Oligonucleotide Name	Sequence: 5' → 3'
CDK5-K33T-F	CTC ATG AGA TCG TGG CTC TGA CGC GGG TGA GGC
CDK5-K33T-R	AGC CTC ACC CGC GTC AGA GCC ACG ATC TCA TGA G
CDK5-K56R-F	CGG GAG ATC TGC CTA CTC AGG GAG CTG AAG
CDK5-K56R-R	CTT CAG CTC CCT GAG TAG GCA GAT CTC CCG
FOXO1-attB1-F	GGG GAC AAG TTT GTA CAA AAA AGC AGG CTC CAT GGC CGA GGC GCC TCA GGT GGT
FOXO1-attB2-R	GGG GAC CAC TTT GTA CAA GAA AGC TGG GTC TCA GCC TGA CAC CCA GCT ATG TG
FOXO1-sh#1_1	GAT CCC CGC AAT GAT GAC TTT GAT AAC TGC TTC CTG TCA CAG TTA TCA AAG TCA TCA TTG CTT TTT GGA AA
FOXO1-sh#1_2	AGC TTT TCC AAA AAG CAA TGA TGA CTT TGA TAA CTG TGA CAG GAA GCA GTT ATC AAA GTC ATC ATT GCG GG
FOXO1-sh#2_1	GAT CCC CGG ACA ATA AGT CGA GTT ATG GGC TTC CTG TCA CCC ATA ACT CGA CTT ATT GTC CTT TTT GGA AA
FOXO1-sh#2_2	AGC TTT TCC AAA AAG GAC AAT AAG TCG AGT TAT GGG TGA CAG GAA GCC CAT AAC TCG ACT TAT TGT CCG GG
FOXO1-sh#3_1	GAT CCC CGA GTT ATG GAG GTA TGA GTC AGC TTC CTG TCA CTG ACT CAT ACC TCC ATA ACT CTT TTT GGA AA
FOXO1-sh#3_2	AGC TTT TCC AAA AAG AGT TAT GGA GGT ATG AGT CAG TGA CAG GAA GCT GAC TCA TAC CTC CAT AAC TCG GG
FOXO1-sh#4_1	GAT CCC CGG TAT GAG TCA GTA TAA CTG TGC TTC CTG TCA CAC AGT TAT ACT GAC TCA TAC CTT TTT GGA AA
FOXO1-sh#4_2	AGC TTT TCC AAA AAG GTA TGA GTC AGT ATA ACT GTG TGA CAG GAA GCA CAG TTA TAC TGA CTC ATA CCG GG
HDAC6-1614-F	CTG TCA CAG TGC TGA GTA CGT
HDAC6-2552-F	GTC ACC AAG AAG GCA CCC CAA
HDAC6-832-F	TAC GAG CAG GGT AGG TTC T
HDAC6-attB1-F	GGG GAC AAG TTT GTA CAA AAA AGC AGG CTC TAT GAC CTC AAC CGG CCA GGA TTC C

Oligonucleotide Name	Sequence: 5' → 3'
HDAC6-attB2-R	GGG GAC CAC TTT GTA CAA GAA AGC TGG GTC CTT AGT GTG GGT GGG GCA TAT CCT C
hSIRT2-560-R	AGT GTG ATG TGT AGA AGG TGC CGT
p35-attB1-F	GGG GAC AAG TTT GTA CAA AAA AGC AGG CTT GAT GGG CAC GGT GCT GTC CCT GTC TC
p35-attB2-R	GGG GAC CAC TTT GTA CAA GAA AGC TGG GTC TCA CCG ATC CAG GCC TAG GAG GAG C
SIRT2-CT-attB1-F	GGG GAC AAG TTT GTA CAA AAA AGC AGG CTG GGC GGG GGT CCC CAA CCC CAG CAC
SIRT2-CT-attB2-R	GGG GAC CAC TTT GTA CAA GAA AGC TGG GTT TCA CTG GGG TTT CTC CCT CTC TGT
SIRT2-ΔATG-F	ACA AAA AAG CAG GCT ACG ACT TCC TGC GGA ACT T
SIRT2-ΔATG-R	AAG TTC CGC AGG AAG TCG TAG CCT GCT TTT TTG T
SIRT2-ΔG320-F	AGA TGC CCA GTC GTA GGC GGG GGT CCC C
SIRT2-ΔG320-R	GGG GAC CCC CGC CTA CGA CTG GGC ATC T
SIRT2-H150Y-STUI-F	GGA GGC CTA CGG CAC CTT CTA CAC ATC ACA C
SIRT2-H150Y-STUI-R	GTG TGA TGT GTA GAA GGT GCC GTA GGC CTC C
SIRT2-S331/335A-F	GCC CCC AAG AAG GCC CCG CCA CCT
SIRT2-S331/335A-F	CAA CCC CAG CAC TTC AGC TGC CCC CAA GAA
SIRT2-S331/335A-R	AGG TGG CGG GGC CTT CTT GGG GGC
SIRT2-S331/335A-R	TTC TTG GGG CA GCT GAA GTG CTG GGG TTG
SIRT2-S331A-PstI-F	CCC AGC ACT TCT GCA GCC CCC AAG AAG TCC CC
SIRT2-S331A-PstI-R	GGG GAC TTC TTG GGG GCT GCA GAA GTG CTG GG
SIRT2-S331E-F	CAA CCC CAG CAC TTC AGC TGA GCC CAA GAA GGA GCC G
SIRT2-S331E-R	CGG CTC CTT CTT GGG CTC AGC TGA AGT GCT GGG GTT G
SIRT2-S335A-F	TTC CCC CAA GAA GGC CCC GCC ACC TG
SIRT2-S335A-R	CAG GTG GCG GGG CCT TCT TGG GGA A

Oligonucleotide Name	Sequence: 5' → 3'
SIRT2-S335E-F	AGC TTC CCC CAA GAA GGA GCC GCC ACC TGC CAA G
SIRT2-S335E-R	CTT GGC AGG TGG CGG CTC CTT CTT GGG GGA AGC T
SIRT2-sh#3_1	GAT CCC CGT CGC AGA GTC ATC TGT TTT CA AGA GAA AAC AGA TGA CTC TGC GAC TTT TTG GAA A
SIRT2-sh#3_2	AGC TTT TCC AAA AAG TCG CAG AGT CAT CTG TTT TCT CTT GAA AAA CAG ATG ACT CTG CGA CGG G
SIRT2-sh#4_1	GAT CCC CCA TCC ACC GGC CTC TAT GAT CA AGA GAT CAT AGA GGC CGG TGG ATG TTT TTG GAA A
SIRT2-sh#4_2	AGC TTT TCC AAA AAC ATC CAC CGG CCT CTA TGA TCT CTT GAA TCA TAG AGG CCG GTG GAT GGG G

4.3 Plasmids

4.3.1 Cloning vectors/Gateway entry vectors

Plasmid name	Description
pDONR/Zeo	This vector allows for the recombination of *attB*-PCR products into its *att*P1 and *att*P2 sites replacing the Gateway cassette containing the negative selective *ccdB* gene. M13 priming sites allow sequencing of the cloned PCR product in both directions. The EM7 promoter drives expression of the Zeocin resistance genes used for selection in *E. coli*. *rrnB* T1 and T2 transcription terminators protect the cloned gene from expression by vector-encoded promoters (from Invitrogen).
pDONR/Zeo-CDK5	This entry vector was created by a Gateway BP reaction with pDONR/Zeo and GW-pHA-CDK5 (F. Flick).
pDONR/Zeo-CDK5-K33T	This entry vector was created by a Gateway BP reaction with pDONR/Zeo and GW-pHA-CDK5-K33T (F. Flick).
pDONR/Zeo-CDK5-K56R	This entry vector was created by a Gateway BP reaction with pDONR/Zeo and GW-pHA-CDK5-K56R (F. Flick).
pDONR/Zeo-FOXO1	This entry vector was created by a Gateway BP reaction with pDONR/Zeo and an *attB*-PCR product of full length human FOXO1 cDNA amplified from pcDNA3-Flag-FOXO1 (N. Schall).
PDONR/Zeo-HDAC6	This entry vector was created by a Gateway BP reaction with pDONR/Zeo and an *attB*-PCR product of full length human HDAC6 cDNA amplified from pcDNA3-HDAC6-Flag (F. Flick).

Plasmid name	Description
pDONR/Zeo-SIRT2	This entry vector was created by a Gateway BP reaction with pDONR/Zeo and GW-pHA-SIRT2 (F. Flick).
pDONR/Zeo-SIRT2-ΔATG	This entry vector was created by a Gateway BP reaction with pDONR/Zeo and GW-pHA-SIRT2-ΔATG (F. Flick).
pDONR/Zeo-SIRT2-ΔATG-H150Y	This entry vector was obtained from pDONR/Zeo-SIRT2-ΔATG by site-directed mutagenesis using the primers SIRT2-H150Y-STUI-F and SIRT2-H150Y-STUI-R (F. Flick).
pDONR/Zeo-SIRT2-ΔATG-S331/335A	This entry vector was obtained from pDONR/Zeo-SIRT2-ΔATG-S331A by site-directed mutagenesis using the primers SIRT2-S335A-F and SIRT2-S335A-R (F. Flick).
pDONR/Zeo-SIRT2-ΔATG-S331/335E	This entry vector was obtained from pDONR/Zeo-SIRT2-ΔATG-S335E by site-directed mutagenesis using the primers SIRT2-S331E-F and SIRT2-S331E-R (F. Flick).
pDONR/Zeo-SIRT2-ΔATG-S331A	This entry vector was obtained from pDONR/Zeo-SIRT2-ΔATG by site-directed mutagenesis using the primers SIRT2-S331A-PstI-F and SIRT2-S331A-PstI-R (F. Flick).
pDONR/Zeo-SIRT2-ΔATG-S331E	This entry vector was obtained from pDONR/Zeo-SIRT2-ΔATG by site-directed mutagenesis using the primers SIRT2-S331E-F and SIRT2-S331E-R (F. Flick).
pDONR/Zeo-SIRT2-ΔATG-S335A	This entry vector was obtained from pDONR/Zeo-SIRT2-ΔATG by site-directed mutagenesis using the primers SIRT2-S335A-F and SIRT2-S335A-R (F. Flick).
pDONR/Zeo-SIRT2-ΔATG-S335E	This entry vector was obtained from pDONR/Zeo-SIRT2-ΔATG by site-directed mutagenesis using the primers SIRT2-S335E-F and SIRT2-S335E-R (F. Flick).
pDONR/Zeo-SIRT2-ΔATG-ΔG320	This entry vector was obtained from pDONR/Zeo-SIRT2-ΔATG by site-directed mutagenesis using the primers SIRT2-ΔG320-F and SIRT2-ΔG320-R (F. Flick).
pDONR/Zeo-SIRT2-CT	This entry vector was created by a Gateway BP reaction with pDONR/Zeo and an *attB*-PCR product covering the last 33 amino acids of GW-pHA-SIRT2 (F. Flick).
pDONR/Zeo-SIRT2-CT-S331/335A	This entry vector was created by a Gateway BP reaction with pDONR/Zeo and an *attB*-PCR product covering the last 33 amino acids of GW-pHA-SIRT2-S331/335A (F. Flick).
pDONR/Zeo-SIRT2-CT-S331/335E	This entry vector was created by a Gateway BP reaction with pDONR/Zeo and an *attB*-PCR product covering the last 33 amino acids of GW-pHA-SIRT2-ΔATG-S331/335E (F. Flick).

Plasmid name	Description
pDONR/Zeo-SIRT2-CT-S331A	This entry vector was created by a Gateway BP reaction with pDONR/Zeo and an *attB*-PCR product covering the last 33 amino acids of GW-pHA-SIRT2-S331A (F. Flick).
pDONR/Zeo-SIRT2-CT-S331E	This entry vector was created by a Gateway BP reaction with pDONR/Zeo and an *attB*-PCR product covering the last 33 amino acids of GW-pHA-SIRT2-ΔATG-S331E (F. Flick).
pDONR/Zeo-SIRT2-CT-S335A	This entry vector was created by a Gateway BP reaction with pDONR/Zeo and an *attB*-PCR product covering the last 33 amino acids of GW-pHA-SIRT2-S335A (F. Flick).
pDONR/Zeo-SIRT2-CT-S335E	This entry vector was created by a Gateway BP reaction with pDONR/Zeo and an *attB*-PCR product covering the last 33 amino acids of GW-pHA-SIRT2-ΔATG-S335E (F. Flick).
pDONR/Zeo-SIRT2-ΔG320, pDONR/Zeo-SIRT2-H150Y, pDONR/Zeo-SIRT2-S331A, pDONR/Zeo-SIRT2-S335A, pDONR/Zeo-SIRT2-S331/335A	These entry vectors were created by a Gateway BP reaction with pDONR/Zeo and the corresponding GW-pHA vectors (F. Flick).
pDONR201	This vector allows for the recombination of *attB*-PCR products into its *att*P1 and *att*P2 sites replacing the Gateway cassette containing the negative selective *ccdB* gene. *attP* priming sites allow sequencing of the cloned PCR product in both directions. It contains a Kanamycin resistance gene used for selection in *E. coli*. *rrnB* T1 and T2 transcription terminators protect the cloned gene from expression by vector-encoded promoters (from Invitrogen).
pDONR201-CDK5	This entry vector was created by a Gateway BP reaction with pDONR201 and an *attB*-PCR product of full length CDK5 amplified from cDNA of SY5Y neuroblastoma cells (R. Pandithage).
pDONR201-SIRT2	This entry vector was created by a Gateway BP reaction with pDONR201 and an *attB*-PCR product of full length cDNA of SIRT2 isoform 2. The plasmid pLafmid-BA-SIRT2 was used as template for the *attB*-PCR reaction (R. Pandithage).
pDONR201-SIRT2-ΔATG	This entry vector was obtained from pDONR201-SIRT2 by site-directed mutagenesis using the primers SIRT2-ΔATG-F and SIRT2-ΔATG-R (F. Flick).

Plasmid name	Description
pDONR201-SIRT2-H150Y	This entry vector was obtained from pDONR201-SIRT2 by site-directed mutagenesis using the primers SIRT2-H150Y-STUI-F and SIRT2-H150Y-STUI-R (R. Pandithage).
pDONR201-SIRT2-S331/335A	This entry vector was obtained from pDONR201-SIRT2-S335A by site-directed mutagenesis using the primers SIRT2-S331/335A-F and SIRT2-S331/335A-R (F. Flick).
pDONR201-SIRT2-S331A	This entry vector was obtained from pDONR201-SIRT2 by site-directed mutagenesis using the primers SIRT2-S331A-PstI-F and SIRT2-S331A-PstI-R (R. Pandithage).
pDONR201-SIRT2-S331E	This entry vector was obtained from pDONR201-SIRT2 by site-directed mutagenesis using the primers SIRT2-S331E-F and SIRT2-S331E-R (R. Pandithage).
pDONR201-SIRT2-S335A	This entry vector was obtained from pDONR201-SIRT2 by site-directed mutagenesis using the primers SIRT2-S335A-F and SIRT2-S335A-R (F. Flick).
pLafmid-BA-SIRT2	The vector was purchased from RZPD, Berlin and encodes the clone IMAGp998N11146q2, which encompasses the full length cDNA of human SIRT2 isoform 2. According to sequencing analysis the cDNA sequence was identical to the sequence described by Ashfar and Murnane (Afshar and Murnane, 1999).
pSuper	This vector contains the PolIII promoter of H1 and drives the expression of shRNAs when appropriate oligonucleotides are inserted in *Bgl*II/*Hind*III sites (R. Lilischkis).

4.3.2 Prokaryotic expression plasmids

Plasmid name	Description
GW-pGST	This vector is derived from pGEX-4T-2 (GE Healthcare), which was made compatible with the Gateway system by insertion of the Gateway cassette Reading frame A (RfA) into the MCS. It allows for the IPTG-inducible gene expression of an N-terminally GST-tagged protein under control of a *tac* promoter and the *lac* operator (R. Lilischkis).
GW-pGST-SIRT2-CT, (S331A), (S335A), (S331/335A), (S331E), (S335E), (S331/335E)	These vectors were created by a LR reaction with GW-pGST and the corresponding pDONR/Zeo entry vectors (F. Flick).

Plasmid name	Description
GW-pGST-SIRT2-ΔATG, (S331A), (S335A), (S331/335A), (S331E), (S335E), (S331/335E), (ΔG320), (H150Y)	These vectors were created by a LR reaction with GW-pGST and the corresponding pDONR/Zeo entry vectors (F. Flick).

4.3.3 Eukaryotic expression plasmids

Plasmid name	Description
GW-pBac-GST	This vector was derived from pVL1392 (BD Bioscience) and made compatible with the Gateway system by insertion of the Gateway cassette Reading frame C1 (RfC1). It is a Baculovirus Transfer Vector that drives the gene expression of GST-fusion proteins under the polyhedrin promoter of AcNPV (R. Pandithage).
GW-pBac-GST-CDK5	This vector was created by a LR reaction with GW-pBAC-GST and the corresponding pDONR/Zeo entry vector (N. Schall).
GW-pBS-CassA-T3	This vector was derived from pBluscript II KS+ and made compatible with the Gateway system by insertion of the Gateway cassette Reading frame A (RfA) into the *Eco*RV site. It drives the *in vitro* transcription from the T3 promoter (R. Lilischkis).
GW-pBS-CassA-T3-CDK5	This vector was created by a LR reaction with GW-pBS-CassA-T3 and the corresponding pDONR/Zeo entry vector (F. Flick).
GW-pBS-CassA-T3-FOXO1	This vector was created by a LR reaction with GW-pBS-CassA-T3 and the corresponding pDONR/Zeo entry vector (N. Schall).
GW-pBS-CassA-T3-HDAC6	This vector was created by a LR reaction with GW-pBS-CassA-T3 and the corresponding pDONR/Zeo entry vector (D. Otten).
GW-pcDNA5/FRT/TO	This vector was derived from pcDNA5/FRT/TO and made compatible with the Gateway system by insertion of the Gateway cassette Reading frame A (RfA) into the *Hind*III site (A. Forst).
GW-pcDNA5/FRT/TO-SIRT2, (S331A), (S335A), (S331/335A), (S331E), (S335E), (S331/335E), (ΔG320), (H150Y)	These vectors were created by a LR reaction with GW-pcDNA5/FRT/TO and the corresponding pDONR/Zeo entry vectors (F. Flick).

Plasmid name	Description
GW-pECFP	The vector pECFP was made compatible with the Gateway system by insertion of the Gateway cassette Reading frame C1 (RfC1) into the *Sma*I site. It allows for the gene expression of N-terminally ECFP-tagged proteins (K. Montzka).
GW-pECFP-CDK5, (K33T), (K56R)	These vectors were created by a LR reaction with GW-pECYFP and the corresponding pDONR/Zeo entry vectors (F. Flick).
GW-pECFP-SIRT2-ΔATG, (S331A), (S335A), (S331/335A), (S331E), (S335E), (S331/335E), (ΔG320), (H150Y)	These vectors were created by a LR reaction with GW-pECYFP and the corresponding pDONR/Zeo entry vectors (F. Flick).
GW-pHA	This vectors allows for the gene expression of N-terminally HA-tagged proteins in eukaryotic cells under control of a strong CMV promoter (Matthias et al., 1989). The vector contains the pSP65 plasmid sequences, a human CMV promoter/enhancer, the translation initiation region from the HSV thymidine kinase, the splicing and polyadenylation signals from the rabbit ß-globin gene and the SV40 origin of replication. It was made compatible with the Gateway system by insertion of the Gateway cassette Reading frame C1 (RfC1) into the *Sma*I site (R. Lilischkis).
GW-pHA-CDK5	This vector was created by a LR reaction with GW-pHA and the corresponding pDONR201 entry vector (R. Pandithage).
GW-pHA-CDK5-K33T	This vector was obtained from GW-pHA-CDK5 by site-directed mutagenesis using the primers CDK5-K33T-F and CDK5-K33T-R (F. Flick).
GW-pHA-CDK5-K56R	This vector was obtained from GW-pHA-CDK5 by site-directed mutagenesis using the primers CDK5-K56R-F and CDK5-K56R-R (F. Flick).
GW-pHA-HDAC6	This vector was created by a LR reaction with GW-pHA and the corresponding pDONR/Zeo entry vector (D. Otten).
GW-pHA-SIRT2-S335A, GW-pHA-SIRT2-S331/335A	These vectors were created by a LR reaction with GW-pHA and the corresponding pDONR201 entry vectors (F. Flick).
GW-pHA-SIRT2-ΔATG	This vector was created by a LR reaction with GW-pHA and the corresponding pDONR201 entry vector (F. Flick).

Plasmid name	Description
GW-pHA-SIRT2-ΔATG, (S331A), (S335A), (S331/335A), (S331E), (S335E), (S331/335E), (ΔG320), (H150Y)	These vectors were created by a LR reaction with GW-pHA and the corresponding pDONR/Zeo entry vectors (F. Flick).
GW-pHA-SIRT2-ΔG320	This vector was obtained from GW-pHA-SIRT2 by site-directed mutagenesis using the primers SIRT2-ΔG320-F and SIRT2-ΔG320-R (A. Wolf).
GW-pHA-SIRT2, (H150Y), (S331A)	These vectors were created by a LR reaction with GW-pHA and the corresponding pDONR201 entry vectors (R. Pandithage).
pBabe Puro	This is a retroviral mammalian expression vector driving the expression of a puromycin resistance gene under the control of a SV40 early promoter (Morgenstern and Land, 1990).
pBluescript II KS+	This vector is designed for DNA cloning, didesoxy-DNA sequencing, *in vitro* mutagenesis and *in vitro* transcription. It contains the intergenic region of phage f1; the pMB1 replicon responsible for the replication of the vector; the *bla*-gene, coding for β-lactamase, that confers resistance to ampicillin and *lacZ,* the 5'-terminal part of the *lacZ* gene encoding the N-terminal fragment of β-galactosidase (from Fermentas).
pcDNA3-Flag-FOXO1	This vector was obtained from the pcDNA3-Flag backbone vector by inserting full length human FOXO1 cDNA between the *Bam*H1 and *Xba*I sites and drives the mammalian gene expression of N-terminally Flag-tagged FOXO1 from a CMV-promoter. It contains an Ampicillin resistance gene used for selection in *E. coli* (from Addgene).
pcDNA3-HDAC6-Flag	This vector was obtained from the pcDNA3.1+ backbone vector by inserting full length human HDAC6 cDNA at the *Not*1 site and it drives the mammalian gene expression of C-terminally Flag-tagged HDAC6 from a CMV-promoter. Furthermore it contains an Ampicillin resistance gene used for selection in *E. coli* (from Addgene).

Plasmid name	Description
pcDNA5/FRT/TO	This vector is a 5.1 kb inducible gene expression vector designed for usage with the Flp-In-T-REx-System from Invitrogen. It features a CMV-promoter for high level tetracycline-regulated expression of the gene of interest in a wide range of mammalian cells; a multiple cloning site with 10 unique restriction sites to facilitate cloning of the gene of interest; a FLP Recombination Target (FRT) site for Flp recombinase-mediated integration of the vector into the Flp-In-T-REx-host cell line and a Hygromycin resistance gene for selection of stable cell lines (from Invitrogen).
pCMV-myc-p35	This vector drives the gene expression of the myc-tagged p35 protein in mammalian cells from a CMV promoter (R. Pandithage).
pEGFP-Tubulin	This vector drives the gene expression of the EGFP-tubulin fusion protein in mammalian cells. The protein incorporates directly into microtubules and thereby allows the observation of microtubules in living or fixed cells by fluorescence microscopy. The vector was used as a control for transfection efficiency (from BD Bioscience/Clontech).
pEQ176P2	This vector was routinely used for control transfections for CMV-containing vectors if the respective backbone vector for the transfected plasmid was not available. It is derived from pEQ176, which drives expression of the ß-galactosidase gene under control of a CMV promoter. Most of the cDNA encoding ß-galactosidase was cut out by a *Pvu*II restriction digest (J. Lüscher-Firzlaff).
pSuper r Ash #5 false	This vector drives the gene expression from the histone H1 PolIII promoter of a non-functional shRNA targeted against the Ash2 mRNA. This vector was routinely used for control transfections for PolIII promoter-containing vectors (J. Lüscher-Firzlaff).
pSuper-sh-FOXO1#1,2,3,4	These vectors were derived from pSuper by insertion of the hybridized oligonucleotides sihSIRT2#3,4 between the *Bgl*II and *Hind*III sites. They drive the gene expression of shRNAs designed for targeting the human FOXO1 mRNA (F. Flick).
pSuper-sh-hSIRT2#3,4	These vectors were derived from pSuper by insertion of the hybridized oligonucleotides sihSIRT2#3,4 between the *Bgl*II and *Hind*III sites. They drive the gene expression of shRNAs designed for targeting the human SIRT2 mRNA (F. Flick).

4.4 Antibodies

Antibody name	Description
α-acetylated-Tubulin (6-11B-1)	Monoclonal mouse IgG_{2b} antibody that recognizes an epitope located on α-tubulin within four residues of K40 when this amino acid is acetylated. It is raised against acetylated tubulin from the outer arm of *Strongylocentrotus purpuratus* (sea urchin) (Sigma).
α-alpha-Tubulin (B-5-1-2)	Monoclonal mouse IgG_1 antibody that recognizes an epitope located at the C-terminal end of the α-tubulin isoform in a variety of organisms. It is raised against Sarkosyl-resistant ribbons from *Strongylocentrotus purpuratus* (Sea Urchin) sperm axonemes (Sigma).
α-GFP (JM-3999-100)	Polyclonal rabbit antibody, that recognizes the wildtype Green Fluorescence protein (GFP) from the pacific jellyfish, *Aequorea victoria* and its variants EGFP and EBFP, etc., even though it is introduced into unrelated recombinant proteins by "epitope tagging" (MBL).
α-GFP (9F9-F9)	Monoclonal mouse IgG_{2a} antibody that recognizes the Green Fluorescence protein (GFP) and its variants rGFP and eGFP, even though GFP is introduced into unrelated recombinant proteins by "epitope tagging". The antibody was raised against a GST-GFP fusion protein corresponding to the full length amino acid sequence (246 aa) derived from the jellyfish *Aequorea victoria* (Rockland).
α-GST (6G9)	Monoclonal rat IgG_{2a} antibody recognizing Glutathione S-Transferase (GST) from *Schistosoma japonicum*, even though it is introduced into unrelated recombinant proteins by "epitope tagging". It was raised against a GST-fusion protein (E. Kremmer).
α-HA (3F10)	Monoclonal rat IgG1 antibody that recognizes the HA peptide sequence (YPYDVPDYA) derived from the influenza hemagglutinin protein, even when the HA peptide is introduced into unrelated recombinant proteins by "epitope tagging" (Roche).
α-mouse IgG + IgM (H+L) HRP-conjugated (115-036-068)	Horseradish Peroxidase conjugated secondary antibody from goat recognizing the heavy and light chains of mouse IgG and IgM antibodies (Jackson Immuno Research).
α-rabbit IgG (H+L) HRP-conjugated (111-035-140)	Horseradish Peroxidase conjugated secondary antibody from goat recognizing the heavy and light chains of rabbit IgG antibodies (Jackson Immuno Research).
α-rat IgG + IgM (H+L) HRP-conjugated (112-035-068)	Horseradish Peroxidase conjugated secondary antibody from goat recognizing the heavy and light chains of rat IgG and IgM antibodies (Jackson Immuno Research).

Antibody name	Description
α-SIRT2 (11F11)	Monoclonal rat IgG antibody recognizing SIRT2 when both S331 and S335 are phosphorylated. It was raised against a C-terminal SIRT2 peptide, which was phosphorylated at S335 (E. Kremmer).
α-SIRT2 (11H2)	Monoclonal rat IgG antibody recognizing SIRT2 when S331 is phosphorylated. It was raised against a C-terminal SIRT2 peptide, which was phosphorylated at S331 (E. Kremmer).
α-SIRT2 (1C5)	Monoclonal rat IgG antibody recognizing SIRT2 when both S331 and S335 are phosphorylated. It was raised against a C-terminal SIRT2 peptide, which was phosphorylated at S331 and S335 (E. Kremmer).
α-SIRT2 (3C8)	Monoclonal rat IgG antibody recognizing SIRT2 when S335 is not phosphorylated. It was raised against a C-terminal SIRT2 peptide, which was phosphorylated at S331 (E. Kremmer).
α-SIRT2 (4C4)	Monoclonal mouse IgG$_1$ antibody recognizing SIRT2 when S331 and S335 are phosphorylated. It was raised against a C-terminal SIRT2 peptide, which was phosphorylated at S331 and S335 (E. Kremmer).
α-SIRT2 (6B5)	Monoclonal rat IgG antibody recognizing SIRT2 when S331 is phosphorylated and S335 is not phosphorylated. It was raised against a C-terminal SIRT2 peptide, which was phosphorylated at S331 (E. Kremmer).
α-SIRT2 (6H10) and (7F2)	Monoclonal mouse IgG antibodies recognizing SIRT2 when S331 is not phosphorylated. It was raised against a C-terminal SIRT2 peptide, which was phosphorylated at S335 (E. Kremmer).
α-SIRT2 (7G5)	Monoclonal rat IgG antibody recognizing SIRT2 independent of phosphorylation at S331 or S335. It was raised against a C-terminal SIRT2 peptide, which was phosphorylated at S331 (E. Kremmer).
α-SIRT2 T749	Polyclonal rabbit antiserum recognizing SIRT2 (E. Kremmer).

4.5 Work with nucleic acids

4.5.1 Enzymatic manipulation of plasmid DNA

10x "Magic" buffer   200 mM Tris Cl pH 7.5
                                         700 mM NaCl
                                         200 mM KCl
                                         100 mM Magnesium chloride
                                         0.5 mM Spermine
                                         0.125 mM Spermidine

Restriction endonucleases recognize short DNA sequences and cleave double-stranded DNA at specific sites within or adjacent to the recognition sequence. In this work restriction digests were used to identify plasmids and to transfer restriction fragments between plasmids.

Restriction enzymes and buffers were purchased from Fermentas and used according to manufacturer's instructions in a 20 µl reaction volume with 0.5 µl of each restriction enzyme used and 2 µl of the appropriate 10x buffer. Reactions were incubated for 1 hour to over-night at the appropriate temperature, in general 37 °C. Double digests were transformed in magic buffer.

A thermosensitive alkaline phosphatase FastAP (Fermentas) was used to dephosphorylate terminal 5' phosphates according to manufacturer's instructions.

DNA was ligated using T4 DNA ligase (Fermentas). Sticky-end ligations were carried out for 1-2 hours at room temperature. For blunt-end ligations, 5 % PEG2000 was included in the reaction, and the reaction was incubated over-night at 16 °C.

4.5.2 The Polymerase Chain Reaction

The polymerase chain reaction (PCR) is an *in vitro* assay to enzymatically amplify a specific segment of double stranded DNA. The assay requires two oligonucleotides (primers), which are complementary to flanking sequences of the target DNA segment and provide a free 3' hydroxyl group (3'-OH). After denaturation of the template DNA double strand the primers hybridize to opposite strands of DNA with their 3' ends facing each other. Then a thermostable DNA polymerase catalyzes the synthesis of a new strand in 5' $\rightarrow$ 3' direction starting at the 3'-OH group of each primer. After the first cycle these two new strands are of indeterminate length and serve as templates for following cycles, which result in the exponential accumulation of a discrete DNA product exactly the length of sequence between both primer ends (Saiki et al., 1988).

PCR amplifications were performed using 1-2 Units of Phusion® High-Fidelity DNA Polymerase (Finnzymes) according to manufacturer's instructions. PCR products were analyzed by agarose gel electrophoresis for yield and specificity.

4.5.3 Agarose gel electrophoresis

TBE   89 mM Tris base
                                         89 mM Boric acid
                                         2 mM EDTA

10x Agarose loading buffer	50 mM Tris Cl, pH 8
	50 mM EDTA
	50 % (v/v) Glycerine
	0.25 % (w/v) Bromphenol blue
	0.25 % (w/v) Xylene cyanol
Agarose gel solution	0.8-2 % (w/v) Agarose Low EEO
	or 3.5-4 % (w/v) Biozym Sieve GP Agarose
	0.01 % (v/v) Ethidium bromide
	TBE

The following protocol was used to separate and identify DNA fragments by their length in an electric field as they run through an agarose gel towards the anode. Ethidium bromide was used to visualize DNA fragments upon illumination with UV light and fragment size was estimated on basis of a molecular weight marker.

For preparation of the agarose gel the melted gel solution was poured into a gel casting platform and a gel comb was inserted. After the gel hardened the comb was removed and the gel placed in an electrophoresis tank. The tank was filled with TBE buffer until gel and sample slots were covered. DNA samples in 10x loading buffer and a molecular weight marker (GeneRuler™ DNA ladder from Fermentas) were loaded into sample wells and electrophoretically separated at 10 V/ cm gel distance. Ethidium bromide stained DNA fragments were visualized and photographed in a gel imaging system from BioRad (ChemiDoc™).

4.5.4 Gel extraction of DNA

Purification and concentration of DNA from agarose gels after electrophoresis was performed using the Zymoclean Gel DNA Recovery Kit™ (Zymo Research) according to manufacturer's instructions.

4.5.5 Gateway cloning

The Gateway Technology (Invitrogen) is a universal cloning method based on the site-specific recombination properties of bacteriophage lambda (Landy, 1989). It provides a way to move DNA sequences into multiple vector systems (Hartley et al., 2000).

According to this cloning strategy the desired DNA sequence is amplified by PCR using primers possessing the recombination sites (*att*-sites). Afterwards the PCR product flanked by *att*-sites is recombined into a so-called entry vector. This entry vector then can be used to recombine the DNA sequence of interest into different destination vectors depending on the intended use.

Gateway cloning was performed according to the manufacturer's instructions with slight modifications. PCR amplification was performed using 1-2 Units of Phusion High-Fidelity DNA Polymerase (Finnzymes) according to manufacturer's instructions. The recombination reactions were carried out over-night with half the amount of reagents as recommended.

4.5.6 Site-directed mutagenesis

Site directed mutagenesis was performed according to Stratagene's QuikChange® II Site-Directed Mutagenesis protocol. It is a three step procedure, in which both strands of a

methylated double-stranded DNA vector with an insert of interest are replicated using primers containing the desired mutation. After replication the product is treated with *Dpn* I, an endonuclease specific for methylated and hemimethylated DNA. *Dpn* I digests the parental DNA template and thus selects the mutation-containing synthesized DNA, which is then transformed into competent *Escherichia coli* (*E. coli*) cells for amplification (Stratagene).

Primers for site-directed mutagenesis were designed using the online available QuikChange Primer Design tool (Stratagene). The mutagenesis was carried out following the manufacturer's instructions. All obtained plasmids were checked for correct amplification by sequencing of the whole insert DNA (MWG or SeqLab).

4.5.7 Generation of pSuper-based siRNA constructs

RNA interference to suppress specific gene expression was induced by using the pSUPER RNAi system in, which a mammalian expression vector directs intracellular synthesis of short interfering RNAs (siRNAs) from a polymerase-III H1-RNA gene promoter (Brummelkamp et al., 2002).

siRNA oligonucleotides targeting the desired sequence were designed using the online available program siDirect (Naito et al., 2004). Chosen sequences were verified to be specific for both strands by using the BLAST algorithm. An oligonucleotide was designed according to the following scheme: 5'-GAT CCC C-*target sequence*-TTC AAG AGA-*complementary sequence*-TTT TTG GAA A-3'. Another oligonucleotide was designed according to the following scheme: 5'-AGC TTT TCC AAA AA-*target sequence*-TCT CTT GAA-*complementary sequence*-GGG-3'. The hybridized oligonucleotides were cloned into pSuper (Brummelkamp et al., 2002) digested with *Bgl*II and *Hind*III.

4.6 Work with prokaryotic cells

4.6.1 Bacteria strains

Name of the bacterial strain	Genotype
E.coli XL10-Gold (Stratagene)	Tet^r D (*mcrA*)*183* D(*mcrCB-hsdSMR-mrr*)*173 endA1 supE44 thi-1 recA1 gyrA96 relA1 lac* Hte [F' *proAB lacI^q Z*D*M15* Tn*10* (Tet^r) Amy Cam^r]
E.coli DH5α (Invitrogen)	F$^-$ φ80dlacZΔM15 Δ(lacZYA-argF) U169 deoR, re-cA1 endA1 hsdR17(r$_k$$^-$ m$_k$$^+$) phoA supE44 λ$^-$ thi-1 gyrA96 relA1
E.coli BL21 (DE3) pLysS (Stratagene)	B F$^-$ *dcm ompT hsdS*(r$_B$$^-$ m$_B$$^-$) *gal* λ(DE3) [pLysS Cam^r]

4.6.2 Materials for work with prokaryotic cells

LB medium   1 % (w/v) Tryptone
                                              0.5 % (w/v) Yeast extract
                                              1 % (w/v) NaCl
                                              pH 7

Low salt LB medium	1 % (w/v) Tryptone
	0.5 % (w/v) Yeast extract
	0.5 % (w/v) NaCl
	pH 7.5

Agar plates (Ampicillin/Kanamycin)	LB medium
	1.5 % (w/v) Agar Bacteriology grade
	100 g/ml Ampicillin
	30 g/ml Kanamycin

Agar plates (Zeocin)	Low salt LB medium
	1.5 % (w/v) Agar Bacteriology grade
	50 g/ml Zeocin

4.6.3 Bacterial transformation

Introduction of plasmid DNA into bacterial cells (transformation) was essentially performed according to the basic protocol 1 from chapter 1.8 of "Current Protocols in Molecular Biology" (Seidman and Struhl, 2001).

100 µl chemically competent bacteria were rapidly thawed by warming between hands and mixed with plasmid DNA, in general 100-500 ng. After up to 30 minutes incubation on ice cells were heat-shocked by placing the tube into a 42 °C water bath for 45 seconds. After heat shock the tube was immediately placed back on ice. 1 ml of LB medium (heated up to 37 °C) was added after 2 minutes incubation on ice and bacteria incubated for 1 hour at 37 °C and 250 rpm. Afterwards bacteria were pelleted by centrifugation, resuspended in 100 µl of LB medium and seeded on LB agar plates containing the appropriate antibiotic. Plates were incubated over-night at 37 °C until bacterial colonies got visible.

4.6.4 DNA preparation

| TE buffer | 10 mM Tris Cl, pH 7.5 |
| | 1 mM EDTA |

Plasmid DNA was extracted from transformed bacteria using the Qiagen Plasmid Maxi Kit (Qiagen) for large-scale preparation and the GeneJET™ Plasmid Miniprep Kit (Fermentas) for small-scale preparation according to manufacturer's instructions. Both protocols are based on a modified alkaline lysis procedure, in which the differential denaturation capacities of chromosomal and plasmid DNA are used to separate them (Ehrt and Schnappinger, 2003). Isolated plasmid DNA is either concentrated and desalted by isopropanol precipitation (Qiagen) or by binding on a silica membrane and after several washing steps, subsequent elution in a smaller volume of TE buffer or sterile water (Fermentas).

4.6.5 Purification of GST fusion proteins

TNE buffer	20 mM Tris Cl pH 8.0
	150 mM NaCl
	1 mM EDTA
	5 mM DTT
	1 mM Pefabloc SC
	14 µg /ml Aprotinin

GST washing buffer	100 mM Tris Cl pH 8.0
	120 mM NaCl

GST elution buffer	100 mM Tris Cl pH 8.0
	120 mM NaCl
	20 mM Glutathione

Purification of GST fusion proteins was essentially performed according to the basic protocol 1 from chapter 6.6 of "Current Protocols in Protein Science" (Harper and Speicher, 2008).

BL21 bacteria were transformed with the corresponding GW-pGST plasmid. Two to three colonies of transformed bacteria were used to inoculate a starter culture of usually 50 ml LB medium supplemented with 1 % Glucose, 1 mM $ZnCl_2$ (Merck) and the appropriate antibiotic, which was grown over-night at 37 °C.

The main culture was started by dilution of the starter culture at least 1:30 in the same type of medium and grown at 37 °C. When the culture reached an OD_{600} of 0.5-0.7 gene expression of GST-fusion protein was induced by addition of 1 mM IPTG. Gene expression was allowed over-night at room temperature.

Bacteria were pelleted by centrifugation at 3500x g, resuspended in ice-cold TNE buffer and lysed for 30 minutes on ice in the presence of 100 μg/ ml lysozyme (AppliChem). Cells were solubilized by sonication and lysates cleared from cell debris by centrifugation at 10,000 g for 30 minutes.

The supernatant was incubated with 500 μl equilibrated Glutathione Sepharose 4B beads (Amersham Biosciences) per 30 ml of lysate for 1 hour at 4 °C. Beads were washed three times with PBS and transferred to a 0.8 x 4 cm chromatography column (Bio-Rad). After washing with 1 ml of GST wash buffer bound proteins were eluted in three fractions à 300 μl with GST elution buffer.

Aliquots of the eluted proteins were subjected to SDS-PAGE and subsequent Coomassie staining in order to estimate the concentration of the purified proteins in comparison to a BSA standard series.

4.7 Work with eukaryotic cells (Cell culture)

4.7.1 Eukaryotic cell lines

Name of the eukaryote cell line	Description
HEK 293 (ATCC CRL-1573)	This is an adherent epithelial cell line derived from human embryonic kidney (HEK) cells transformed with Adenovirus 5 DNA. The Ad5 insert is integrated into chromosome 19q13.2. It is a hypotriploid cell line with a modal chromosome number of 64, occurring in 30 % of cells.
HCT 116 (ATCC CCL247)	This is an adherent epithelial cell line derived from human a colorectal carcinoma. The stem line chromosome number is near diploid with the modal

Name of the eukaryote cell line	Description
	number at 45 (62 %) and polyploids occurring at 6.8 %. The cells have been reported to be positive for keratin by immunoperoxidase staining and for transforming growth factors beta 1 and 2 (TGFβ1, 2) gene expression. This line has a mutation in codon 13 of the ras protooncogene
HeLa (ATCC CCL-2)	This is an adherent epithelial cell line derived from a cervical adenocarcinoma of a 31 year old black female. 100 % aneuploidy is observed with a modal chromosome number of 82. HeLa cells have been reported to contain HPV-18 sequences, p53 gene expression was reported to be low, and normal levels of pRB were found.
Flp-In T-REx-HeLa (Invitrogen #R714-07)	This cell line was derived from HeLa. It expresses the Tet-repressor gene from pcDNA6/TR and contains a single integrated Flp recombination target (FRT) site from pFRT/lacZeo resulting in expression of a lacZ-Zeocin fusion gene. This cell line can be used to generate a tetracycline-inducible expression cell line by cotransfecting the pcDNA5/FRT/TO expression vector containing your gene of interest and the Flp recombinase expression plasmid, pOG44.
Flp-In T-REx-HeLa-SIRT2, -S331A, -S335A, -S331/335A, -S331E, -S335E, -S331/335E, -ΔG320, -H150Y	This stably transfected cell lines were generated by transfection of Flp-In T-REx-HeLa cells with pOG44 and pcDNA5/FRT/TO or the corresponding GW-pcNA5/FRT/TO construct. Stable cell lines were obtained by selection with Hygromycin B and Blasticidin S.

4.7.2 Materials for cell culture work

PBS   140 mM NaCl
                                    2.6 mM KCl
                                    2 mM Na_2HPO_4
                                    1.45 mM KH_2PO_4

McCoy's 5A (Gibco)

DMEM (Gibco) with 4.5 g/ l Glucose

10 mg/ml Blasticidin S (Invitrogen)

1 mg/ml Doxycyclin (Sigma)

100 mg/ml Hygromycin B (InvivoGen)

10 000 Units/ml Penicillin/10 000 μg/ml Streptomycin (Seromed)

0.5/0.2 % (w/v) Trypsin/EDTA in PBS (Seromed)

FCS (Gibco)

Dimethyl Sulfoxide (DMSO) Cell culture grade (AppliChem)

∅ 6 cm/10 cm Tissue culture dishes (Sarstedt)

6-Well Tissue culture plates (TPP)

1 ml Cryotubes (Nalgene)

4.7.3 Cell Culture conditions

All cell lines were cultured under humidified atmosphere of 5 % CO_2 at 37 °C.

HEK 293 and HeLa cells were cultured in DMEM supplemented with 10 % (v/v) FCS and 1 % (v/v) Penicillin/Streptomycin.

HCT 116 cells were cultured in McCoy's 5A supplemented with 10 % (v/v) FCS and 1 % (v/v) Penicillin/Streptomycin.

Stably transfected Flp-In T-REx-HeLa cell lines were maintained in regular DMEM supplemented with 15 μg/ml Blasticidin S and 200 μg/ml Hygromycin B.

4.7.4 Trypsinizing and subculturing cells from a monolayer

For subculturing of an adherent monolayer cell culture grown to confluency in a ∅ 10 cm tissue culture dish the old tissue culture medium was removed and cells rinsed with PBS to remove any residual FCS that may inhibit trypsin reaction. 1 ml Trypsin/EDTA was added to the cells and the dish swayed until the whole surface was covered before it was placed into a cell culture incubator. When cells detached from the dish surface fresh medium was added and an aliquot of trypsinized cells transferred to a new prepared tissue culture dish.

4.7.5 Cryo-conservation and thawing of cells

For cryo-conservation, $5-8x10^6$ pelleted cells grown to log phase were resuspended in 1 ml FCS supplemented with 10 % (v/v) DMSO and transferred into a cryotube. After incubation on ice for 30 minutes, the cryotubes were wrapped in several layers of tissue paper, put into an isolating box and slowly cooled down for 16-48 hours at -80 °C. Afterwards, the cryotubes were transferred to -150 °C for long-term storage.

For thawing of frozen cells, cryotubes were rapidly thawed in a water bath at 37 °C. Immediately after melting of ice crystals, cells were suspended in 10 ml culture medium, pelleted by centrifugation, resuspended in 10 ml culture medium and transferred to an appropriate culture dish or flask.

4.7.6 Transfection of DNA into eukaryotic cells

Calcium Phosphate Transfection

2x Hebs buffer   274 mM NaCl
                              42 mM HEPES
                              9.6 mM KCl
                              1.5 mM Na_2HPO_4
                              pH 7.1

HEPES buffer	142 mM NaCl
	10 mM HEPES
	6.7 mM KCl
	pH 7.3

The transient transfection of HEK293 and HeLa cells was performed according to the calcium phosphate method (Chen and Okayama, 1988). This method is based on the precipitate formation of calcium-phosphate-DNA complexes, which are taken up by cells through endocytosis.

The day prior to the transfection, about $1x10^6/4x10^5$ cells were seeded on $\varnothing$ 10 cm/$\varnothing$ 6 cm tissue culture dishes. For transfection, 20 µg/4 µg of total DNA was diluted in 500 µl/200 µl 250 mM CaCl$_2$. Subsequently, 500 µl/200 µl 2x Hebs buffer was added, the solution briefly vortexed for 3 seconds and incubated for 15 minutes at ambient temperature. Afterwards the solution was pipetted onto the cell monolayer. The dishes were swayed and put back into the incubator. After 5-6 hours incubation time, the cells were freed from residual precipitate by washing with 5 ml/2 ml HEPES buffer. Subsequently, fresh medium was added.

Calcium phosphate transfection of HeLa cells was performed according to the standard instructions with slight modifications. For transfection of a 40 % confluent $\varnothing$ 10 cm plate of HeLa cells 20 µg DNA was diluted in 950 µl 1x Hebs buffer, pH 6.95. Precipitate formation was induced by adding 50 µl 2.5 M CaCl$_2$.

Cationic Lipid-mediated Transfection

Cationic lipid-mediated transfection of eukaryotic cells is based on the ability of positively charged (cationic) lipids to form complexes with nucleic acid polymers due to ionic interactions. The cationic and lipophilic character of these aggregates then allows crossing of the negatively charged and hydrophobic cell membrane of target cells (Felgner et al., 1987).

Transfection of HeLa cells was performed by using ExGen 500 (Fermentas) according to manufacturer's instructions with an ExGen 500/DNA ratio of 3.3:1.

FuGeneHD (Roche) was used for the transfection of HCT 116 cells according to the manufacturer's instructions with an FuGeneHD/DNA ratio of 6:2.

4.7.7 Preparation of cell lysates

RIPA buffer	10 mM Tris Cl, pH 7.4
	150 mM NaCl
	1 % Nonidet P40 Substitute
	1 % Sodium deoxycholate
	0.1 % SDS

CoIP buffer	10 mM HEPES, pH 7.5
	50 mM NaCl
	30 mM tetra-Sodium pyrophosphate
	50 mM Sodium fluoride
	5 µM Zinc chloride
	0.2 % Triton X-100
	10 % Glycerine
	pH 7.05

Phosphatase Inhibitors	100 µM Sodium ortho-vanadate
	20 mM Sodium ß-glycerophosphate
	0.05 µM Ocadaic acid
	50 mM Sodium fluoride

Cells of a $\varnothing$ 10 cm tissue culture dish grown to confluency were gathered in the supernatant or fresh culture medium and pelleted by centrifugation at 200x g for 3 minutes at 4 °C. Pelleted cells were washed in 5 ml PBS and pelleted by centrifugation again.

Cell pellets were stored at -20 °C for at least 1 hour before lysis in 750 µl CoIP buffer or RIPA buffer supplemented with ProteoBlock Protease Inhibitor Cocktail (Fermentas) and phosphatase inhibitors. CoIP-lysates were incubated on ice for 30 minutes before cell debris was spun down at 16 000x g for 30 minutes at 4 °C. RIPA-lysates were sonicated for 15 minutes at high level in the Bioruptor from Diagenode at 4 °C before cell debris was spun down. The supernatant was transferred to a new reaction tube and used immediately for further analysis.

4.8 Work with proteins

4.8.1 Immunoprecipitation

This method describes the isolation of an antigen by binding to a specific antibody, which is attached to a sedimentable matrix. For this work proteins were immunoprecipitated from whole cell lysates using protein A or protein G-conjugated sepharose. Protein A and protein G from *Staphylococcus aureus* are immunoadsorbants that can non-covalently bind antibodies (Bonifacino et al., 2001).

For immunoprecipitation the suitable antibody (5 µl of a polyclonal antiserum, 1 µg of purified monoclonal antibody or 10 µl of culture supernatant containing monoclonal antibody) was added to 700 µl of whole cell lysate and incubated for 2 hours or over-night at 4 °C while mixing end over end in a tube rotator. Meanwhile 25 µl of 50 % protein A- or G sepharose bead slurry were washed twice with 0.5 ml lysis buffer. Then the lysate-antibody mixture was combined with the prepared sepharose beads and incubated 1 to 2 hours at 4 °C while mixing end over end in a tube rotator.

After incubation the protein-antibody-complexes bound to the sepharose beads were sedimented at 200x g for 1 minute in a microcentrifuge and the supernatant aspirated using a disposable pipet tip connected to a vacuum aspirator. To remove unspecific bound proteins beads were resuspended in 1 ml ice-cold lysis buffer and sedimented. After aspiration of the supernatant this washing step was repeated 2 to 3 times. Immunoprecipitated proteins were used for enzymatic assays (4.9) or directly analyzed by SDS-PAGE (4.8.2) and immunoblot (4.8.5).

4.8.2 Denaturing (SDS) Discontinuous Polyacrylamide Gel Electrophoresis (SDS-PAGE)

2x/4x Sample buffer	160 mM/320 mM Tris Cl, pH 6.8
	20 %/40 % (v/v) Glycerine
	10 %/8 % (w/v) SDS
	0.25 %/0.5 % (w/v) Bromphenol blue
	100 mM/200 mM ß-Mercaptoethanol

Laemmli buffer   25 mM Tris base
                                                  250 mM Glycerine
                                                  0.1 % (w/v) SDS

Discontinuous polyacrylamide gel electrophoresis under denaturing conditions (presence of 0.1 % SDS) separates proteins based on molecular size as they move through a gel matrix toward the anode. The polyacrylamide gel is cast as a separating gel topped by a stacking gel and secured in an electrophoresis apparatus.(BioRad). Sample proteins are solubilized by boiling in the presence of SDS (sample buffer), applied to a gel lane and separated electrophoretically. Binding of SDS to the denatured proteins generates a negative net charge of the proteins due to its anionic properties and allows separation solely by molecular weight (Gallagher, 2001).

The SDS-PAGE was performed according to the Laemmli buffer system (Laemmli, 1970) with a 5 % stacking gel and 10-15 % separating gels. The molecular weight of separated proteins was estimated by comparison with the PageRuler™ Prestained Protein Ladder (Fermentas).

4.8.3 Rapid Coomassie blue staining

Fixing solution   25 % (v/v) Isopropanol
                                                  10 % (v/v) Acetic acid

Rapid Coomassie blue staining solution 10 % (v/v) Acetic acid
                                                  0.006 % (w/v) Coomassie brilliant blue G-250

Detection of protein bands in a polyacrylamide gel by Coomassie blue staining depends on nonspecific binding of a dye, Coomassie brilliant blue R, to proteins. In this procedure proteins separated by SDS-PAGE were precipitated by gently shaking the polyacrylamide gel in the fixing solution for 30 minutes. Then the location of the precipitated proteins were detected by exchanging the fixing solution for the rapid Coomassie blue solution and incubation for 1 hour. Background staining was removed by incubation with water containing a tissue paper over-night. All incubations took place at room temperature. The gel was photographed and dried on Whatman paper to maintain a permanent record (Echan and Speicher, 2002).

4.8.4 Electroblotting from polyacrylamide gels

The electrophoretic transfer of proteins from polyacrylamide gels on retentive membranes (nitrocellulose or PVDF) results in a replica of the original gel pattern, which can be visualized by Ponceau S staining and detected by respective antibodies (= immunoblot or Western blot). The method was essentially performed according to Towbin (Towbin et al., 1979).

Semi-dry transfer buffer   25 mM Tris base
                                                  192 mM Glycine
                                                  20% (v/v) methanol

Tank blot transfer buffer	25 mM Tris base
	192 mM Glycine
	0.1% (w/v) SDS

For the transfer the polyacrylamide gel and the membrane were soaked in the respective transfer buffer and packed between three layers of Whatman papers, which were soaked in the buffer as well. PVDF membranes were pre-soaked in methanol. For even blotting results it was necessary to remove all air bubbles between the different sheets of the so called "sandwich". Then the sandwich was placed in a semi-dry blotting chamber between two electrode plates or into a tank-blot apparatus. Proteins were transferred to the membrane for 1 hour at 2 mA/ cm^2 of membrane size.

Ponceau S staining

Ponceau staining solution	0.2 % (w/v) Ponceau S
	3 % (v/v) Trichloroacetic acid

Transfer efficiency was controlled by incubating the membrane in Ponceau staining solution for 2 minutes. Excessive staining was removed by washing off the membrane with water.

4.8.5 Immunoblot detection

Detection of a specific protein transferred by Western blotting on a membrane was achieved by a two-step antibody incubation, in which first a primary antibody specifically bound the protein of interest. Then a secondary antibody was used that targeted the invariable part of the primary antibody and was conjugated with horseradish peroxidase (HRP). Protein-antibody complexes were visualized by a chemiluminescence reaction, in which a substrate was locally turned-over under emission of light by the peroxidase. The emission was detected by a CCD camera imaging device.

TBS-T	20 mM Tris base
	137 mM NaCl
	0.05 % (v/v) Tween-20

Blocking buffer	5 % (w/v) Nonfat dried milk powder
	TBS-T

Antibody buffer	5 % (w/v) BSA
	TBS-T

For immunodetection of proteins the membrane was incubated with blocking buffer for 30 minutes at room temperature to block unspecific binding sites. After three washing steps with TBS-T the membrane was incubated with the primary antibody, diluted in antibody buffer for 1 hour at room temperature or over-night at 4 °C. Afterwards the membrane was thoroughly washed thrice and incubated with the secondary antibody, diluted in blocking buffer for 30 minutes at room temperature. Prior to detection the membrane was washed for 30 minutes and at least three times with TBS-T. The ECL solution from Pierce was used as a substrate according to manufacturer's instructions. The detection was carried out with a computer-assisted camera (LAS-3000, Fuji).

4.8.6 Autoradiography

Autoradiography was used to detect radioisotope-labeled proteins or peptides in dried gel with commercially available autoradiography films. These films are covered with an emulsion of silver halide grains, which interact with emitted ionizing radiation. The resulting latent image is then amplified by incubation with a developer (Bundy, 2001).

For detection of ^{32}P-labeled samples an intensifying screen was located on the other side of a autoradiography film, which converted the ionizing radiation to blue or green light thereby intensifying the signal.

Detection of ^{35}S-labeled samples was enhanced by fluorography. For that purpose the Coomassie-stained gel was soaked in scintillant prior to drying. The reagent emitted visible light upon absorbing ionizing radiation.

For both detection methods the dried gel and the autoradiography film (SuperRX FUJI) were incubated in a light-tight cassette at -80 °C. After exposure the cassette was warmed to room temperature and manually processed in a developer and fixing solution from Tetenal according to manufacturer's instructions.

4.9 Enzymatic Assays

4.9.1 Acetylation Assay

In this gel assay, a lysine acetyltransferase catalyzed acetylation of substrates with acetyl-CoA as the coenzyme. Acetylated proteins were separated from each other, as well as from free acetyl-CoA, by SDS-PAGE (4.8.2) for subsequent detection by immunoblot (4.8.5). The *in vitro* assay was essentially performed according to the basic protocol 2 from chapter 14.11 of "Current Protocols in Protein Science" with slight differences (John E. Coligan, 2011.).

5x Buffer A1	250 mM Tris Cl, pH 8.0
	50 % (v/v) Glycerine
	5 mM DTT
	0.5 mM EDTA
5x Buffer A2	250 mM Tris Cl, pH 8.0
	50 % (v/v) Glycerine
	0.5 M NaCl
	20 mM $MgCl_2$
	1 mM $ZnCl_2$
HDAC inhibitors	10 mM Sodium butyrate
	3 μM TSA
	5 mM Nicotinamide
	10 μM AGK2

A 20 μl acetylation reaction was prepared in a 1.5 ml sterile microcentrifuge tube on ice containing 4 μl of 5x buffer A, HDAC inhibitors, ProteoBlock Protease Inhibitor Cocktail (Fermentas), 0.5 μg substrate and 0.25 mM acetyl-CoA. If there were many samples, a master mix was prepared.

The lysine acetyltransferase was diluted to a concentration of 250 ng/μl in 1x buffer A and

1 µl enzyme added to a reaction mix. The tube was gently mixed and transferred into a Thermo Shaker (BioRad) preheated to 30 °C. After an incubation at 30 °C at 1400 rpm for 30 minutes the reaction was terminated by addition of 7 µl 4x sample buffer (4.8.2). The samples were analyzed by SDS-PAGE (4.8.2) and immunoblot (4.8.5).

4.9.2 Deacetylation Assay

The following protocol describes an enzymatic assay to detect SIRT2 activity by using purified porcine tubulin (Cytoskeleton, T240) as a substrate. The deacetylation of tubulin was detected through immunoblot (4.8.5) with a specific antibody detecting acetylated tubulin.

A 19 µl deacetylation reaction was prepared in a 1.5 ml sterile microcentrifuge tube on ice containing 4.8 µl of 5x buffer A1 (4.9.1), ProteoBlock Protease Inhibitor Cocktail (Fermentas), 0.5 µg tubulin and 1 µg GST-SIRT2. If there were many samples, a master mix was prepared.

The enzymatic reaction was initiated by adding 2.5 mM NAD$^+$ cofactor (5 µl). The reaction tube was gently mixed and transferred into a Thermo Shaker preheated to 30 °C. After an incubation at 30 °C and 1400 rpm for up to 90 minutes the reaction was terminated by addition of 8 µl 4x sample buffer (4.8.2). The samples were analyzed by SDS-PAGE (4.8.2) and immunoblot (4.8.5).

4.9.3 Kinase Assay

The following protocol describes an enzymatic assay to detect the phosphorylation of a substrate by CDK5. The assay was essentially performed according to a protocol from Sigma-Aldrich to measure CDK5 activity with slight differences. Purified GST-fusion proteins (4.6.5) were used as substrates and *CDK5* was transiently overexpressed in HEK293 cells (4.7.6) and immunoprecipitated (4.8.1). Results were evaluated by SDS-PAGE (4.8.2) and autoradiography (4.8.6).

Kinase assay buffer   25 mM MOPS, pH 7.2
                                 12.5 mM Sodium ß-glycerophosphate
                                 25 mM MgCl$_2$
                                 5 mM EGTA
                                 2 mM EDTA
                                 0.25 mM DTT
                                 (0.25 mM ATP)

Kinase dilution buffer   20 % (v/v) kinase assay buffer <u>without</u> ATP

Immunoprecipitated p35/CDK5 complexes were washed once with kinase dilution buffer for equilibration and gathered in 10 µl of the same buffer. 1 µg GST-substrate was diluted in sterile water and added to the kinase solution. 2 µC [γ-^{32}P]-ATP were added to 60 µl kinase assay buffer. Out of this "hot mix" 5 µl were used to initiate the enzymatic reaction. The reaction tube was gently mixed and transferred into a Thermo Shaker (BioRad) preheated to 30 °C. After an incubation at 30 °C and 1400 rpm for 15 minutes the reaction was terminated by addition of 8.3 µl 4x sample buffer (4.8.2). The samples were separated by SDS-PAGE (4.8.2) and the gel subjected to a Coomassie blue staining (4.8.3). Afterwards the gel was dried on Whatman paper and analyzed by autoradiography (4.8.6).

4.9.4 Phosphatase Assay

The following protocol describes an enzymatic assay to dephosphorylate proteins with a commercially available unspecific phosphatase (FastAP™, Fermentas). The assay was essentially performed according to manufacture's instructions. Results were evaluated by SDS-PAGE (4.8.2) and immunoblot (4.8.5).

1x Alkaline phosphatase buffer	10 mM Tris Cl, pH 8
	5 mM $MgCl_2$
	100 mM KCl
Phosphatase inhibitors	100 µM Sodium ortho-vanadate
	20 mM Sodium ß-glycerophosphate
	0.05 µM Ocadaic acid
	50 mM Sodium fluoride

Immunoprecipitated substrates (4.8.1) were washed once with 1x alkaline phosphatase buffer for equilibration and gathered in 5 µl of 10x FastAP buffer (Fermentas). 37 µl sterile water were added to achieve a reaction volume of 50 µl. As a negative control phosphatase inhibitors were included in the reaction. The assay was initiated by addition of 8 µl enzyme and incubated at 37 °C and 1400 rpm in a Thermo Shaker (BioRad). After 1 hour the reaction was terminated by addition of 16.7 µl 4x sample buffer (4.8.2) and the samples were analyzed by SDS-PAGE (4.8.2) and immunoblot (4.8.5).

5. References

Afshar, G., and Murnane, J.P. (1999). Characterization of a human gene with sequence homology to Saccharomyces cerevisiae SIR2. Gene *234*, 161-168.

Ahuja, N., Schwer, B., Carobbio, S., Waltregny, D., North, B.J., Castronovo, V., Maechler, P., and Verdin, E. (2007). Regulation of insulin secretion by SIRT4, a mitochondrial ADP-ribosyltransferase. The Journal of biological chemistry *282*, 33583-33592.

Allfrey, V.G., and Mirsky, A.E. (1964). Structural Modifications of Histones and their Possible Role in the Regulation of RNA Synthesis. Science *144*, 559.

Allis, C.D., Berger, S.L., Cote, J., Dent, S., Jenuwien, T., Kouzarides, T., Pillus, L., Reinberg, D., Shi, Y., Shiekhattar, R.*, et al.* (2007). New nomenclature for chromatin-modifying enzymes. Cell *131*, 633-636.

Amerik, A.Y., and Hochstrasser, M. (2004). Mechanism and function of deubiquitinating enzymes. Biochimica et biophysica acta *1695*, 189-207.

Ashraf, N., Zino, S., Macintyre, A., Kingsmore, D., Payne, A.P., George, W.D., and Shiels, P.G. (2006). Altered sirtuin expression is associated with node-positive breast cancer. British journal of cancer *95*, 1056-1061.

Back, J.H., Rezvani, H.R., Zhu, Y., Guyonnet-Duperat, V., Athar, M., Ratner, D., and Kim, A.L. (2011). Cancer cell survival following DNA damage-mediated premature senescence is regulated by mammalian target of rapamycin (mTOR)-dependent Inhibition of sirtuin 1. The Journal of biological chemistry *286*, 19100-19108.

Bell, E.L., Emerling, B.M., Ricoult, S.J., and Guarente, L. (2011). SirT3 suppresses hypoxia inducible factor 1alpha and tumor growth by inhibiting mitochondrial ROS production. Oncogene *30*, 2986-2996.

Besset, V., Rhee, K., and Wolgemuth, D.J. (1999). The cellular distribution and kinase activity of the Cdk family member Pctaire1 in the adult mouse brain and testis suggest functions in differentiation. Cell growth & differentiation : the molecular biology journal of the American Association for Cancer Research *10*, 173-181.

Bhoj, V.G., and Chen, Z.J. (2009). Ubiquitylation in innate and adaptive immunity. Nature *458*, 430-437.

Blanco-Garcia, N., Asensio-Juan, E., de la Cruz, X., and Martinez-Balbas, M.A. (2009). Autoacetylation regulates P/CAF nuclear localization. The Journal of biological chemistry *284*, 1343-1352.

Bonifacino, J.S., Dell'Angelica, E.C., and Springer, T.A. (2001). Immunoprecipition. Curr Protoc Protein Sci *Chapter 9*, Unit 9 8.

Brachmann, C.B., Sherman, J.M., Devine, S.E., Cameron, E.E., Pillus, L., and Boeke, J.D. (1995). The SIR2 gene family, conserved from bacteria to humans, functions in silencing, cell cycle progression, and chromosome stability. Genes Dev *9*, 2888-2902.

Braunstein, M., Rose, A.B., Holmes, S.G., Allis, C.D., and Broach, J.R. (1993). Transcriptional silencing in yeast is associated with reduced nucleosome acetylation. Genes Dev *7*, 592-604.

Brummelkamp, T.R., Bernards, R., and Agami, R. (2002). A system for stable expression of short interfering RNAs in mammalian cells. Science *296*, 550-553.

Bundy, D.C. (2001). Autoradiography. Curr Protoc Protein Sci *Chapter 10*, Unit 10 11.

Burnett, C., Valentini, S., Cabreiro, F., Goss, M., Somogyvari, M., Piper, M.D., Hoddinott, M., Sutphin, G.L., Leko, V., McElwee, J.J.*, et al.* (2011). Absence of effects of Sir2 overexpression on lifespan in C. elegans and Drosophila. Nature *477*, 482-485.

Chacinska, A., Koehler, C.M., Milenkovic, D., Lithgow, T., and Pfanner, N. (2009). Importing mitochondrial proteins: machineries and mechanisms. Cell *138*, 628-644.

Chae, T., Kwon, Y.T., Bronson, R., Dikkes, P., Li, E., and Tsai, L.H. (1997). Mice lacking p35, a neuronal specific activator of Cdk5, display cortical lamination defects, seizures, and adult lethality. Neuron *18*, 29-42.

Chambon, P., Weill, J.D., and Mandel, P. (1963). Nicotinamide mononucleotide activation of new DNA-dependent polyadenylic acid synthesizing nuclear enzyme. Biochemical and Biophysical Research Communications *11*, 39-43.

Chen, C.A., and Okayama, H. (1988). Calcium phosphate-mediated gene transfer: a highly efficient transfection system for stably transforming cells with plasmid DNA. Biotechniques *6*, 632-638.

Chen, W.Y., Wang, D.H., Yen, R.C., Luo, J., Gu, W., and Baylin, S.B. (2005). Tumor suppressor HIC1 directly regulates SIRT1 to modulate p53-dependent DNA-damage responses. Cell *123*, 437-448.

Chen, Y., Zhang, J., Lin, Y., Lei, Q., Guan, K.L., Zhao, S., and Xiong, Y. (2011). Tumour suppressor SIRT3 deacetylates and activates manganese superoxide dismutase to scavenge ROS. EMBO reports *12*, 534-541.

Cheng, H.-L., Mostoslavsky, R., Saito, S.a.i., Manis, J.P., Gu, Y., Patel, P., Bronson, R., Appella, E., Alt, F.W., and Chua, K.F. (2003). Developmental defects and p53 hyperacetylation in Sir2 homolog (SIRT1)-deficient mice. Proceedings of the National Academy of Sciences of the United States of America *100*, 10794-10799.

Cheng, K., Li, Z., Fu, W.-Y., Wang, J.H., Fu, A.K.Y., and Ip, N.Y. (2002). Pctaire1 interacts with p35 and is a novel substrate for Cdk5/p35. The Journal of biological chemistry *277*, 31988-31993.

Choudhary, C., Kumar, C., Gnad, F., Nielsen, M.L., Rehman, M., Walther, T.C., Olsen, J.V., and Mann, M. (2009). Lysine acetylation targets protein complexes and co-regulates major cellular functions. Science (New York, NY) *325*, 834-840.

Choudhary, C., Weinert, B.T., Wagner, S.A., Horn, H., Henriksen, P., Liu, W.S.R., Olsen, J.V., and Jensen, L.J. (2011). Proteome-Wide Mapping of the Drosophila Acetylome Demonstrates a High Degree of Conservation of Lysine Acetylation. Science Signaling *4*.

Cicero, S., and Herrup, K. (2005). Cyclin-dependent kinase 5 is essential for neuronal cell cycle arrest and differentiation. The Journal of neuroscience : the official journal of the Society for Neuroscience *25*, 9658-9668.

Ciechanover, A., and Ben-Saadon, R. (2004). N-terminal ubiquitination: more protein substrates join in. Trends in cell biology *14*, 103-106.

Cohen, P. (2000). The regulation of protein function by multisite phosphorylation--a 25 year update. Trends in biochemical sciences *25*, 596-601.

Conacci-Sorrell, M., Ngouenet, C., and Eisenman, R.N. (2010). Myc-Nick: A Cytoplasmic Cleavage Product of Myc that Promotes alpha-Tubulin Acetylation and Cell Differentiation. Cell *142*, 480-493.

Courapied, S., Sellier, H., de Carné Trécesson, S., Vigneron, A., Bernard, A.-C., Gamelin, E., Barré, B., and Coqueret, O. (2010). The cdk5 kinase regulates the STAT3 transcription factor to prevent DNA damage upon topoisomerase I inhibition. The Journal of biological chemistry *285*, 26765-26778.

Cuschieri, L., Nguyen, T., and Vogel, J. (2007). Control at the cell center: the role of spindle poles in cytoskeletal organization and cell cycle regulation. Cell Cycle *6*, 2788-2794.

de Ruijter, A.J., van Gennip, A.H., Caron, H.N., Kemp, S., and van Kuilenburg, A.B. (2003). Histone deacetylases (HDACs): characterization of the classical HDAC family. The Biochemical journal *370*, 737-749.

Dephoure, N., Zhou, C., Villen, J., Beausoleil, S.A., Bakalarski, C.E., Elledge, S.J., and Gygi, S.P. (2008). A quantitative atlas of mitotic phosphorylation. Proceedings of the National Academy of Sciences of the United States of America *105*, 10762-10767.

Deshaies, R.J., Koch, B.D., Werner-Washburne, M., Craig, E.A., and Schekman, R. (1988). A subfamily of stress proteins facilitates translocation of secretory and mitochondrial precursor polypeptides. Nature *332*, 800-805.

Desterro, J.M., Rodriguez, M.S., and Hay, R.T. (1998). SUMO-1 modification of IkappaBalpha inhibits NF-kappaB activation. Molecular Cell *2*, 233-239.

Di Lorenzo, A., and Bedford, M.T. (2011). Histone arginine methylation. FEBS letters *585*, 2024-2031.

Dikic, I., Wakatsuki, S., and Walters, K.J. (2009). Ubiquitin-binding domains - from structures to functions. Nat Rev Mol Cell Biol *10*, 659-671.

Dryden, S.C., Nahhas, F.A., Nowak, J.E., Goustin, A.-S., and Tainsky, M.A. (2003). Role for human SIRT2 NAD-dependent deacetylase activity in control of mitotic exit in the cell cycle. Mol Cell Biol *23*, 3173-3185.

Echan, L.A., and Speicher, D.W. (2002). Protein detection in gels using fixation. Curr Protoc Protein Sci *Chapter 10*, Unit 10 15.

Ehrt, S., and Schnappinger, D. (2003). Isolation of plasmids from E. coli by alkaline lysis. Methods Mol Biol *235*, 75-78.

Felgner, P.L., Gadek, T.R., Holm, M., Roman, R., Chan, H.W., Wenz, M., Northrop, J.P., Ringold, G.M., and Danielsen, M. (1987). Lipofection: a highly efficient, lipid-mediated DNA-transfection procedure. Proceedings of the National Academy of Sciences of the United States of America *84*, 7413-7417.

Finley, L.W., Carracedo, A., Lee, J., Souza, A., Egia, A., Zhang, J., Teruya-Feldstein, J., Moreira, P.I., Cardoso, S.M., Clish, C.B.*, et al.* (2011). SIRT3 opposes reprogramming of cancer cell metabolism through HIF1alpha destabilization. Cancer cell *19*, 416-428.

Ford, E., Voit, R., Liszt, G., Magin, C., Grummt, I., and Guarente, L. (2006). Mammalian Sir2 homolog SIRT7 is an activator of RNA polymerase I transcription. Genes Dev *20*, 1075-1080.

Frye, R.A. (2000). Phylogenetic classification of prokaryotic and eukaryotic Sir2-like proteins. Biochemical and Biophysical Research Communications *273*, 793-798.

Fulco, M., Cen, Y., Zhao, P., Hoffman, E.P., McBurney, M.W., Sauve, A.A., and Sartorelli, V. (2008). Glucose restriction inhibits skeletal myoblast differentiation by activating SIRT1 through AMPK-mediated regulation of Nampt. Developmental Cell *14*, 661-673.

Gakh, O., Cavadini, P., and Isaya, G. (2002). Mitochondrial processing peptidases. Biochimica et biophysica acta *1592*, 63-77.

Gallagher, S.R. (2001). One-dimensional SDS gel electrophoresis of proteins. Curr Protoc Protein Sci *Chapter 10*, Unit 10 11.

Geiss-Friedlander, R., and Melchior, F. (2007). Concepts in sumoylation: a decade on. Nat Rev Mol Cell Biol *8*, 947-956.

Giralt, A., Hondares, E., Villena, J.A., Ribas, F., Diaz-Delfin, J., Giralt, M., Iglesias, R., and Villarroya, F. (2011). Peroxisome proliferator-activated receptor-gamma coactivator-1alpha controls transcription of the Sirt3 gene, an essential component of the thermogenic brown adipocyte phenotype. The Journal of biological chemistry *286*, 16958-16966.

Gottlieb, S., and Esposito, R.E. (1989). A new role for a yeast transcriptional silencer gene, SIR2, in regulation of recombination in ribosomal DNA. Cell *56*, 771-776.

Grob, A., Roussel, P., Wright, J.E., McStay, B., Hernandez-Verdun, D., and Sirri, V. (2009). Involvement of SIRT7 in resumption of rDNA transcription at the exit from mitosis. Journal of cell science *122*, 489-498.

Guarente, L. (2011). Franklin H. Epstein Lecture: Sirtuins, aging, and medicine. N Engl J Med *364*, 2235-2244.

Haigis, M.C., Mostoslavsky, R., Haigis, K.M., Fahie, K., Christodoulou, D.C., Murphy, A.J., Valenzuela, D.M., Yancopoulos, G.D., Karow, M., Blander, G.*, et al.* (2006). SIRT4 inhibits glutamate dehydrogenase and opposes the effects of calorie restriction in pancreatic beta cells. Cell *126*, 941-954.

Hallows, W.C., Lee, S., and Denu, J.M. (2006). Sirtuins deacetylate and activate mammalian acetyl-CoA synthetases. Proceedings of the National Academy of Sciences of the United States of America *103*, 10230-10235.

Hallows, W.C., Yu, W., Smith, B.C., Devries, M.K., Ellinger, J.J., Someya, S., Shortreed, M.R., Prolla, T., Markley, J.L., Smith, L.M.*, et al.* (2011). Sirt3 promotes the urea cycle and fatty acid oxidation during dietary restriction. Molecular Cell *41*, 139-149.

Han, Y., Jin, Y.-H., Kim, Y.-J., Kang, B.Y., Choi, H.-J., Kim, D.-W., Yeo, C.-Y., and Lee, K.-Y. (2008). Acetylation of Sirt2 by p300 attenuates its deacetylase activity. Biochemical and Biophysical Research Communications *375*, 576-580.

Harper, S., and Speicher, D.W. (2008). Expression and purification of GST fusion proteins. Curr Protoc Protein Sci *Chapter 6*, Unit 6 6.

Hartley, J.L., Temple, G.F., and Brasch, M.A. (2000). DNA cloning using in vitro site-specific recombination. Genome Res *10*, 1788-1795.

He, X., Takahashi, S., Suzuki, H., Hashikawa, T., Kulkarni, A.B., Mikoshiba, K., and Ohshima, T. (2011). Hypomyelination phenotype caused by impaired differentiation of oligodendrocytes in Emx1-cre mediated Cdk5 conditional knockout mice. Neurochemical research *36*, 1293-1303.

Hietakangas, V., Anckar, J., Blomster, H.A., Fujimoto, M., Palvimo, J.J., Nakai, A., and Sistonen, L. (2006). PDSM, a motif for phosphorylation-dependent SUMO modification. Proceedings of the National Academy of Sciences of the United States of America *103*, 45-50.

Hirschey, M.D., Shimazu, T., Goetzman, E., Jing, E., Schwer, B., Lombard, D.B., Grueter, C.A., Harris, C., Biddinger, S., Ilkayeva, O.R.*, et al.* (2010). SIRT3 regulates mitochondrial fatty-acid oxidation by reversible enzyme deacetylation. Nature *464*, 121-125.

Hisahara, S., Chiba, S., Matsumoto, H., Tanno, M., Yagi, H., Shimohama, S., Sato, M., and Horio, Y. (2008). Histone deacetylase SIRT1 modulates neuronal differentiation by its nuclear translocation. Proceedings of the National Academy of Sciences of the United States of America *105*, 15599-15604.

Hochstrasser, M. (2009). Origin and function of ubiquitin-like proteins. Nature *458*, 422-429.

Hottiger, M.O., Hassa, P.O., Luscher, B., Schuler, H., and Koch-Nolte, F. (2010). Toward a unified nomenclature for mammalian ADP-ribosyltransferases. Trends in biochemical sciences *35*, 208-219.

Huang, X., Auinger, P., Eberly, S., Oakes, D., Schwarzschild, M., Ascherio, A., Mailman, R., and Chen, H. (2011). Serum Cholesterol and the Progression of Parkinson's Disease: Results from DATATOP. PLoS ONE *6*, e22854.

Hunter, T. (2007). The age of crosstalk: phosphorylation, ubiquitination, and beyond. Molecular Cell *28*, 730-738.

Imai, S., Armstrong, C.M., Kaeberlein, M., and Guarente, L. (2000). Transcriptional silencing and longevity protein Sir2 is an NAD-dependent histone deacetylase. Nature *403*, 795-800.

Inoue, T., Hiratsuka, M., Osaki, M., Yamada, H., Kishimoto, I., Yamaguchi, S., Nakano, S., Katoh, M., Ito, H., and Oshimura, M. (2007). SIRT2, a tubulin deacetylase, acts to block the entry to chromosome condensation in response to mitotic stress. Oncogene *26*, 945-957.

Inoue, T., Nakayama, Y., Yamada, H., Li, Y.C., Yamaguchi, S., Osaki, M., Kurimasa, A., Hiratsuka, M., Katoh, M., and Oshimura, M. (2009). SIRT2 downregulation confers resistance to microtubule inhibitors by prolonging chronic mitotic arrest. Cell cycle (Georgetown, Tex) *8*, 1279-1291.

Ji, S., Doucette, J.R., and Nazarali, A.J. (2011). Sirt2 is a novel in vivo downstream target of Nkx2.2 and enhances oligodendroglial cell differentiation. Journal of molecular cell biology.

Jing, E., Gesta, S., and Kahn, C.R. (2007). SIRT2 regulates adipocyte differentiation through FoxO1 acetylation/deacetylation. Cell metabolism *6*, 105-114.

Jintang Du, Y.Z., Xiaoyang Su, Jiu Jiu Yu, Saba Khan, Hong Jiang, Jungwoo Kim, Jimin Woo, Jun Huyn Kim, Brian Hyun Choi, Bin He, Wei Chen, Sheng Zhang, Richard A. Cerione, Johan Auwerx, Quan Hao, Hening Lin (2011). Sirt5 Is a NAD-Dependent Protein Lysine Demalonylase and Desuccinylase. Science *334*, 806-809.

John E. Coligan, B.M.D., David W. Speicher, Paul T. Wingfield, ed. (2011). Current Protocols in Protein Science (Wiley).

Johnson, E.S. (2004). Protein modification by SUMO. Annual review of biochemistry *73*, 355-382.

Kaeberlein, M., McVey, M., and Guarente, L. (1999). The SIR2/3/4 complex and SIR2 alone promote longevity in Saccharomyces cerevisiae by two different mechanisms. Genes Dev *13*, 2570-2580.

Kaidi, A., Weinert, B.T., Choudhary, C., and Jackson, S.P. (2010). Human SIRT6 promotes DNA end resection through CtIP deacetylation. Science *329*, 1348-1353.

Kang, H., Suh, J.Y., Jung, Y.S., Jung, J.W., Kim, M.K., and Chung, J.H. (2011). Peptide switch is essential for sirt1 deacetylase activity. Molecular Cell *44*, 203-213.

Karanam, B., Jiang, L., Wang, L., Kelleher, N.L., and Cole, P.A. (2006). Kinetic and mass spectrometric analysis of p300 histone acetyltransferase domain autoacetylation. The Journal of biological chemistry *281*, 40292-40301.

Kawahara, T.L., Michishita, E., Adler, A.S., Damian, M., Berber, E., Lin, M., McCord, R.A., Ongaigui, K.C., Boxer, L.D., Chang, H.Y.*, et al.* (2009). SIRT6 links histone H3 lysine 9 deacetylation to NF-kappaB-dependent gene expression and organismal life span. Cell *136*, 62-74.

Kawahara, T.L., Rapicavoli, N.A., Wu, A.R., Qu, K., Quake, S.R., and Chang, H.Y. (2011). Dynamic chromatin localization of sirt6 shapes stress- and aging-related transcriptional networks. PLoS genetics *7*, e1002153.

Kim, E.J., Kho, J.H., Kang, M.R., and Um, S.J. (2007). Active regulator of SIRT1 cooperates with SIRT1 and facilitates suppression of p53 activity. Molecular Cell *28*, 277-290.

Kim, H.S., Patel, K., Muldoon-Jacobs, K., Bisht, K.S., Aykin-Burns, N., Pennington, J.D., van der Meer, R., Nguyen, P., Savage, J., Owens, K.M.*, et al.* (2010). SIRT3 is a mitochondria-localized tumor suppressor required for maintenance of mitochondrial integrity and metabolism during stress. Cancer cell *17*, 41-52.

Kim, J.E., Chen, J., and Lou, Z. (2008). DBC1 is a negative regulator of SIRT1. Nature *451*, 583-586.

Kleine, H., and Luscher, B. (2009). Learning how to read ADP-ribosylation. Cell *139*, 17-19.

Kong, X., Wang, R., Xue, Y., Liu, X., Zhang, H., Chen, Y., Fang, F., and Chang, Y. (2010). Sirtuin 3, a new target of PGC-1alpha, plays an important role in the suppression of ROS and mitochondrial biogenesis. PLoS ONE *5*, e11707.

Kornberg, M.D., Sen, N., Hara, M.R., Juluri, K.R., Nguyen, J.V., Snowman, A.M., Law, L., Hester, L.D., and Snyder, S.H. (2010). GAPDH mediates nitrosylation of nuclear proteins. Nature cell biology *12*, 1094-1100.

Laemmli, U.K. (1970). Cleavage of structural proteins during the assembly of the head of bacteriophage T4. Nature *227*, 680-685.

Lalioti, V., Pulido, D., and Sandoval, I.V. (2010). Cdk5, the multifunctional surveyor. Cell cycle (Georgetown, Tex) *9*, 284-311.

Landry, J., Slama, J.T., and Sternglanz, R. (2000). Role of NAD(+) in the deacetylase activity of the SIR2-like proteins. Biochemical and Biophysical Research Communications *278*, 685-690.

Landy, A. (1989). Dynamic, structural, and regulatory aspects of lambda site-specific recombination. Annual review of biochemistry *58*, 913-949.

Lau, L.-F., and Ahlijanian, M.K. (2003). Role of cdk5 in the pathogenesis of Alzheimer's disease. Neurosignals *12*, 209-214.

Lew, J., Beaudette, K., Litwin, C.M., and Wang, J.H. (1992). Purification and characterization of a novel proline-directed protein kinase from bovine brain. The Journal of biological chemistry *267*, 13383-13390.

Li, A., Xue, Y., Jin, C., Wang, M., and Yao, X. (2006). Prediction of Nepsilon-acetylation on internal lysines implemented in Bayesian Discriminant Method. Biochemical and Biophysical Research Communications *350*, 818-824.

Li, W., Zhang, B., Tang, J., Cao, Q., Wu, Y., Wu, C., Guo, J., Ling, E.-A., and Liang, F. (2007). Sirtuin 2, a mammalian homolog of yeast silent information regulator-2 longevity regulator, is an oligodendroglial protein that decelerates cell differentiation through deacetylating alpha-tubulin. Journal of Neuroscience *27*, 2606-2616.

Liebl, J., Furst, R., Vollmar, A.M., and Zahler, S. (2011). Twice switched at birth: Cell cycle-independent roles of the "neuron-specific" cyclin-dependent kinase 5 (Cdk5) in non-neuronal cells. Cellular signalling *23*, 1698-1707.

Liszt, G., Ford, E., Kurtev, M., and Guarente, L. (2005). Mouse Sir2 homolog SIRT6 is a nuclear ADP-ribosyltransferase. The Journal of biological chemistry *280*, 21313-21320.

Liu, X., Wang, D., Zhao, Y., Tu, B., Zheng, Z., Wang, L., Wang, H., Gu, W., Roeder, R.G., and Zhu, W.G. (2011). Methyltransferase Set7/9 regulates p53 activity by interacting with Sirtuin 1 (SIRT1). Proceedings of the National Academy of Sciences of the United States of America *108*, 1925-1930.

Lombard, D.B., Alt, F.W., Cheng, H.L., Bunkenborg, J., Streeper, R.S., Mostoslavsky, R., Kim, J., Yancopoulos, G., Valenzuela, D., Murphy, A.*, et al.* (2007). Mammalian Sir2 homolog SIRT3 regulates global mitochondrial lysine acetylation. Mol Cell Biol *27*, 8807-8814.

Lu, S.P., and Lin, S.J. (2010). Regulation of yeast sirtuins by NAD(+) metabolism and calorie restriction. Biochimica et biophysica acta *1804*, 1567-1575.

Luo, J., Nikolaev, A.Y., Imai, S., Chen, D., Su, F., Shiloh, A., Guarente, L., and Gu, W. (2001). Negative control of p53 by Sir2alpha promotes cell survival under stress. Cell *107*, 137-148.

Luthi-Carter, R., Taylor, D.M., Pallos, J., Lambert, E., Amore, A., Parker, A., Moffitt, H., Smith, D.L., Runne, H., Gokce, O.*, et al.* (2010). SIRT2 inhibition achieves neuroprotection by decreasing sterol biosynthesis. Proceedings of the National Academy of Sciences of the United States of America *107*, 7927-7932.

Madeo, F., Eisenberg, T., and Kroemer, G. (2009). Autophagy for the avoidance of neurodegeneration. Genes & Development *23*, 2253-2259.

Mahlknecht, U., Ho, A.D., Letzel, S., and Voelter-Mahlknecht, S. (2006a). Assignment of the NAD-dependent deacetylase sirtuin 5 gene (SIRT5) to human chromosome band 6p23 by in situ hybridization. Cytogenet Genome Res *112*, 208-212.

Mahlknecht, U., Ho, A.D., and Voelter-Mahlknecht, S. (2006b). Chromosomal organization and fluorescence in situ hybridization of the human Sirtuin 6 gene. International journal of oncology *28*, 447-456.

Mahlknecht, U., and Voelter-Mahlknecht, S. (2009). Fluorescence in situ hybridization and chromosomal organization of the sirtuin 4 gene (Sirt4) in the mouse. Biochemical and Biophysical Research Communications *382*, 685-690.

Malumbres, M., Harlow, E., Hunt, T., Hunter, T., Lahti, J.M., Manning, G., Morgan, D.O., Tsai, L.-H., and Wolgemuth, D.J. (2009). Cyclin-dependent kinases: a family portrait. Nature cell biology *11*, 1275-1276.

Mao, Z., Hine, C., Tian, X., Van Meter, M., Au, M., Vaidya, A., Seluanov, A., and Gorbunova, V. (2011). SIRT6 promotes DNA repair under stress by activating PARP1. Science *332*, 1443-1446.

Matsushita, N., Yonashiro, R., Ogata, Y., Sugiura, A., Nagashima, S., Fukuda, T., Inatome, R., and Yanagi, S. (2011). Distinct regulation of mitochondrial localization and stability of two human Sirt5 isoforms. Genes Cells *16*, 190-202.

Matthias, P., Muller, M.M., Schreiber, E., Rusconi, S., and Schaffner, W. (1989). Eukaryotic expression vectors for the analysis of mutant proteins. Nucleic Acids Res *17*, 6418.

McBurney, M.W., Yang, X., Jardine, K., Hixon, M., Boekelheide, K., Webb, J.R., Lansdorp, P.M., and Lemieux, M. (2003). The mammalian SIR2alpha protein has a role in embryogenesis and gametogenesis. Mol Cell Biol *23*, 38-54.

McCord, R.A., Michishita, E., Hong, T., Berber, E., Boxer, L.D., Kusumoto, R., Guan, S., Shi, X., Gozani, O., Burlingame, A.L.*, et al.* (2009). SIRT6 stabilizes DNA-dependent protein kinase at chromatin for DNA double-strand break repair. Aging (Albany NY) *1*, 109-121.

Michishita, E., McCord, R.A., Berber, E., Kioi, M., Padilla-Nash, H., Damian, M., Cheung, P., Kusumoto, R., Kawahara, T.L., Barrett, J.C.*, et al.* (2008). SIRT6 is a histone H3 lysine 9 deacetylase that modulates telomeric chromatin. Nature *452*, 492-496.

Michishita, E., Park, J.Y., Burneskis, J.M., Barrett, J.C., and Horikawa, I. (2005). Evolutionarily conserved and nonconserved cellular localizations and functions of human SIRT proteins. Molecular biology of the cell *16*, 4623-4635.

Moorhead, G.B., De Wever, V., Templeton, G., and Kerk, D. (2009). Evolution of protein phosphatases in plants and animals. The Biochemical journal *417*, 401-409.

Morgan, D.O. (2008). SnapShot: cell-cycle regulators I. Cell *135*, 764-764 e761.

Morgenstern, J.P., and Land, H. (1990). Advanced mammalian gene transfer: high titre retroviral vectors with multiple drug selection markers and a complementary helper-free packaging cell line. Nucleic Acids Res *18*, 3587-3596.

Mostoslavsky, R., Chua, K.F., Lombard, D.B., Pang, W.W., Fischer, M.R., Gellon, L., Liu, P., Mostoslavsky, G., Franco, S., Murphy, M.M.*, et al.* (2006). Genomic instability and aging-like phenotype in the absence of mammalian SIRT6. Cell *124*, 315-329.

Nahhas, F., Dryden, S.C., Abrams, J., and Tainsky, M.A. (2007). Mutations in SIRT2 deacetylase which regulate enzymatic activity but not its interaction with HDAC6 and tubulin. Molecular and cellular biochemistry *303*, 221-230.

Naito, Y., Yamada, T., Ui-Tei, K., Morishita, S., and Saigo, K. (2004). siDirect: highly effective, target-specific siRNA design software for mammalian RNA interference. Nucleic Acids Res *32*, W124-129.

Nakagawa, T., Lomb, D.J., Haigis, M.C., and Guarente, L. (2009). SIRT5 Deacetylates carbamoyl phosphate synthetase 1 and regulates the urea cycle. Cell *137*, 560-570.

Nakamura, Y., Ogura, M., Tanaka, D., and Inagaki, N. (2008). Localization of mouse mitochondrial SIRT proteins: shift of SIRT3 to nucleus by co-expression with SIRT5. Biochemical and Biophysical Research Communications *366*, 174-179.

Nasrin, N., Kaushik, V.K., Fortier, E., Wall, D., Pearson, K.J., de Cabo, R., and Bordone, L. (2009). JNK1 phosphorylates SIRT1 and promotes its enzymatic activity. PLoS ONE *4*, e8414.

Nasrin, N., Wu, X., Fortier, E., Feng, Y., Bare, O.C., Chen, S., Ren, X., Wu, Z., Streeper, R.S., and Bordone, L. (2010). SIRT4 regulates fatty acid oxidation and mitochondrial gene expression in liver and muscle cells. The Journal of biological chemistry *285*, 31995-32002.

North, B.J., Marshall, B.L., Borra, M.T., Denu, J.M., and Verdin, E. (2003). The human Sir2 ortholog, SIRT2, is an NAD+-dependent tubulin deacetylase. Molecular Cell *11*, 437-444.

North, B.J., and Verdin, E. (2004). Sirtuins: Sir2-related NAD-dependent protein deacetylases. Genome biology *5*, 224.

North, B.J., and Verdin, E. (2007a). Interphase nucleo-cytoplasmic shuttling and localization of SIRT2 during mitosis. PLoS ONE *2*, e784.

North, B.J., and Verdin, E. (2007b). Mitotic regulation of SIRT2 by cyclin-dependent kinase 1-dependent phosphorylation. The Journal of biological chemistry *282*, 19546-19555.

Ohshima, T., Gilmore, E.C., Longenecker, G., Jacobowitz, D.M., Brady, R.O., Herrup, K., and Kulkarni, A.B. (1999). Migration defects of cdk5(-/-) neurons in the developing cerebellum is cell autonomous. The Journal of neuroscience : the official journal of the Society for Neuroscience *19*, 6017-6026.

Olsen, J.V., Vermeulen, M., Santamaria, A., Kumar, C., Miller, M.L., Jensen, L.J., Gnad, F., Cox, J., Jensen, T.S., Nigg, E.A.*, et al.* (2010). Quantitative phosphoproteomics reveals widespread full phosphorylation site occupancy during mitosis. Science Signaling *3*, ra3.

Outeiro, T.F., Kontopoulos, E., Altmann, S.M., Kufareva, I., Strathearn, K.E., Amore, A.M., Volk, C.B., Maxwell, M.M., Rochet, J.-C., McLean, P.J.*, et al.* (2007). Sirtuin 2 inhibitors rescue alpha-synuclein-mediated toxicity in models of Parkinson's disease. Science (New York, NY) *317*, 516-519.

Pandithage, R., Lilischkis, R., Harting, K., Wolf, A., Jedamzik, B., Lüscher-Firzlaff, J., Vervoorts, J., Lasonder, E., Kremmer, E., Knöll, B.*, et al.* (2008). The regulation of SIRT2 function by cyclin-dependent kinases affects cell motility. J Cell Biol *180*, 915-929.

Patrick, G.N., Zukerberg, L., Nikolic, M., de la Monte, S., Dikkes, P., and Tsai, L.H. (1999). Conversion of p35 to p25 deregulates Cdk5 activity and promotes neurodegeneration. Nature *402*, 615-622.

Pickart, C.M. (2001). Mechanisms underlying ubiquitination. Annual review of biochemistry *70*, 503-533.

Pradhan, S., Chin, H.G., Esteve, P.O., and Jacobsen, S.E. (2009). SET7/9 mediated methylation of non-histone proteins in mammalian cells. Epigenetics *4*, 383-387.

Prudden, J., Pebernard, S., Raffa, G., Slavin, D.A., Perry, J.J., Tainer, J.A., McGowan, C.H., and Boddy, M.N. (2007). SUMO-targeted ubiquitin ligases in genome stability. The EMBO journal *26*, 4089-4101.

Qiu, X., Brown, K., Hirschey, M.D., Verdin, E., and Chen, D. (2010). Calorie restriction reduces oxidative stress by SIRT3-mediated SOD2 activation. Cell metabolism *12*, 662-667.

Rahman, S., and Islam, R. (2011). Mammalian Sirt1: insights on its biological functions. Cell Commun Signal *9*, 11.

Rodier, F., Campisi, J., and Bhaumik, D. (2007). Two faces of p53: aging and tumor suppression. Nucleic Acids Res *35*, 7475-7484.

Rothgiesser, K.M., Erener, S., Waibel, S., Lüscher, B., and Hottiger, M.O. (2010). SIRT2 regulates NF-κB dependent gene expression through deacetylation of p65 Lys310. Journal of cell science *123*, 4251-4258.

Sabò, A., Lusic, M., Cereseto, A., and Giacca, M. (2008). Acetylation of conserved lysines in the catalytic core of cyclin-dependent kinase 9 inhibits kinase activity and regulates transcription. Mol Cell Biol *28*, 2201-2212.

Saher, G., Brugger, B., Lappe-Siefke, C., Mobius, W., Tozawa, R., Wehr, M.C., Wieland, F., Ishibashi, S., and Nave, K.A. (2005). High cholesterol level is essential for myelin membrane growth. Nature neuroscience *8*, 468-475.

Saiki, R.K., Gelfand, D.H., Stoffel, S., Scharf, S.J., Higuchi, R., Horn, G.T., Mullis, K.B., and Erlich, H.A. (1988). Primer-directed enzymatic amplification of DNA with a thermostable DNA polymerase. Science *239*, 487-491.

Samson, F., Donoso, J.A., Heller-Bettinger, I., Watson, D., and Himes, R.H. (1979). Nocodazole action on tubulin assembly, axonal ultrastructure and fast axoplasmic transport. J Pharmacol Exp Ther *208*, 411-417.

Sasaki, T., Maier, B., Koclega, K., Chruszcz, M., and Gluba, W. (2008a). Phosphorylation Regulates SIRT1 Function. PLoS ONE.

Sasaki, T., Maier, B., Koclega, K.D., Chruszcz, M., Gluba, W., Stukenberg, P.T., Minor, W., and Scrable, H. (2008b). Phosphorylation regulates SIRT1 function. PLoS ONE *3*, e4020.

Sasaki, Y., Cheng, C., Uchida, Y., Nakajima, O., Ohshima, T., Yagi, T., Taniguchi, M., Nakayama, T., Kishida, R., Kudo, Y*., et al.* (2002). Fyn and Cdk5 mediate semaphorin-3A signaling, which is involved in regulation of dendrite orientation in cerebral cortex. Neuron *35*, 907-920.

Scher, M.B., Vaquero, A., and Reinberg, D. (2007). SirT3 is a nuclear NAD+-dependent histone deacetylase that translocates to the mitochondria upon cellular stress. Genes Dev *21*, 920-928.

Schlicker, C., Gertz, M., Papatheodorou, P., Kachholz, B., Becker, C.F., and Steegborn, C. (2008). Substrates and regulation mechanisms for the human mitochondrial sirtuins Sirt3 and Sirt5. J Mol Biol *382*, 790-801.

Schwer, B., North, B.J., Frye, R.A., Ott, M., and Verdin, E. (2002). The human silent information regulator (Sir)2 homologue hSIRT3 is a mitochondrial nicotinamide adenine dinucleotide-dependent deacetylase. J Cell Biol *158*, 647-657.

Seidman, C.E., and Struhl, K. (2001). Introduction of plasmid DNA into cells. Curr Protoc Neurosci *Appendix 1*, Appendix 1L.

Shi, T., Wang, F., Stieren, E., and Tong, Q. (2005). SIRT3, a mitochondrial sirtuin deacetylase, regulates mitochondrial function and thermogenesis in brown adipocytes. The Journal of biological chemistry *280*, 13560-13567.

Shimazu, T., Hirschey, M.D., Hua, L., Dittenhafer-Reed, K.E., Schwer, B., Lombard, D.B., Li, Y., Bunkenborg, J., Alt, F.W., Denu, J.M*., et al.* (2010). SIRT3 deacetylates mitochondrial 3-hydroxy-3-methylglutaryl CoA synthase 2 and regulates ketone body production. Cell metabolism *12*, 654-661.

Smith, J.S., Brachmann, C.B., Celic, I., Kenna, M.A., Muhammad, S., Starai, V.J., Avalos, J.L., Escalante-Semerena, J.C., Grubmeyer, C., Wolberger, C., *et al*. (2000). A phylogenetically conserved NAD+-dependent protein deacetylase activity in the Sir2 protein family. Proceedings of the National Academy of Sciences of the United States of America *97*, 6658-6663.

Someya, S., Yu, W., Hallows, W.C., Xu, J., Vann, J.M., Leeuwenburgh, C., Tanokura, M., Denu, J.M., and Prolla, T.A. (2010). Sirt3 mediates reduction of oxidative damage and prevention of age-related hearing loss under caloric restriction. Cell *143*, 802-812.

Song, J., Durrin, L.K., Wilkinson, T.A., Krontiris, T.G., and Chen, Y. (2004). Identification of a SUMO-binding motif that recognizes SUMO-modified proteins. Proceedings of the National Academy of Sciences of the United States of America *101*, 14373-14378.

Southwood, C.M., Peppi, M., Dryden, S., Tainsky, M.A., and Gow, A. (2007). Microtubule deacetylases, SirT2 and HDAC6, in the nervous system. Neurochemical research *32*, 187-195.

Stefani, M., and Liguri, G. (2009). Cholesterol in Alzheimer's disease: unresolved questions. Curr Alzheimer Res *6*, 15-29.

Strahl, B.D., and Allis, C.D. (2000). The language of covalent histone modifications. Nature *403*, 41-45.

Sundaresan, N.R., Pillai, V.B., Wolfgeher, D., Samant, S., Vasudevan, P., Parekh, V., Raghuraman, H., Cunningham, J.M., Gupta, M., and Gupta, M.P. (2011). The Deacetylase SIRT1 Promotes Membrane Localization and Activation of Akt and PDK1 During Tumorigenesis and Cardiac Hypertrophy. Science Signaling *4*, ra46.

Suzuki, K., and Koike, T. (2007). Mammalian Sir2-related protein (SIRT) 2-mediated modulation of resistance to axonal degeneration in slow Wallerian degeneration mice: a crucial role of tubulin deacetylation. Neuroscience *147*, 599-612.

Tanner, K.G., Landry, J., Sternglanz, R., and Denu, J.M. (2000). Silent information regulator 2 family of NAD- dependent histone/protein deacetylases generates a unique product, 1-O-acetyl-ADP-ribose. Proceedings of the National Academy of Sciences of the United States of America *97*, 14178-14182.

Tanno, M., Sakamoto, J., Miura, T., Shimamoto, K., and Horio, Y. (2007). Nucleocytoplasmic shuttling of the NAD+-dependent histone deacetylase SIRT1. The Journal of biological chemistry *282*, 6823-6832.

Tennen, R.I., Berber, E., and Chua, K.F. (2010). Functional dissection of SIRT6: identification of domains that regulate histone deacetylase activity and chromatin localization. Mech Ageing Dev *131*, 185-192.

Tennen, R.I., and Chua, K.F. (2011). Chromatin regulation and genome maintenance by mammalian SIRT6. Trends in biochemical sciences *36*, 39-46.

Tong, L., and Denu, J.M. (2010). Function and metabolism of sirtuin metabolite O-acetyl-ADP-ribose. Biochimica et biophysica acta *1804*, 1617-1625.

Towbin, H., Staehelin, T., and Gordon, J. (1979). Electrophoretic transfer of proteins from polyacrylamide gels to nitrocellulose sheets: procedure and some applications. Proceedings of the National Academy of Sciences of the United States of America *76*, 4350-4354.

Turner, N.C., Lord, C.J., Iorns, E., Brough, R., Swift, S., Elliott, R., Rayter, S., Tutt, A.N., and Ashworth, A. (2008). A synthetic lethal siRNA screen identifying genes mediating sensitivity to a PARP inhibitor. The EMBO journal *27*, 1368-1377.

Vakhrusheva, O., Braeuer, D., Liu, Z., Braun, T., and Bober, E. (2008a). Sirt7-dependent inhibition of cell growth and proliferation might be instrumental to mediate tissue integrity during aging. J Physiol Pharmacol *59 Suppl 9*, 201-212.

Vakhrusheva, O., Smolka, C., Gajawada, P., Kostin, S., Boettger, T., Kubin, T., Braun, T., and Bober, E. (2008b). Sirt7 increases stress resistance of cardiomyocytes and prevents apoptosis and inflammatory cardiomyopathy in mice. Circ Res *102*, 703-710.

Vaquero, A., Scher, M., Lee, D., Erdjument-Bromage, H., Tempst, P., and Reinberg, D. (2004). Human SirT1 interacts with histone H1 and promotes formation of facultative heterochromatin. Molecular Cell *16*, 93-105.

Vaquero, A., Scher, M.B., Lee, D.H., Sutton, A., Cheng, H.-L., Alt, F.W., Serrano, L., Sternglanz, R., and Reinberg, D. (2006). SirT2 is a histone deacetylase with preference for histone H4 Lys 16 during mitosis. Genes & Development *20*, 1256-1261.

Vaziri, H., Dessain, S.K., Ng Eaton, E., Imai, S.I., Frye, R.A., Pandita, T.K., Guarente, L., and Weinberg, R.A. (2001). hSIR2(SIRT1) functions as an NAD-dependent p53 deacetylase. Cell *107*, 149-159.

Vempati, R.K., Jayani, R.S., Notani, D., Sengupta, A., Galande, S., and Haldar, D. (2010). p300-mediated acetylation of histone H3 lysine 56 functions in DNA damage response in mammals. The Journal of biological chemistry *285*, 28553-28564.

Voelter-Mahlknecht, S., Ho, A.D., and Mahlknecht, U. (2005). FISH-mapping and genomic organization of the NAD-dependent histone deacetylase gene, Sirtuin 2 (Sirt2). International journal of oncology *27*, 1187-1196.

Voelter-Mahlknecht, S., Letzel, S., and Mahlknecht, U. (2006). Fluorescence in situ hybridization and chromosomal organization of the human Sirtuin 7 gene. International journal of oncology *28*, 899-908.

Voelter-Mahlknecht, S., and Mahlknecht, U. (2006). Cloning, chromosomal characterization and mapping of the NAD-dependent histone deacetylases gene sirtuin 1. Int J Mol Med *17*, 59-67.

Wang, F., Nguyen, M., Qin, F.X.-F., and Tong, Q. (2007). SIRT2 deacetylates FOXO3a in response to oxidative stress and caloric restriction. Aging cell *6*, 505-514.

Wang, F., and Tong, Q. (2009). SIRT2 suppresses adipocyte differentiation by deacetylating FOXO1 and enhancing FOXO1's repressive interaction with PPARgamma. Molecular biology of the cell *20*, 801-808.

Wang, J., and Chen, J. (2010). SIRT1 regulates autoacetylation and histone acetyltransferase activity of TIP60. The Journal of biological chemistry *285*, 11458-11464.

Welihinda, A.A., Tirasophon, W., and Kaufman, R.J. (1999). The cellular response to protein misfolding in the endoplasmic reticulum. Gene Expr *7*, 293-300.

Werner, H.B., Kuhlmann, K., Shen, S., Uecker, M., Schardt, A., Dimova, K., Orfaniotou, F., Dhaunchak, A., Brinkmann, B.G., Möbius, W.*, et al.* (2007). Proteolipid protein is required for transport of sirtuin 2 into CNS myelin. Journal of Neuroscience *27*, 7717-7730.

Wilson, J.M., Le, V.Q., Zimmerman, C., Marmorstein, R., and Pillus, L. (2006). Nuclear export modulates the cytoplasmic Sir2 homologue Hst2. EMBO reports *7*, 1247-1251.

Wold, F. (1981). In vivo chemical modification of proteins (post-translational modification). Annual review of biochemistry *50*, 783-814.

Yan, S.C., Grinnell, B.W., and Wold, F. (1989). Post-translational modifications of proteins: some problems left to solve. Trends in biochemical sciences *14*, 264-268.

Yang, B., Zwaans, B.M.M., Eckersdorff, M., and Lombard, D.B. (2009). The sirtuin SIRT6 deacetylates H3 K56Ac in vivo to promote genomic stability. Cell cycle (Georgetown, Tex) *8*, 2662-2663.

Yang, X., and Seto, E. (2008). Lysine Acetylation: Codified Crosstalk with Other Posttranslational Modifications. Molecular Cell *31*, 449-461.

Yang, Y., Fu, W., Chen, J., Olashaw, N., Zhang, X., Nicosia, S.V., Bhalla, K., and Bai, W. (2007). SIRT1 sumoylation regulates its deacetylase activity and cellular response to genotoxic stress. Nature cell biology *9*, 1253-1262.

Yi, J., and Luo, J. (2010). SIRT1 and p53, effect on cancer, senescence and beyond. Biochimica et biophysica acta *1804*, 1684-1689.

Yu, L.R., Zhu, Z., Chan, K.C., Issaq, H.J., Dimitrov, D.S., and Veenstra, T.D. (2007). Improved titanium dioxide enrichment of phosphopeptides from HeLa cells and high confident phosphopeptide identification by cross-validation of MS/MS and MS/MS/MS spectra. Journal of proteome research *6*, 4150-4162.

Yuan, F., Xie, Q., Wu, J., Bai, Y., Mao, B., Dong, Y., Bi, W., Ji, G., Tao, W., Wang, Y.*, et al.* (2011). MST1 promotes apoptosis through regulating Sirt1-dependent p53 deacetylation. The Journal of biological chemistry *286*, 6940-6945.

Zhang, J. (2003). Are poly(ADP-ribosyl)ation by PARP-1 and deacetylation by Sir2 linked? BioEssays : news and reviews in molecular, cellular and developmental biology *25*, 808-814.

Zhang, J., Cicero, S.A., Wang, L., Romito-Digiacomo, R.R., Yang, Y., and Herrup, K. (2008). Nuclear localization of Cdk5 is a key determinant in the postmitotic state of neurons. Proceedings of the National Academy of Sciences of the United States of America *105*, 8772-8777.

Zhang, J., Li, H., and Herrup, K. (2010). Cdk5 nuclear localization is p27-dependent in nerve cells: implications for cell cycle suppression and caspase-3 activation. The Journal of biological chemistry *285*, 14052-14061.

Zhao, K., Chai, X., Clements, A., and Marmorstein, R. (2003). Structure and autoregulation of the yeast Hst2 homolog of Sir2. Nature structural biology *10*, 864-871.

Zhao, Y., Wang, L., Yang, J., Zhang, P., Ma, K., Zhou, J., Liao, W., and Zhu, W.-G. (2010a). Anti-neoplastic activity of the cytosolic FoxO1 results from autophagic cell death. Autophagy *6*, 988-990.

Zhao, Y., Yang, J., Liao, W., Liu, X., Zhang, H., Wang, S., Wang, D., Feng, J., Yu, L., and Zhu, W.-G. (2010b). Cytosolic FoxO1 is essential for the induction of autophagy and tumour suppressor activity. Nature cell biology *12*, 665-675.

Zhong, L., D'Urso, A., Toiber, D., Sebastian, C., Henry, R.E., Vadysirisack, D.D., Guimaraes, A., Marinelli, B., Wikstrom, J.D., Nir, T.*, et al.* (2010). The histone deacetylase Sirt6 regulates glucose homeostasis via Hif1alpha. Cell *140*, 280-293.

Zschoernig, B., and Mahlknecht, U. (2009). Carboxy-terminal phosphorylation of SIRT1 by protein kinase CK2. Biochemical and Biophysical Research Communications *381*, 372-377.

Zukerberg, L.R., Patrick, G.N., Nikolic, M., Humbert, S., Wu, C.L., Lanier, L.M., Gertler, F.B., Vidal, M., Van Etten, R.A., and Tsai, L.H. (2000). Cables links Cdk5 and c-Abl and facilitates Cdk5 tyrosine phosphorylation, kinase upregulation, and neurite outgrowth. Neuron *26*, 633-646.

6. Appendices

6.1 Abbreviations

A	Ampere
A.dest.	Destilled water
aa	Amino acid
Ab	Antibody
AD	Alzheimer's disease
ADP	Adenosine diphosphate
Amp	Ampicillin
AMP	Adenosine monophosphate
APS	Ammonium persulfate
ATCC	American Tissue Culture Collection
ATP	Adenosine triphosphate
bp	Base pair
BSA	Bovine serum albumine
°C	Degree Celsius
C-	Carboxy-
ca.	Circa
CDK	Cyclin-dependent kinase
CFP	Cyan-fluorescent protein
CMV	Cytomegalie virus
Da	Dalton
DMEM	Dulbecco's modified Eagle's medium
DMSO	Dimethyl sulfoxid
DNA	Desoxyribonucleic acid
DSB	Double strand break
DTT	Dithiothreitol
DUB	Deubiquitinating enzyme
DUSP	Dual-specific enzyme
E	Glutamate
E. coli	*Escherichia coli*
e.g.	For example
ECL	Enhanced chemoluminescense
EDTA	Ethylene-diamine-tetra-acedic acid
EGTA	Ethylene-glycol-bis(2-aminoethylether)-N,N,N',N'-tetraacetic acid
EST	Expressed sequence tag
et al.	at alii
FAD	Flavin adenine dinucleotide
FAK	Focal adhesion kinase

FAO	Fatty acid oxidation
FCS	Fetal calf serum
g	Gram
g	Gravitation constant
GFP	Green fluorescent protein
HAT	Histone acetyltransferase
HDAC	Histone deacetylase
HeBS	Hepes buffered saline
HEK	Human embryonic kidney
HIF-1α	Hypoxia inducible factor 1α
HRP	Horseradish peroxidase
IgG	Immunoglobuline G
IMP	Inner membrane peptidase
IMS	Intermembrane space
IP	Immunoprecipitation
IPTG	Isopropyl-β-D-1-thiogalactopyranoside
k	Kilo
K	Lysine
KAT	Lysine acetyltransferase
KDAC	Lysine deacetylase
KDM	Lysine specific demethylase
KMT	Lysine methyltransferases
l	Liter
LB	Luria Broth
M	Molar (mol/l)
m	Milli
m	Meter
MARH	Mono-ADP-ribose-protein hydrolase
MART	Mono-ADP-ribosylating enzyme
MBP	Myelin basic protein
MCS	Multiple cloning site
MEF	Murine embryonic fibroblast
min	Minute
MIP	Mitochondrial intermediate peptidase
MPP	Mitochondrial processing peptidase
mRNA	Messenger RNA
MS	Mass spectrometry
n	Nano
N-	Amino-
NAD$^+$	Nicotinamide adenindinucleotide
NAM	Nicotinamide

NAMPT	NAM phosphoribosyltransferase
NES	Nuclear export signal
NLS	Nuclear localization signal
O-AADP	*Ortho*-Acetyl-ADP
OD	Optical density
OL	Oligodendrocyte
p.a.	Pro analysi
PAGE	Polyacrylamide gel electrophoresis
PAR	Poly-ADP-ribose
PARG	Poly-ADP-ribose glycohydrolase
PARP	Poly-ADP-ribose polymerase
PBS	Phosphate buffered saline
PD	Parkinson's disease
PPAR	Peroxisome proliferator-activated receptors
PPP	Phospho-protein phosphatases
PRMT	Protein arginine methyltransferases
PTM	Posttranslational modification
PTP	Protein tyrosine phosphatases
RNA	Ribonucleic acid
ROS	Reactive oxygen species
rpm	Rounds per minute
S	Serine
SAM	S-adenosyl-L-methionine
shRNA	Short hairpin RNA
SIM	SUMO-interaction motifs
SOD	Superoxide dismutase
SREBP	Sterol response element binding protein
SUMO	Small ubiquitin-related modifiers
TE	Tris-EDTA
TIM	Translocase of the inner membrane
TOM	Translocase of the outer membrane
U	Unit
UBD	Ubiquitin-binding domain
v/v	volume per volume
w/v	weight per volume
WB	Western blot
wt	Wildtype
Y	Tyrosine
YFP	Yellow fluorescent protein
μ	Micro

6.2 Curriculum vitae

Angaben zur Person

Nachname/Vorname	Franziska Flick
Geburtsdatum	14. Oktober, 1981
Geburtsort	Ludwigslust
Nationalität	Deutsch

Ausbildung

Seit 04/2008	RWTH Aachen, Universitätsklinikum Promotionsstudentin im Institut für Biochemie und Molekularbiologie AG Prof. B. Lüscher
09/2001-03/2008	RWTH Aachen Diplomstudiengang Biologie mit den Fachschwerpunkten Mikrobiologie, Humanbiologie, Molekulare Medizin und Molekulare Biotechnologie
03/2008	Diplom Diplomarbeit am Institut für Humangenetik am Universitätsklinikum Aachen, Titel: „*Validierung der Proteininteraktion von SH3TC2 (KIAA1985) und Rad23 in Bezug auf eine Charcot Marie Tooth Typ 4C-Erkrankung*"
09/2004	Vordiplom
08/1992-06/2001	Landrat Lukas Schule, Leverkusen Abitur
08/1988-07/1992	Grundschule - Johannis-Widmann-Schule, Sindelfingen - 26. Schule – Berlin Hellersdorf - Oberschule Friedrich Schiller, Jena

Berufstätigkeit

Seit 04/2008	RWTH Aachen, Universitätsklinikum Wissenschaftliche Angestellte im Institut für Biochemie und Molekularbiologie AG Prof. B. Lüscher

6.3 Eidesstattliche Erklärung

Ich erkläre eidesstattlich, dass ich die vorliegende Dissertation selbstständig verfasst und alle in Anspruch genommenen Hilfen in der Dissertation angegeben habe. Des weiteren erkläre ich, dass die vorliegende Dissertation nicht bereits als Diplomarbeit oder vergleichbare Prüfungsarbeit verwendet worden ist.

Aachen, den 06.02.12   Franziska Flick

6.4 Danksagung

Ich danke allen, die dazu beigetragen haben, dass diese Arbeit geschrieben werden konnte. Insbesondere natürlich meinem Mentor Prof. Dr. Bernhard Lüscher, der mir die Möglichkeit einer Promotion in seiner Arbeitsgruppe gab. Er nahm sich immer die Zeit, meine vielen Fragen zu beantworten und zeigte mir neue Perspektiven auf. Vielen Dank dafür.

Herrn Prof. Dr. Werner Baumgartner möchte ich für die bereitwillige Übernahme des Zweitgutachtens danken.

Andrea Ullius danke ich unter anderem dafür, dass sie sich die Zeit genommen hat, meine literarischen Ergüsse zu korrigieren.

Ich bedanke mich bei Nadine Schall für ihren Beitrag zu dieser Arbeit. Es hat mir viel Spaß gemacht dich zu betreuen.

Den aktuellen und ehemalige Kollegen aus der Arbeitsgruppe Lüscher möchte ich für das besonders gute Arbeitsklima, die wissenschaftlichen Gespräche, die unverzichtbaren „Arbeiten im Hintergrund" und die Organisation bedanken: Nicolas Herzog, Georgios Agalaridis, Sophie Willnow, Mark Dohmen, Maryna Levikova, Kusum Singh, Jens Schirrmacher, Stephanie Speckgens Heike Chauvistre, Stephan Dreschers, Nora Honke, Stefan Brüning, Gabriele Lützeler, Elke Meyer, Angelika Szameit, Elena Buerova, Marcel Robbertz, Angelina Kriescher, Barbara Lippok.

Meinen aktuellen und ehemaligen Kollegen aus Labor 6 Karla Feijs, Patrice Verheugd, Jürgen Stahl, Andrea Graf, Daniela Otten, Juliane Lüscher-Firzlaff, Henning Kleine und Anne Braczynski danke ich für die vielen unterhaltsamen Stunden, die Gespräche, die Musik und die Späße, die mir über Rückschläge hinweghalfen und dafür verantwortlich waren, dass ich immer gerne hier war.

In diesem Zuge möchte ich auch meinen Kollegen und Freunden aus meinem Büro danken: Alexandra Forst für ihre fachliche Kompetenz und Hilfsbereitschaft, aber auch für viele kurzweilige und tanzbare Treffen; Henning Kleine für seine wissenschaftliche Betreuung und für herausfordernde Badminton-Spiele, Nadine Hein für ihren Zuspruch, wenn es mal nicht so gut lief und viele lustige Abende u.a. auf dem Weihnachtsmarkt oder beim Grillen; Christian Cornelissen u.a. fürs Blumengießen und Bierkästen schleppen, und Jörg Verfoorts-Weber für Zuspruch, Betreuung und konstruktive Kritik.

Sehr großer Dank geht an Ulli Linzen für ihre Kritik und Unterstützung und für alles, was

diese Zeit so unvergesslich macht.

Meinen Eltern Axel und Angela Flick danke ich dafür, dass sie mich ermutigt haben diesen Weg zu gehen und mir auch währenddessen immer mit Zuspruch zur Seite standen.

Besonderer Dank geht an Andreas Bollermann dafür, dass er nicht aufgegeben hat und immer für mich da war.

Vielen Dank!